# INFORMATION TO USERS

This manuscript has been reproduced from the microfilm master. UMI films the text directly from the original or copy submitted. Thus, some thesis and dissertation copies are in typewriter face, while others may be from any type of computer printer.

**The quality of this reproduction is dependent upon the quality of the copy submitted.** Broken or indistinct print, colored or poor quality illustrations and photographs, print bleedthrough, substandard margins, and improper alignment can adversely affect reproduction.

In the unlikely event that the author did not send UMI a complete manuscript and there are missing pages, these will be noted. Also, if unauthorized copyright material had to be removed, a note will indicate the deletion.

Oversize materials (e.g., maps, drawings, charts) are reproduced by sectioning the original, beginning at the upper left-hand corner and continuing from left to right in equal sections with small overlaps.

ProQuest Information and Learning
300 North Zeeb Road, Ann Arbor, MI 48106-1346 USA
800-521-0600

# INFLUENCE OF NONLINEAR ASYMMETRIC SUSPENSION PROPERTIES ON THE RIDE CHARACTERISTICS OF ROAD VEHICLE

**Mahmud Niroopam Joarder**

**A Thesis**
**in**
**The Department**
**of**
**Mechanical and Industrial Engineering**

**Presented in Partial Fulfillment of the Requirements**
**for the Degree of Master of Applied Science at**
**Concordia University**
**Montreal, Quebec**
**Canada**

**February, 2003**

## ABSTRACT

INFLUENCE OF NONLINEAR ASYMMETRIC SUSPENSION PROPERTIES ON THE RIDE CHARACTERISTICS OF ROAD VEHICLE

Mahmud Niroopam Joarder

The suspension springs and dampers, employed in road vehicles, typically exhibit nonlinear and asymmetric force-deflection and force-velocity characteristics. The asymmetry in the suspension characteristics is known to yield a shift in the dynamic equilibrium. Such fundamental behavior of the suspension components can be studied through analysis of simple quarter-vehicle model with realistic representation of the suspension characteristics. The asymmetric characteristics of the suspension components are characterized to investigate the phenomenon of drift in dynamic equilibrium, also known as the 'ride height drift'. A quarter-vehicle model, incorporating nonlinear and asymmetric suspension components, is mathematically modeled and simulated using 'simulink'. Suspension damper is represented by multistage nonlinear asymmetric characteristics, while the stiffness is treated as a nonlinear cubical spring, asymmetric in compression and rebound. The simulations are carried out in sequence starting with linear, nonlinear symmetric, single stage asymmetric, and finally the two-stage asymmetric suspension properties. The model results are validated by comparing the responses over a wide frequency range with the published data. A comprehensive parametric study is performed to establish the influence of variation in design and operating parameters of suspension components on 'ride height drifting' phenomenon. The study clearly reveals that the 'ride height drifting' phenomenon is a direct result of asymmetric properties of the suspension damper. The magnitude of the drift increases

with an increase in asymmetry as well as amplitude of excitation, and it approaches maximum corresponding to the wheel hop natural frequency. Reduced damping with a fixed asymmetry also tends to increase the magnitude of drift over the entire frequency range. The results further suggest that, the suspension spring with hardening and softening characteristics in compression and extension, respectively, yields the sprung mass drift in the opposite direction. Suspension springs with asymmetric characteristics may thus reduce the magnitude of the sprung mass drift.

## ACKNOWLEDGEMENTS

The author is greatly indebted to his supervisors, Dr. Subhash Rakheja and Dr. A. K. W. Ahmed for their guidance, financial support, suggestions, continued encouragement and their tireless efforts during the completion of this dissertation.

The author wishes to express his thanks to CONCAVE personnel, who gave time during the work, particularly Arlene Zimmerman and Weimin Pu.

Thanks to CONCAVE students, who have assisted the author with the kind advices while under taking this work.

The support and encouragement of author's parents, his brothers, and lots of his friends, have been greatly appreciated.

Above all, the author would like to thank his wife, Sharmin for her love and patience to complete this investigation.

Finally, The author would like to give a special thank to Dr. A. K. W. Ahmed for his unforgettable efforts to complete this dissertation.

This thesis is dedicated to the author's wife, Sharmin.

## TABLE OF CONTENTS

## CHAPTER 3

## VEHICLE RIDE ANALYSIS



## CHAPTER 4

## INFLUENCE OF DAMPER PARAMETERS ON RIDE HEIGHT DRIFTING

## LIST OF FIGURES

## NOMENCLATURE

| Symbols | Description |
|---|---|
| $\alpha$ | Preset velocity of the damper |
| $\alpha_c$ | Preset velocity during compression |
| $\alpha_e$ | Preset velocity during extension |
| $a_e$ | Effective fluid flow |
| $a_E$ | Effective area of the spring |
| $\beta$ | Compressibility of the liquid |
| $C_1$ | Damping coefficient at low piston velocity in compression |
| $C_2$ | Damping coefficient at high piston velocity in compression |
| $C_3$ | Damping coefficient at low piston velocity in rebound |
| $C_4$ | Damping coefficient at high piston velocity in rebound |
| $C_d$ | Discharge coefficient of fluid |
| $C_{eq}$ | Linear suspension damping coefficient |
| $C_s$ | Suspension damping coefficient |
| $C_t$ | Tire damping coefficient |
| $\delta_t$ | Static tire deflection |
| $F_0$ | Vehicle load supported by the spring |
| $F_d$ | Damping force |
| $F_{dT}$ | Damping force at temperature T |
| $F_{dT_{ref}}$ | Damping force at reference temperature $T_{ref}$ |
| $f_s$ | Spring force |
| $g$ | Gravitational acceleration |
| $K_1$ | Linear stiffness coefficient |
| $K_2$ | Cubic stiffness coefficient |
| $K_{eq}$ | Linear suspension spring coefficient |
| $K_s$ | Suspension stiffness coefficient |
| $K_t$ | Tire stiffness coefficient |
| $m_s$ | Sprung mass |

| | |
|---|---|
| $m_u$ | Unsprung mass |
| $n$ | Polytropic constant |
| $P$ | Fluid Pressure inside the damper |
| $p$ | Asymmetry factor of the damper |
| $p_A$ | Absolute gas pressure |
| $V$ | Piston velocity of the damper |
| $V_0$ | Static volume of the air |
| $V_c$ | Chamber volume |
| $V_{OILTref}$ | Volume of oil at reference temperature $T_{ref}$ |
| $V_{OILT}$ | Volume of oil at temperature T |
| $z$ | Relative Displacement |
| $z_1$ | Relative displacement of the tire |
| $\dot{z}$ | Relative Velocity |
| $X_0$ | Road input |
| $X$ | Displacement |
| $X_s$ | Displacement of the sprung mass |
| $X_u$ | Displacement of the unsprung mass |
| $\delta_{st}$ | Static deflection of the spring |
| $\gamma$ | Damping reduction factor of the damper |
| $\gamma_c$ | Compression reduction factor of the damper |
| $\gamma_e$ | Expansion reduction factor of the damper |
| $\rho$ | Fluid Density |

# CHAPTER 1

# INTRODUCTION AND LITERATURE REVIEW

## 1.1 General

A vehicle suspension system comprises springs, shock absorbers, torsion bars, joints, arms, etc., and it cushions the vehicle over the road irregularities. A vehicle suspension is designed to maintain adequate tire-road contact to provide desirable directional control and stability, and ride quality of the vehicle. The performance objectives associated with vehicle ride, road holding and control often require conflicting suspension design parameters. Harder suspensions yield improved handling and directional performance, while adequate ride performance is achieved with lightly damped soft suspension. A lightly damped soft suspension, on the other hand, would require increased rattle space.

Owing to the conflicting performance requirements, the vehicle suspensions are invariably designed to achieve an acceptable compromise among the ride, handling and control performance. Such a design compromise is often achieved through highly nonlinear and asymmetric properties of suspension springs and dampers (Warner, 1996; Rengarajan, 1991; Oueslati, 1990; Ahmed, 2001; Rakheja and Ahmed, 1993; Harrison and Harmond, 1986). The suspension springs yield relatively low stiffness in the ride zone and progressively hardening characteristics under higher deflections. Air springs employed in commercial vehicles yield soft ride in the vicinity of the desired ride height and asymmetric hardening and softening properties in compression and rebound, respectively. Motion limiting bump stops are often incorporated to limit the suspension

travel within the available rattle space. Vehicle suspensions employ hydraulic dampers with either dual or multi-stage force-velocity characteristics. The dampers yield high viscous damping coefficient corresponding to low velocity and considerably lower damping coefficients at medium and high velocities to achieve a better compromise between vehicle ride and handling performance (Warner, 1996). The transition from high to low damping coefficients occurs at a preset velocity, and is achieved through pressure-sensitivity valving. Moreover, the hydraulic dampers are designed to yield asymmetric force-velocity characteristics in compression and rebound in order to achieve better road-handling performance and adequate control of wheel hop motions.

The nonlinear and asymmetric properties of vehicle suspension pose considerable challenges in modeling and analysis. Consequently, the majority of the reported studies on analysis of vehicle ride consider either linear or nonlinear but symmetric properties of the suspension dampers and springs. The vehicle suspension with asymmetric damping properties are known to exhibit 'packing down' behavior, which refers to downward shift of the dynamic equilibrium. Such findings have been limited to experimental observations alone either in the field or in the laboratory (Warner, 1996) while this phenomenon has been briefly analyzed in a recent study (Rajalingham and Rakheja, 2003). The experimental (field and laboratory) finding of the 'downward packing' behavior has been attributed to asymmetric damping properties of the suspension. Although the dynamic responses of the vehicle and suspensions have been extensively investigated through analysis of various analytical models of suspension components (Bastow, 1998; Thompson, 1970; Sharp and Crolla, 1987; Rengarajan, 1991; Wong, 1993; Crolla and Horton, 1991) the packing down properties of the suspensions have not

been addressed in the reported studies. This is perhaps attributed to the consideration of either linear or nonlinear but symmetric characteristics of the suspension components, and response analysis in terms of root mean square (rms) accelerations or acceleration spectra.

The 'packing down' or downward drift in the dynamic equilibrium is dependent upon force-displacement and force-velocity characteristics of the suspension, specially the degree of damping asymmetry. The time varying equilibrium of the vehicle may affect the vehicle ride and dynamic tire loads in a significant manner. In the absence of a ride height control, the packing down behavior would also affect the suspension travel, especially in the compression stroke. In this dissertation, the dynamic responses of the suspension components with symmetric and asymmetric force-displacement and force-velocity characteristics are investigated on the basis of a simple quarter-vehicle model. The suspension properties causing the 'packing down' behavior of the suspension are identified from the simulation results. The influences of excitation amplitudes and frequencies, and suspension parameters on the variations in the dynamic equilibrium are investigated and discussed in sufficient details.

## 1.2 Literature Review

The designs and analyses of vehicle suspension systems have been addressed in a large number of reported studies. These studies focus on various aspects of the performance objectives, such as ride, handling, directional control and variations in the dynamic wheel loads. These studies are also based upon either field or laboratory experimentation, and development and analysis of vehicle and suspension models. The models range from simple single-degree-of-freedom (DOF) models with linear

suspension properties to multi-degree-of-freedom models with nonlinear suspension properties. Moreover, the reported experimental and analytical studies focus on the conventional passive suspension, and on-off and continuously varying semi-active dampers, and active and adaptive vehicle suspension. In this chapter, the relevant published studies are reviewed and briefly discussed to gain knowledge on the modeling and analysis methodologies, and to formulate the scope of the dissertation research.

### 1.2.1 Vehicle Suspension

Vehicles invariably employ suspension systems with passive components, although considerable developments have been realized for both semi-active and active suspensions. A passive suspension system has the ability to store energy via a spring and to dissipate it via a damper. Its parameters are generally fixed, which are chosen to achieve a certain level of compromise between road holding, load carrying and comfort performances. Such suspensions mostly employ leaf, rubber, coil or air springs and hydraulic dampers. The performance characteristics of these suspension are limited due to fixed parameter design, and the fact that the components can temporarily store and dissipate energy at a constant rate, while the suspension forces are generated in response to local relative motions (Bastow, 1988; Youn and Hac, 1995).

Wide ranges of passive suspension designs are being used in light as well as heavy vehicles. These include the McPherson strut suspension, coil spring suspension, wishbone or double-wishbone, multilink suspension that are employed within the light vehicles front axle. Figure 1.1 illustrates the schematics of some of these suspensions (Bacon, 1988; Ellinger, 1989). Heavy vehicles often employ coupled or beam axle suspension comprising springs (leaf, coil, air or rubber) together with hydraulic dampers,

as shown in Figure 1.2 (Parkin, 1999). These passive suspension springs invariably exhibit progressively hardening force-deflection characteristics, while the hydraulic dampers yield nonlinear force-velocity characteristics that are mostly asymmetric in compression and rebound.

The active suspension systems may be classified on the basis of their control algorithm, hardware and power requirements, namely fully active and semi-active (Rajamoni and Hadrick, 1991). A fully active system consists of a force generating actuator, either hydraulic or pneumatic. A medium to high bandwidth servo-valve and controller is employed to modulate the flows to and from the actuator to generate the desired force in order to reduce the body movements caused by the uneven road roughness (Rengarajan, 1991; Tanaka and Kikushima, 1988; Horton and Crolla, 1986). Figure 1.3 illustrates a schematic of an actively controlled suspension force generator in conjunction with a quarter-vehicle model, feedback sensors and controller. Limited bandwidth active suspensions have been proposed to control the vehicle motions near the sprung mass (1-2 hz) and wheel-hop (9-12 hz) resonant frequencies. Based on the signals obtained by the sensors and the prescribed control strategy, the actuator force is modulated to achieve improved ride and handling and performance (Rengarajan, 1991). The controller is designed to track a desired target force, which is derived on the basis of a control law. Active suspension systems require significant amount of power and are thus considered to be feasible only for applications where increased cost and weight can offset the performance benefits.

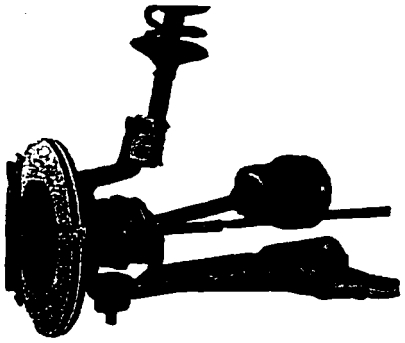

a) McPherson Strut

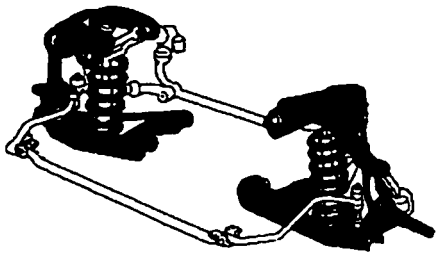

b) Coil Spring Type 1

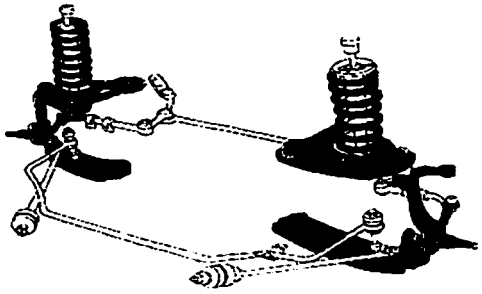

c) Coil Spring System Type 2

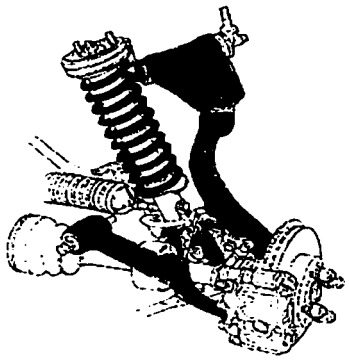

d) Double Wishbone Suspension

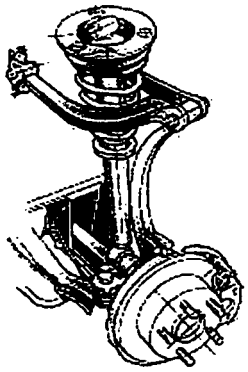

e) Multi link Suspension

Figure 1.1: Schematics of some of the front wheel suspension systems (Parkin, 1999)

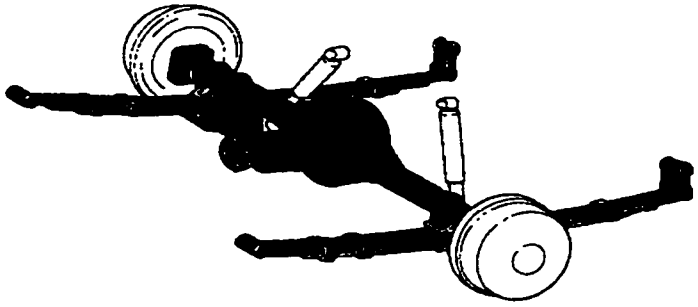

a) Solid Axle, Leaf Spring System

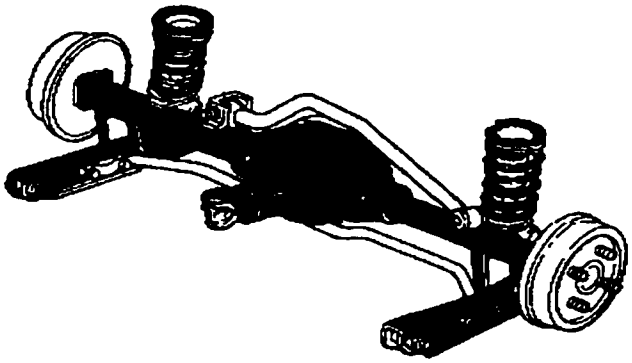

b) Solid Axle, Coil Spring System

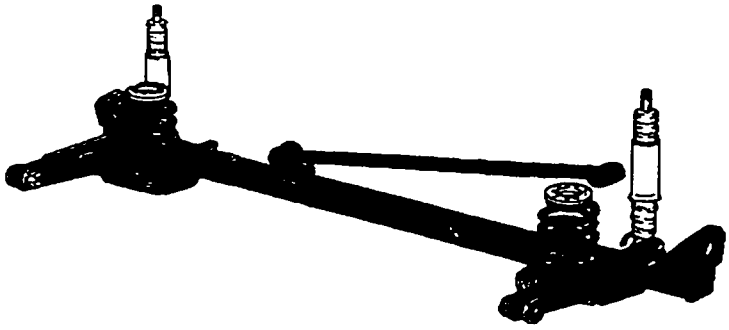

c) Beam Axle system

Figure 1.2: Schematic of some of the rear wheel suspension systems (Parkin, 1999)

A semi active suspension yields variable damping properties with only minimal power that is required to activate a valve. The concept of a Semi-active suspension was initially proposed by Karnopp and Crosby (1973). The variation in the damping force was achieved by modulating the fluid flows within the damper on the basis of. Figure 1.4 illustrates a schematic of a semi active suspension concept in conjunction with a quarter vehicle model. It has been suggested that a semi-active suspension, when properly tuned, can yield performance gains similar to that of a fully active suspension under certain circumstances (Wong, 1993). A number of control concepts have been proposed to achieve semi-actively controlled suspension damping on the basis of flow modulation within a hydraulic damper. The transient responses and limited bandwidth of semi-active suspension damper could limit their performance significantly. In recent years a number of semi-active damping concepts based upon electro (ER) and magneto-rheological (MR) fluids have been developed. These control concepts are based upon both 'on-off' and continuously varying suspension damping (Rakheja, 2002; Wu and Griffin, 1997; Oueslati and Sankar, 1994). The MR fluids offer high viscous damping corresponding to low velocity, attributed to the yield of the fluid, and low damping coefficient due to force limiting in the post-yield. Such properties are considered to be highly desirable for vehicle suspension. Moreover, the damping properties can be varied quite rapidly with the application of only small magnitude of current. The suspension performance potentials of MR dampers have been demonstrated in a few recent studies (Choi et al., 2001; Rakheja et al., 2002; Wu and Griffin, 1997). The MR dampers are being commercially applied in a number of suspension seats and vehicle suspension (Wu and Griffin, 1997).

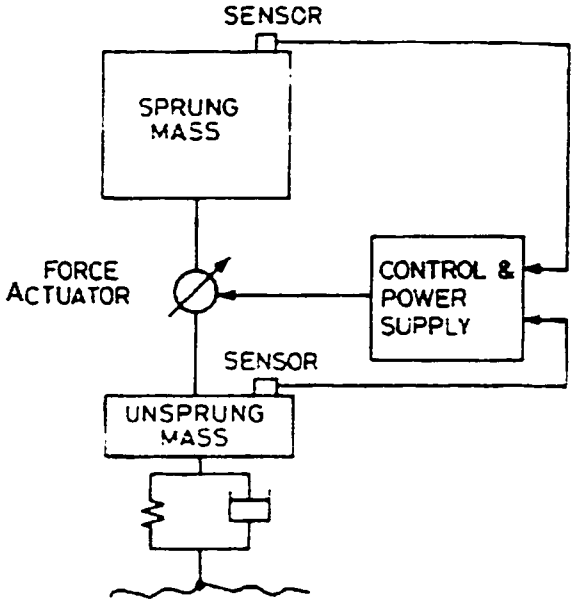


Figure 1.3: Schematic an active suspension concept (Wong, 1993)

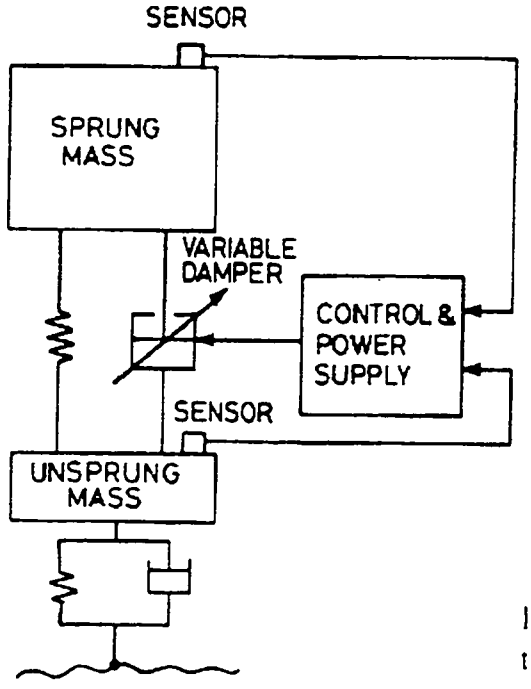


Figure 1.4: Concept of a semi-active suspension system (Wong, 1993)

### 1.2.2 Passive Suspension Dampers

Hydraulic suspension dampers dissipate energy through pressure drops across the orifices or valves. There are two basic designs in use today on the basis of their construction: the twin-tube design and the mono-tube design. Figure 1.5 (a) illustrates the schematic of a twin tube damper. The inner tube is known as the pressure or working cylinder, while the outer tube is known as the reserve tube. The upper mount of the damper connects to the vehicle frame, while the lower mount is connected to the unsprung mass, either directly or indirectly. The piston rod passes through a bushing and seal at the upper end of the pressure tube. The bushing keeps the rod in line with the pressure tube and allows the piston to move freely inside. The seal is usually a multi-lip design made of neoprene or silicone rubber. The outer or reserve tube is partly filled with hydraulic fluid and partly with an inert gas. The gas charge compensates for the flows due to area differential between the two sides of the piston and volume changes due to variations in the temperature. The flow from the pressure tube to the outer tube is controlled through a base valve located at the foot of the pressure tube. The damper piston consists of a series of bleed orifices and valves to permit the flows during compression and rebound.

The mono-tube shock absorber has been widely described in the literatures (Warner, 1996; Causemann, 2000; Gillespie, 1992). These are high-pressure gas shocks with only one tube, which is the pressure tube. The pressure tube houses two pistons; a dividing piston and a working piston, as shown in Figure 1.5 (b). The working piston and rod are very similar to the double tube design. This piston also comprises a number of orifices and valves. The mono-tube design, consisting of the floating piston within the

pressure tube, thus tends to yield considerably longer damper body for a specified rattle space. Alternative design, with an external accumulator containing the floating piston have also been realized to reduce the damper body length, as shown in Figure 1.5 (c) (Sharp and Crolla, 1987; Chaudhary, 1998; Joo, 1991).

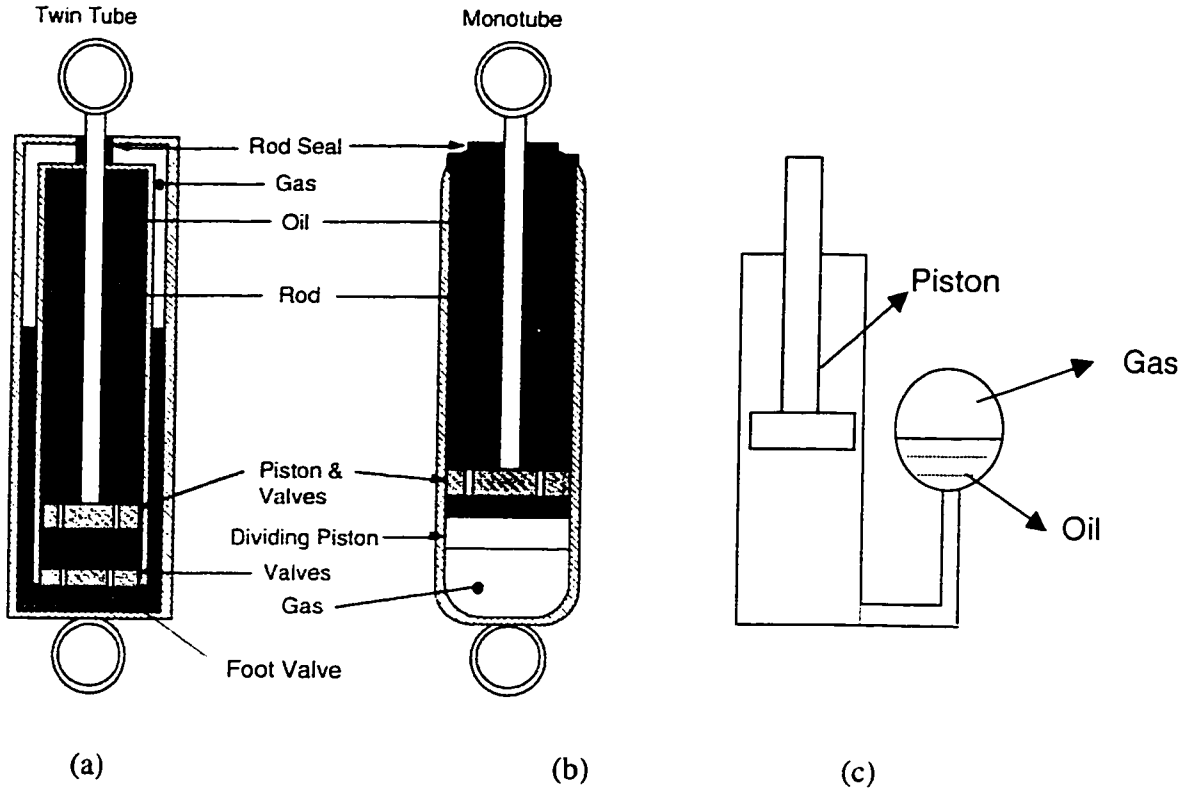


Figure 1.5: a) Twin-tube, b) Mono-tube shock absorbers (Gillespie, 1992) and c) Mono-tube damper with an external accumulator

A twin-tube design, when compared to a mono-tube, has a longer stroke capability and greater oil volume in a similarly sized unit. A twin-tube damper would therefore tend to provide smoother ride characteristics. The twin tube dampers, however, often cause foaming of oil due to entrapped gas under extreme velocities or body temperature condition (Causemann, 2000). The damping properties of such dampers may

thus deteriorate considerably under extreme operating condition. Mono tube dampers offer a number of advantages over the twin tube designs. The mono-tube design eliminates the potential for gas oil mixture and yields superior heat dissipation ability, which could be a critical factor for dampers applied in racing cars. The manufacturing cost of a mono-tube damper, however, is relatively higher due to precision requirements associated with high-pressure gas (Williams, 2000). Other disadvantages of the mono-tube designs include the susceptibility to side loads and dents. The variation of gas pressure caused by the increase in damper temperature tends to affect the ride height, and thus the aerodynamic losses, which could be a critical factor for racing vehicles (Warner, 1996).

#### 1.2.2.1 Damper Force Characteristics

The dynamic force developed by a hydraulic damper comprises these components attributed to seal friction, gas spring effect and hydraulic flows. The damping force, attributed to hydraulic flows, is mostly determined by the flows through the valves and orifices and pressure drop across the valves (hydraulic resistance). The dampers are invariably designed to yield variable hydraulic resistance as a function of magnitude and direction of the piston velocity (Snowdon, 1968; Bert, 1973). Low piston velocity yields lower flow rates across the flow paths, lower pressure drop and thus the lower magnitude of the force. For a given flow path, an increase in piston velocity causes higher flows and pressure drop and thus higher damping force. The multi-stage valving employed in the dampers, however, yield highly complex damping force and velocity characteristics.

Through extensive laboratory measurements and simulations, Warner (1996) described the effect of piston speed on the damper characteristics. The hydraulic resistance in the damper is controlled using various combinations of valving mechanisms, which are effective over different speed ranges. On the basis of the measured force-velocity characteristics of typical hydraulic dampers, the velocity ranges are termed as 'low', 'mid' and 'high'. Figure 1.6 illustrates the typical force-velocity characteristics over the three speed ranges. The force-velocity characteristic curve reveals high damping coefficient (rate of change of the peak force with respect to the peak velocity) corresponding to the low piston velocity, irrespective of the direction of the piston velocity. While the flow rate across the piston is relatively small at low speeds, high flow resistance is achieved through closed piston valves, thereby permitting the flows only through small size. Figure 1.7 illustrates the design of a damper piston comprising deflection disc valves and bleed orifices. The hydraulic fluid displaced due to piston motion will flow from the high-pressure side of the piston to the low-pressure side. During the compression stroke the low-pressure side of the piston is normally the side with the rod. The pressure differential developed across the piston is strongly dependent upon the piston velocity relative to the cylinder.

As shown in the Figure 1.7, the fluid flows at low speeds occur through two paths: *(i)* through the bleed orifice(s); and *(ii)* leakage flows through the piston/wall clearance. The deflection discs remain closed due to relatively low-pressure differential developed at low velocity. While the leakage flows can affect the damping characteristics considerably, the low speed damping characteristics are mostly tuned through selection of number and size of the bleed orifices.

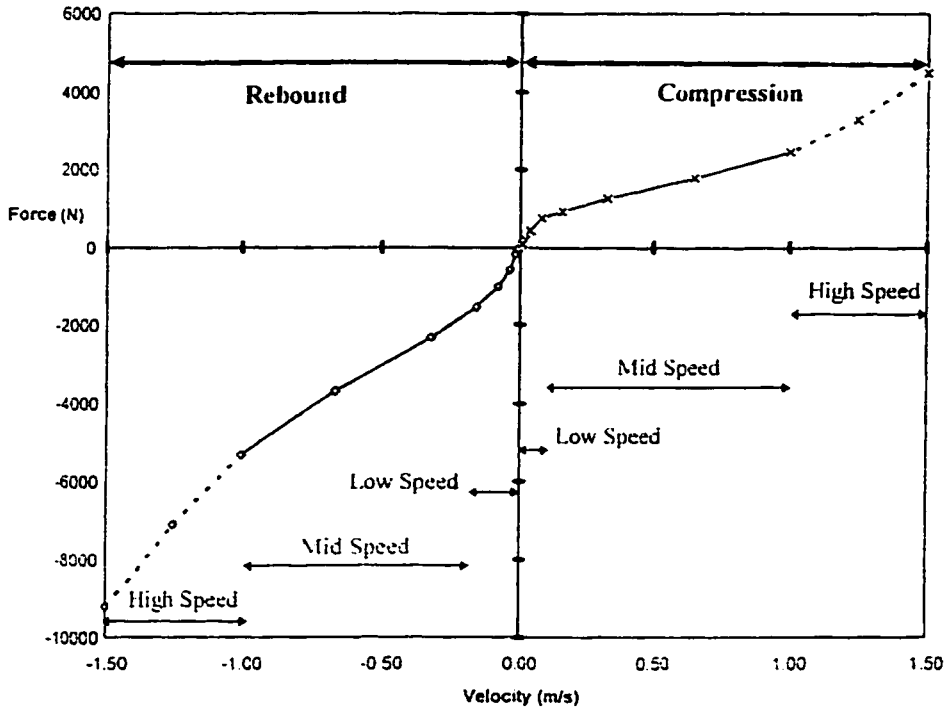


Figure 1.6: Force-velocity characteristics of a hydraulic damper (Warner, 1996)

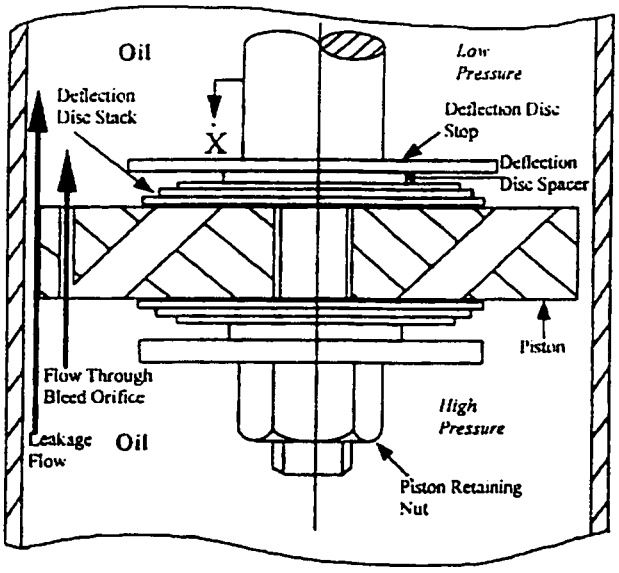


Fig 1.7: Schematic of damper compression mechanism for low velocity (Warner, 1996)

An increase in the piston speed to the mid-speed range causes flows through three paths; (i) leakage flows; (ii) bleed orifice; and (iii) the deflection disc valves. While the flows through the first two are similar to those described for the low speed, the flows through the valve occur due to deflections of the discs caused by high pressure differential, as shown in Figure 1.8. It is essential to note that the valve openings in compression and rebound differ due to different force-deflection characteristics of the deflection disc stack. The mid-speed damping coefficients corresponding to compression and rebound are thus considerably different, as evident from Figure 1.7. The flow areas for leakage and bleed flows are relatively small in comparison with that for the deflection disc stack. The flows through the deflection disc stack, thus, dominate the mid speed damping characteristics. A further increase in the piston velocity to the 'high speed' range yields higher deflection of the discs leading to higher flow path and thus considerably lower damping coefficient. The high piston speed causes high fluid pressure, which in case of twin-tube design could encourages foaming of the oil that yields significant loss of damping. The relative high pressure of the oil-gas mixture in the annular region also causes large pressure drop across the foot-valve.

#### 1.2.2.2 Valving mechanism in dampers

The hydraulic dampers invariably offer variable hydraulic resistance through multiple pressure relief valves. Different valves are employed in the compression and rebound flow paths, which result in asymmetric damping characteristics in compression and rebound (Warner, 1996). Apart from the fixed leakage flow path, the majority of the damper designs, employ two parallel flow paths, (i) a constant area flow path (bleed), which permits flows over; the entire range of speeds; and (ii) a variable flow path, whose

flow area is controlled by the pressure differential across the piston. Desirable damping characteristics are realized through a combination of both flow paths. The flows through a simple orifice valve (bleed valve) generates a damping force which grows with the square of the velocity, attributed to turbulent flows through the orifice (Gillespie, 1992), as shown in Figure 1.9. When designed to provide adequate damping to control body motions at low velocities, simple orifice control yields very high damping at the higher velocities leading to poor vibration attenuations and axle hop motions. The variable flow path is often achieved from the "blow-off' valve or the deflection discs (Figure 1.7 and 1.8) the flow passage is blocked by a spring-loaded valve or disc stack prevent the flows until a desired pressure is reached. As the pressure differential approaches or exceeds the preset value, the flows yield damping force as shown in curve B of Figure 1.9. By combining the orifice and the blow-off controls, a typical shock absorber would yield damping behavior such as that shown in curve C.

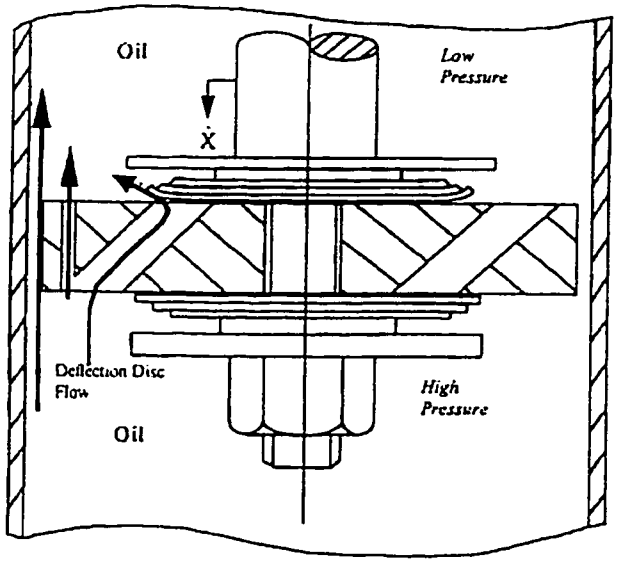


Figure 1.8: Schematic of damper compression mechanism for mid speed (Warner, 1996)

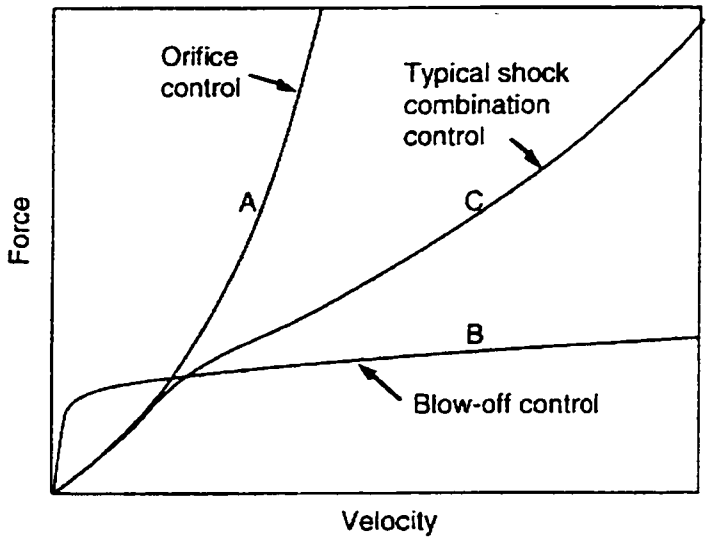


Figure 1.9: Force-velocity properties of shock absorber valving (Gillespie, 1992)

### 1.2.2.3 Suspension Damper Modeling

Although considerable developments in suspension system have been realized during the past few decades, the majority of the studies in vehicle dynamics consider damping through different forms of simplified force-velocity characteristics. The models are therefore limited to either linear or symmetric characteristics of the damper; such models cannot be considered valid for investigating the influence of damping asymmetry on the vehicle response, specially the 'packing down' behavior of the suspensions.

The force-velocity characteristics of a hydraulic damper are complex functions of various design and operating parameters. The total force developed by a damper is dependent upon the fluid flows through the piston and thus the orifice geometry and the valve characteristics, flows through the base valve, gas spring effect, seal friction, fluid compressibility and operating temperature. A large number of mathematical models have

been proposed to characterize the damping force-velocity characteristics of shock absorbers. A vast majority of these models, however, have been based upon the laboratory measured data and regression functions. The models are thus considerable as semi empirical models involving coefficients that are identified from the measured date. These models are thus considered suited for a specific damper and cannot be applied generally.

Owing to complexities associated with analytical models of the hydraulic dampers, the damper characteristics are mostly involved through laboratory tests. These tests involve stroking of the damper mounted between a fixed inertial frame and a motion generator under a specified displacement or velocity magnitude and frequency. The damper is often characterized by its means peak force- mean peak velocity characteristics, hysteresis and force- deflection properties as a function of the operating temperature.

Segel and Lang (1981) have shown that the characteristics of a damper for stroking frequencies up to 10 Hz are understandable in terms of simple orifice and leakage flow models and fluid compressibility. Although dampers are normally characterized by measured peak forces obtained during stroking tests, the dynamic force/velocity relationships typically exhibit hysteresis loops, as shown in Figure 1.10. The force rising faster than velocity is apparent, as also is a marked asymmetry between bump and rebound forces for low speed.

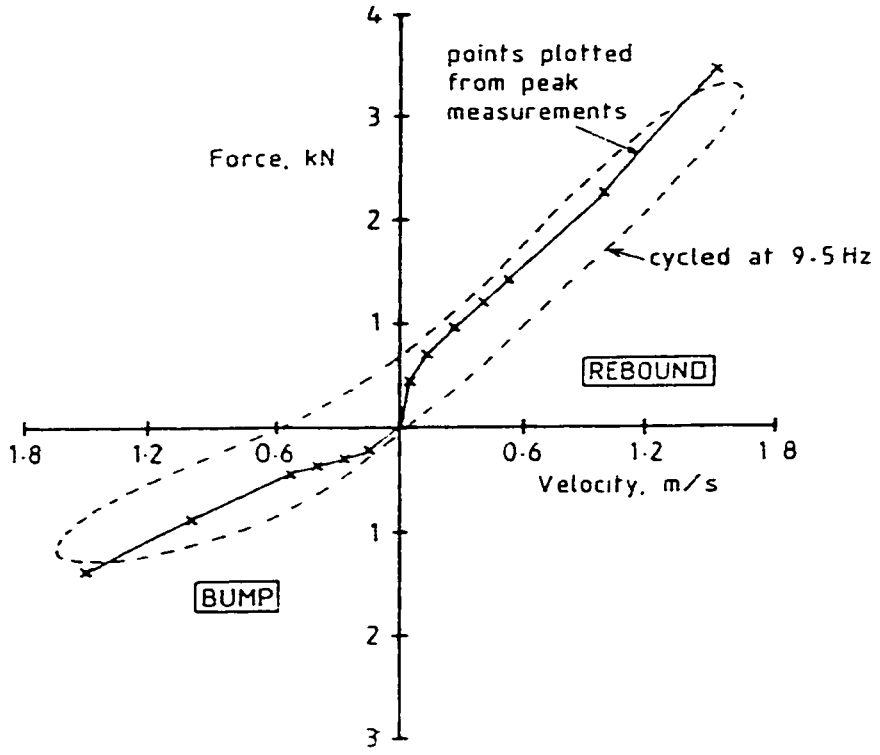


Figure 1.10: Force-velocity characteristics of a typical hydraulic damper (Sharp and Crolla, 1987 )

Thompson (1970) investigated the influence of such damping asymmetry by means of analog simulation of a quarter car model in terms of sprung mass responses to positive and negative step inputs of two different magnitudes. The study concluded that symmetric damping properties are desirable for maintaining adequate contact between the tire and the road under small magnitude excitations. The responses under sufficiently large disturbances leading to loss of contact between tire and ground, suggested that responses the performance under positive steps could be improved by providing greater damping in rebound, which tended to deteriorates response under negative steps. Warner (1996) analyzed the damping behavior of both an integrated and remote-reservoir mono-tube dampers, specially the effects of temperature and fluid compressibility. On the basis

of measured data the study proposed the component models to yield the total damper model for incompressible and compressible flows using series of regression functions. The model concluded that the component forces attributed to hydraulic flows, gas spring and seal friction are strongly dependent upon the operating temperature.

#### 1.2.2.4 Damping Models Applied to Vehicle Models

With different resistance combinations attribute to bleed orifices and valving, it is possible to achieve characteristics with digressive, linear and progressive segments, as evident in Figure 1.6 (Causemann, 2000). A mechanical or servo-hydraulic test machine is frequently used to measure these damper characteristics. At constant speed (rpm), this machine produces various strokes in rebound and compression direction, and subsequently different damper compression and rebound speeds. Figure 1.11 illustrates the force-deflection and force-velocity characteristics typical for nonlinear asymmetric (digressive, A and progressive B) In the view of the complexities associated with characterization and modeling of such phenomena and valving, the force-velocity characteristics are widely used to study the role of damping design on the vehicle responses. The characterization in terms of force-velocity offers the advantage that the association between damping force and compression and rebound velocity can be assessed in a convenient manner. Such formulations, however, yield only maximum values of the damping forces in rebound and compression direction at various strokes or compression and rebound rates. The ride dynamics models of various vehicles reported in the literature have considered different forms of damping models. These include the simple linear viscous model considered adequate for preliminary analyses, and piece-wise linear models.

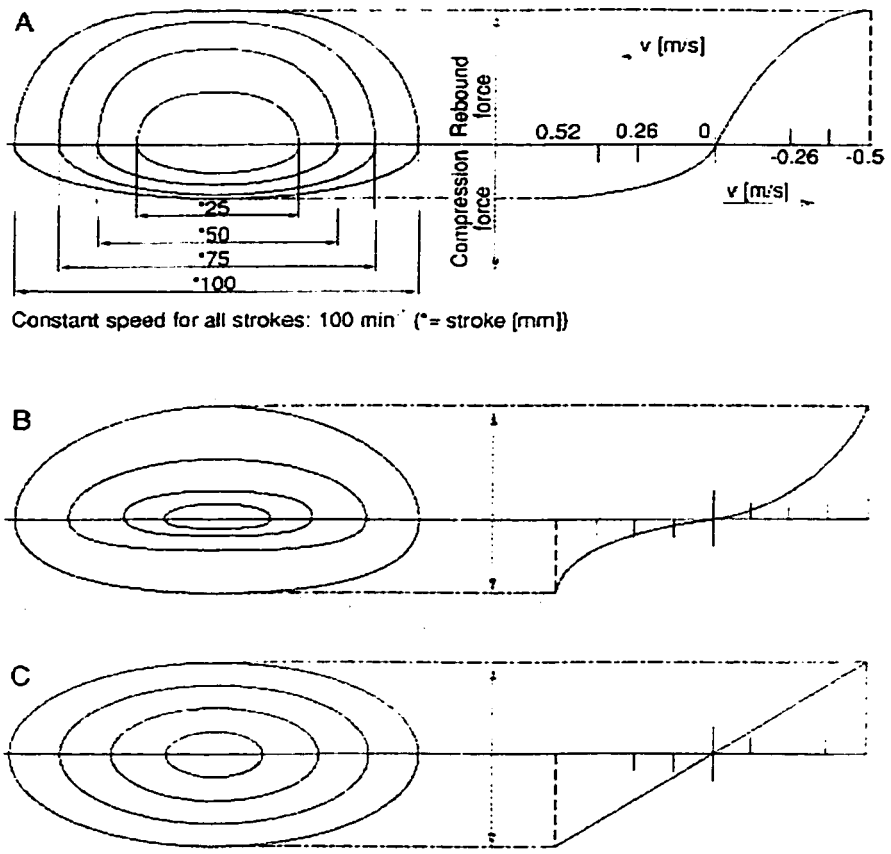


Figure 1.11: Damping characteristics for A. Digressive, B. Progressive, C. Linear (Causemann, 2000)

Rajalingham and Rakheja (2003) investigated the influence of damping asymmetry on the displacement response of the sprung mass of a quarter-car model. The asymmetric damping mass considered as a combination of linear viscous dampers with different damping coefficients in compression and rebound, as shown in Figure 1.12. The solution if differential equation of motion for the model revealed downward shifting of the sprung mass depending upon the degree of damping asymmetry. On the basis of measured means force-velocity data acquired from a large number of suspension dampers, generalized piecewise linear models of suspension dampers have been proposed to characterize both the symmetric and asymmetric force-velocity characteristics, as

shown in Figure 1.13 and 1.14. Such models consider negligible contributions due to damping hysteresis, fluid compressibility and operating temperature, but provide an effective damping model to analyze the vehicle responses under variable damping. The symmetric force-velocity model is derived on the basis of mean damping coefficients, while neglecting the contributions due to asymmetry (Rakheja and Ahmed, 1993). The symmetric model therefore cannot be applied to the packing down behavior of the sprung mass. The piece-wise linear representation of the asymmetric force-velocity characteristics (Figure 1.12) have been applied to study the ride dynamic behavior of an urban bus, dynamic tire loads due to heavy vehicle and the validity of the energy similarity principle. These studies consider either acceleration or rms displacement responses, thereby, ignoring the 'packing down' phenomenon associated with asymmetric damping.

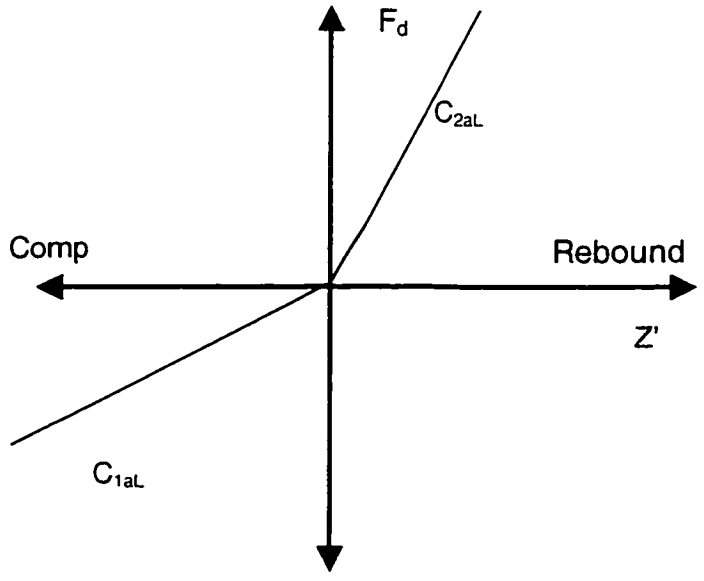


Figure 1.12: Single-stage Asymmetric Damper

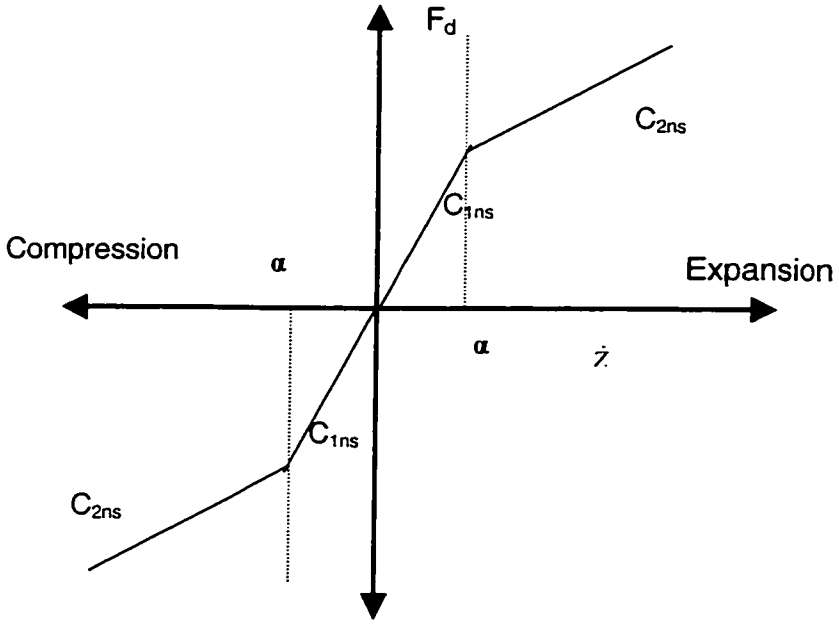


Figure 1.13: Two-Stage Symmetric

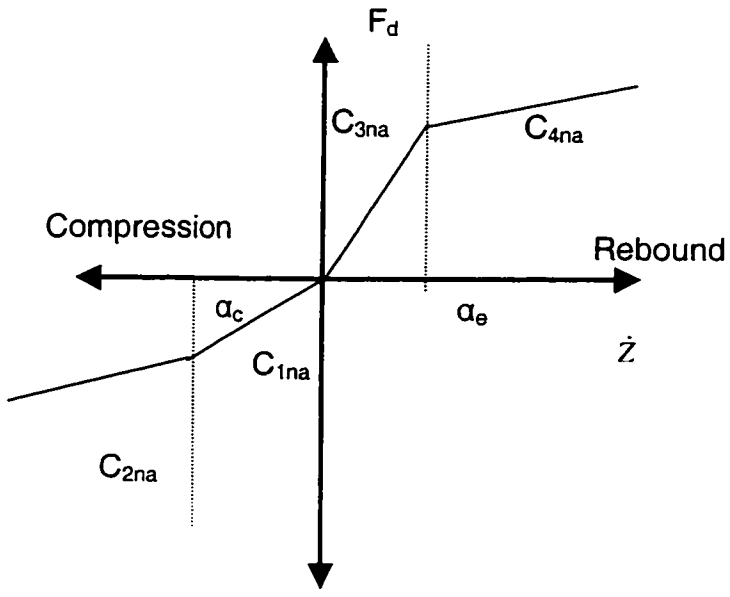


Figure 1.14: Two-Stage Asymmetric

### 1.2.3 Suspension Springs Characteristics

Spring elements used for automobile suspension, in increasing order of their ability to store elastic energy per unit of weight, are leaf springs, coil springs, torsion bars, rubber-in-shear devices, and air springs. An important factor in spring selection is the relationship between the load and the deflection known as the spring rate. A coil or a leaf spring retains a substantially constant rate within its operating range of load (Gillespie, 1992). The torsion bar, a long spring-steel element with one end held rigidly to the frame and the other twisted by a crank connected to the axle, provides an increasing spring rate. A soft-spring suspension provides a comfortable ride on a relatively smooth road, on the other hand, the springs must be stiff enough to limit large deflections at any corresponding to resonant oscillation within the permissible rattle space. Road-handling characteristics also suffer because of what is known as sway or roll, lateral deflection of the car body that results from centrifugal force acting outward on turns. The softer the suspension, the more the outer springs are compressed and the inner springs expanded. Front-end "dive" under brake action is more noticeable with soft front springs.

The sprung mass of a vehicle is mostly supported by the spring, are often designed to yield progressively hardening properties, which are characterized by a cubical force-deflection relationship. Figure 1.15 illustrates the force-deflection characteristics of a progressively hardening cubical spring. The position of the static equilibrium of the sprung mass depends upon spring rate and the static load. As the function of a spring is to store varying amounts of energy, the average of those varying amounts must be approximately the sprung weight of the car multiplied by half the static

deflection of its springs (Bastow, 1998). This approximation arises principally because the geometry of the suspension system is unlikely to provide a constant spring rate at the wheel.

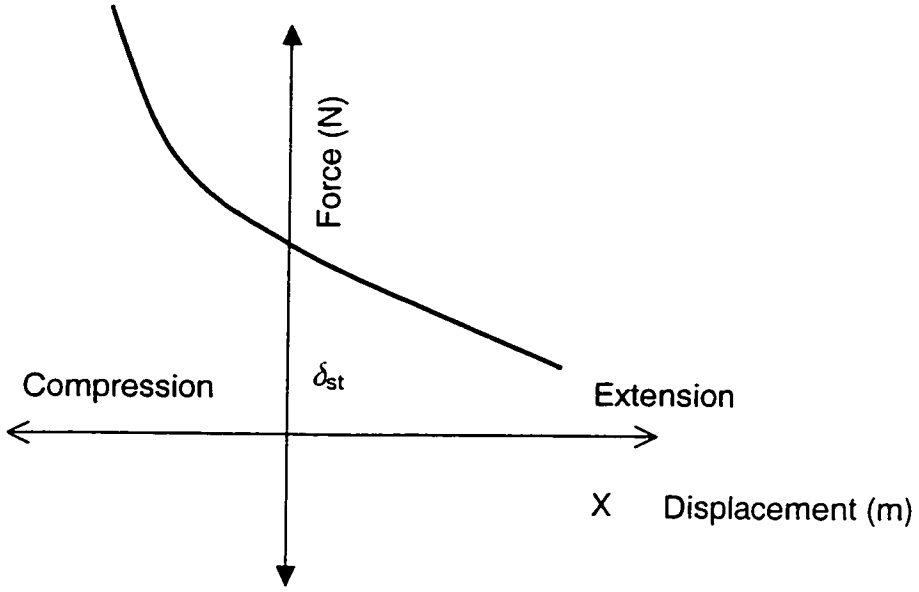


Figure 1.15: Static equilibrium position of a gas spring

### 1.2.4 Vehicle Models

A vehicle represents a complex vibration system which can be modeled from one degrees of freedom to a complex three-dimensional model with hundreds of D.O.F. Different concepts in suspension damping, however, have been mostly evaluated using a quarter car model comprising spring and unsprung masses constrained to move along the vertical axis, as shown in Figure 1.16 (Ahmed, 2001). These models are widely used for studies of different suspension concepts, and vibration isolation and dynamic travel properties of the suspension.

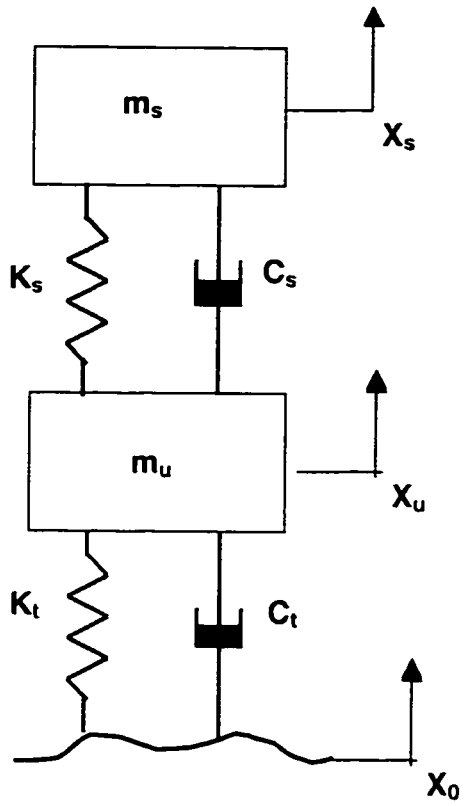


Figure 1.16: A Quarter Car Models with Two-degrees of freedom system

A quarter vehicle model may be formulated as 1 to 3 degrees of freedom system (Michael and Dongsuck, 1995; Genta, 1997), The concepts in suspension design and the role of various asymmetric/symmetric and linear/nonlinear properties of suspension components, however, can be effectively investigated using a Two-DOF model. This model contains no representation of the geometric effects, and longitudinal and lateral dynamics. Important features of a quarter vehicle model are that it includes a proper representation of the problem of controlling the wheel load variations and the suspension system forces, which are properly applied between the wheel mass and the body mass (Sharp and Crolla, 1987).

### 1.2.5 Drifting in the Suspension System

Although extensive developments in suspension system have been studied during the past few decades through repetitive field trials, the effective analytical models of the modern suspension systems, specially the shock absorber, do not yet exist. The analytical models developed so far have not been extensively applied or proven for the analysis of the 'ride height drifting' phenomenon of a suspension system, which has been invariably attributed to the asymmetric properties. Static riding height, often measured from the rocker panel to the ground (Figure 1.17) is considered to be fixed for vehicles where mass variations are relatively small. Ride height drifting is a response of the suspension system generated due to asymmetry of the suspension dampers. This phenomenon of drifting in the ride height researchers often called ' the packing down of the suspension' (Emery, 2002, Warner, 1996) and also 'mean line shifting of the alternating amplitude response' (Rajalingham and Rakheja, 2003). Since majority of the studies are based upon linear or symmetric dampers (Rengarajan, 1991; Oueslati, 1990; Haque et al., 1995, Rakheja and Ahmed, 1993, 1994) the phenomenon associated within ride height drifting could not be investigated.

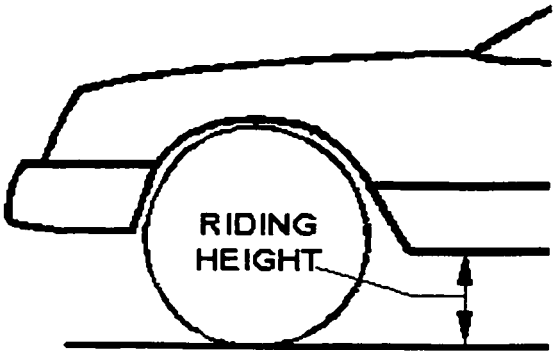


Figure 1.17: Ride height

Furthermore, another recent study (Emery, 2002) has been undergone the characteristics of asymmetry of dampers and cause of 'packing down' of the suspension. The experimental study showed that stiffer rebound can induce 'Packing down' of the suspension. Consequently it may cause considerably less suspension movement and impose higher demands on the tire. Warner (1996) has conducted laboratory experiments to demonstrate that the ride height is significantly influenced by the excitation frequency. The study reported that the average ride height is decreased significantly with the increase in frequency of excitation as shown in Figure 1.18. The average ride height of the sprung mass primarily depends upon the compression to rebound velocity response, and increases with the increase in compression and/or decrease in rebound velocity changes. Asymmetries in low-speed compression or rebound damping causes nearly consistent changes in the ride height in the entire frequency range, while the changes in the mid speed compression or rebound damping result in considerable variations in the ride height at higher damper velocities. Furthermore, an increase in the mid speed compression damping and/or a decrease in the mid speed rebound damping reduces the magnitude of variations in the average ride height with frequency. Variations in high rebound damping yield considerably larger variations in ride height than those caused by proportional changes in the compression damping.

Rajalingham and Rakheja (2003) investigated that the influence of a conceptual single-stage asymmetric damping on dynamic response of the sprung mass of a quarter-car model. Through numerical simulation, the study showed that the damper non-linearity introduces a downward shifting in the mean position of the sprung mass in addition to the vibratory response. However, the response of the unsprung mass doesn't exhibit such a

mean position shift. The mean position shift in the sprung mass is due to the mean compression in the shock absorber spring caused by the force imbalance in the suspension damper during vibrations.

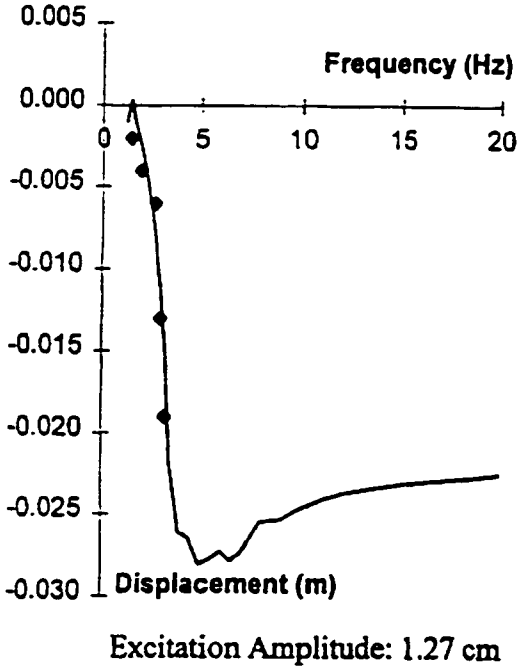


Figure 1.18: Average ride height response characteristics of the quarter car model (Warner, 1996)

It is very imperative to keep the ride height variations within predetermined limits in order to (i) maintain headlight dip angle, (ii) provide adequate suspension stroke, (iii) provide an appropriate ground clearance, (iv) maximize the performance of the car's aerodynamics; while downward drift may be beneficial in view of the aerodynamic drag in racing cars, the build up of pressure under the vehicle body may increase the lift component, which be adversely affected due to reduced suspension travel (Scibor-Rylski, 1975).

## 1.3 Objective and Scope of the present research work

From the literature review, it is evident that nonlinear asymmetric dampers are commonly utilized by road vehicles for enhanced ride and handling performances. Furthermore, system with such damper is known to exhibit ride height drift phenomenon also known as 'packing down'. This behavior causes the vehicle to oscillate about a new equilibrium which is lower than the static equilibrium. This behavior has been reported in only a few studies as the basis of the field or experimental observations. Moreover, nonlinear progressively hardening springs employed in vehicle suspension may further affect the vehicle ride height. This nonlinear property of the spring may infact counter the downward drifting effect of the asymmetric damper. The drifting phenomenon associated with the asymmetric damper, however, has not been adequately investigated.

From the review of published studies, it is apparent that a majority of studies on the suspension systems and vehicle ride dynamics employs either linear or equivalent linear suspension components. While many studies have considered the nonlinear stiffness and damping components, the asymmetry in their force-deflection and force-velocity characteristics is mostly ignored. The phenomenon of ride height shift of the suspension has been documented in only a few studies on the basis of either laboratory or field tests. These are mostly the websites maintained by racing vehicle professionals. Only minimal efforts have been made to systematically investigate the influence of the suspension asymmetry on the overall vehicle response, specifically the ride height. The scope of this dissertation research is thus formulated to investigate the fundamental response behavior of the stiffness and damping asymmetry on the ride height response of a vehicle using a simple quarter vehicle model.

The objective of this work is to demonstrate the phenomenon of ride height drift utilizing a quarter vehicle model. The ride height responses of a nonlinear and asymmetric damper along with a linear and nonlinear spring are investigated. A parametric sensitivity analysis is conducted to study the effects of suspension nonlinearity.

The specific objectives of the thesis are thus as follows:

1. To characterize the nonlinear asymmetric behavior of the suspension damping and stiffness components, and formulate associated models.
2. To formulate a quarter-vehicle model incorporating asymmetric suspension components to study their response behavior.
3. Analyze the vehicle model to study the phenomenon of ride height drift.
4. To perform a parametric sensitivity analysis to identify the role of suspension parameters on the sprung and unsprung mass drift.
5. To establish a relationship between the ride height drift and the suspension component properties.

## 1.4 Organization of the Thesis

In chapter 2, a suspension system with a nonlinear spring and damper has been analytically modeled. A quarter-vehicle model with two degrees of freedom dynamic system has been taken into consideration for this purpose. Since the drifting is due to relative shifting of the sprung and unsprung masses in vertical direction from its mean position; a quarter vehicle model is considered to be sufficient for this investigation. A

conventional nonlinear damper and an air spring that exhibits cubical force-displacement are modeled analytically.

In chapter 3, the ride dynamics of the vehicle model is investigated in terms of responses of the sprung and unsprung masses amplitudes in time domain. The responses are analyzed to examine the drifting effects of different component characteristics in the wheel hop frequency (9.5 Hz).

In chapter 4, a comprehensive parametric study is performed to establish the influence of variation in characteristics of linear, symmetric and asymmetric suspension components on the ride height responses in the wide range of frequency. A normalized drift is also identified to obtain a relationship between drift and other suspension component parameters.

The major conclusions and the needs for further studies are summarized in chapter 5.

# CHAPTER 2

# ANALYTICAL MODELING OF SUSPENSION SYSTEM COMPONENTS

## 2.1 General

The total dynamic force developed by a hydraulic damper is the resultant of the hydraulic, gas spring and frictional forces, which are complex functions of the fluid compressibility, valving, seal friction, velocity, acceleration, temperature, etc. (Su, 1990; Warner, 1996). The suspension dampers are therefore mostly characterized through laboratory tests performed under controlled conditions and a number of analytical models have also been developed. These models may be grouped in three categories on the basis of the modeling approach. The first group of models is derived on the basis of the physical system involving fluid flows through orifices (Ikenaga and Lewis, 1991; Hrovat, 1997). These models, however, do not characterize the asymmetric nature of the damping and valve dynamics, while the seal friction is considered as an ideal friction force. The second group of models is based upon regression analysis of the measured data and involves identification of several coefficients (Warner, 1996; Segel and Lang, 1981; Thompson, 1970). These models can effectively characterize the effects of fluid compressibility, valve dynamics, asymmetry, and temperature. The models, however, are damper specific and thus could not be considered for general applications. The third group of models describes the peak force-peak velocity characteristics in a piecewise manner to study the role of damping characteristics on the vehicle response in a convenient manner (Rajalingham and Rakheja, 2003; Rengarajan, 1991; Oueslati, 1990; Rakheja and Ahmed, 1993, 1994). Such models are also damper-specific and can

effectively characterize the asymmetric force-velocity nature of the damping attributed to the valving. Although a number of models could characterize the asymmetric nature of the damping, only a few studies have explored the effects of damping asymmetry on the vehicle ride response. Through laboratory experiments and simulations, Warner (1996) concluded that asymmetric damping strongly affects the vehicle ride height response that could deteriorate the lap-time performance of racing cars. Apart from the Warner's study, the effects of asymmetric damping have been mostly observed in laboratory situations and the resulting ride height response is often referred to as the 'packing down' behavior of the suspension (Emery, 2002). This 'packing down' behavior would also influence the suspension static equilibrium and thus the suspension spring forces, which have not been explored.

In this chapter, the symmetric as well as asymmetric restoring and damping forces due to suspension components are characterized using simplified models on the basis of the mean measured characteristics. The analytical damping and spring models incorporating their asymmetric and nonlinear properties are also discussed.

## 2.2 Characteristics of a Hydraulic Damper

The dynamic force developed by a hydraulic vehicle suspension damper comprises the following major components: (i) hydraulic force attributed to pressure drop across the flow paths, such as orifices and valves; (ii) restoring force due to gas spring; and (iii) seal friction force. The magnitudes of the two latter components are considerably small when compared to that of the hydraulic force. The suspension dampers are therefore mostly characterized by their hydraulic force components (Sharp and Crolla,

1987; Oueslati, 1990), which are strongly nonlinear function of the velocity. Figure 2.1 illustrates a typical peak force-peak velocity behavior of a hydraulic damper measured under sinusoidal piston velocity (Warner, 1996). The force-velocity curve exhibits hysteretic behavior attributed to fluid compressibility and inertial effects. The contributions due to such factors are often considered to be small such that the damping characteristics are represented by the mean force-velocity curve, as indicated by the bold line in Figure 2.1 (Segel and Lang, 1981; Thompson, 1970; Warner, 1996).

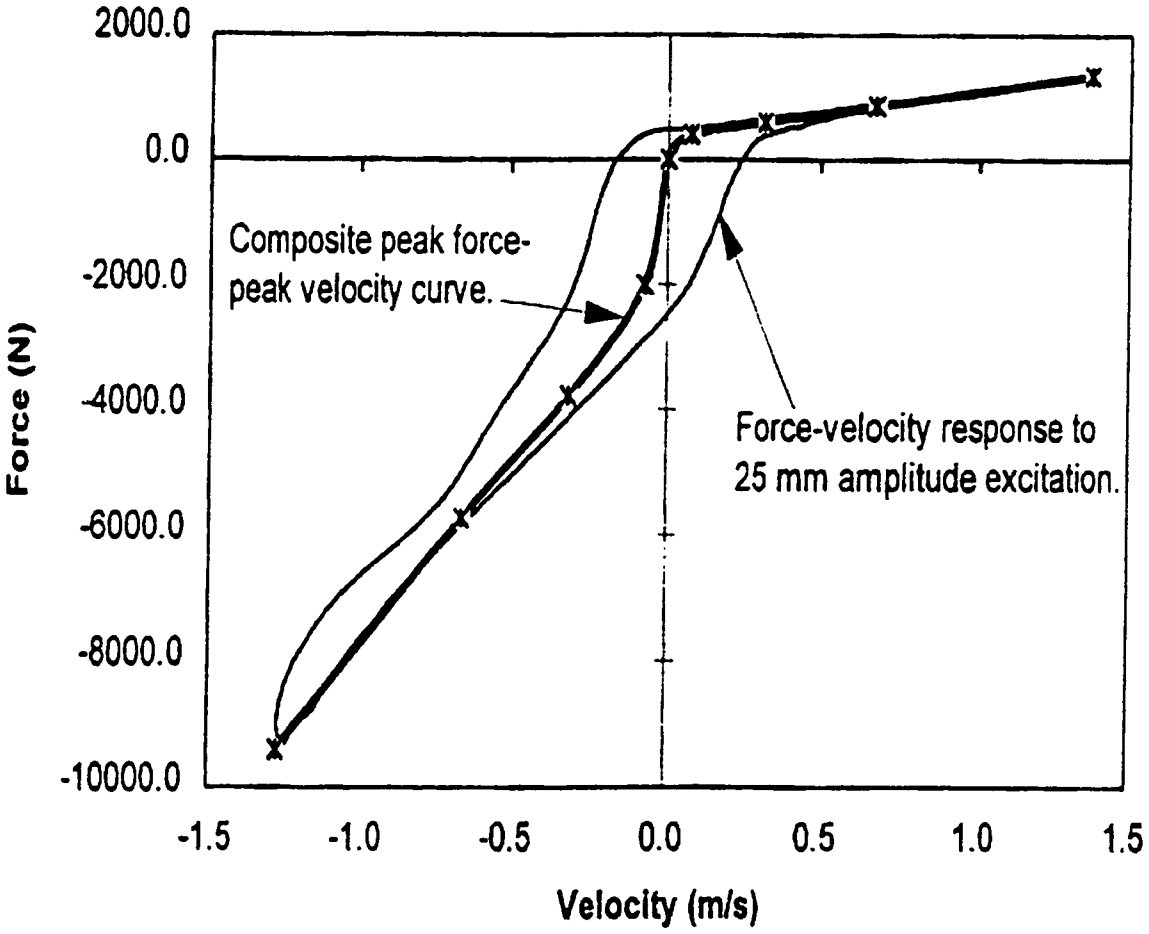


Figure 2.1: Peak force-peak velocity characteristics of a hydraulic damper (Warner, 1996)

The mean force-velocity characteristics suggest that the damper generates highly asymmetric force in compression (v> 0) and rebound (v< 0). The damping force in rebound is nearly 5 times larger than that in compression. The asymmetry in the compression and rebound damping forces is further evident from the force-deflection curves obtained under sinusoidal excitations of varying velocity amplitudes, as shown in Figure 2.2. Moreover, the damping coefficient (the rate of change of force with respect to velocity) corresponding to low velocities tends to be considerably larger than at a higher velocity. The variations in damping coefficient as function of velocity are attained through different forms of valving, such as blow-off valves (Warner, 1989; 1996).

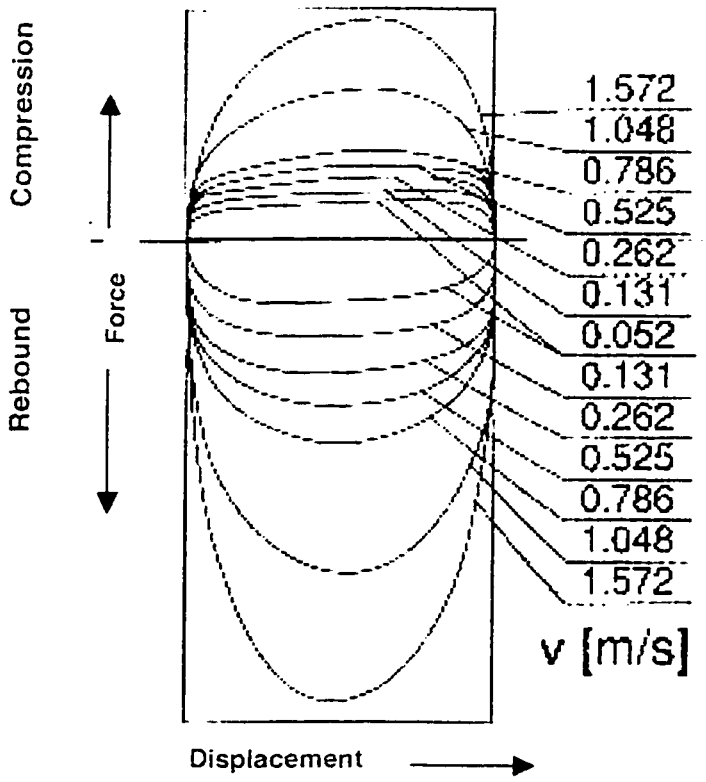


Figure 2.2: Force-velocity characteristics of a hydraulic damper. (Causemann, 2000 )

Dampers invariably employ valving in the form of one or more orifices and pressure relief valves. The flow through the valves may occur under either laminar or turbulent flow conditions (Hanly, 1967; Wahi, 1967; Warner, 1996). Based on the assumption of the turbulent flow, the characteristic equation for flow rate (Q) through an orifice is given by:

$$Q = C_d . A_e \sqrt{(\frac{2.\Delta P}{\rho})} \tag{2.1}$$

Where $\Delta P$ is the pressure drop across the valve or the orifice and $A_e$ is the effective flow area, $\rho$ is the density of the fluid and $C_d$ is the discharge coefficient. $C_d$ is a complex function of fluid pressure, orifice geometry or valve design. A previous study (Lang, 1985) investigated an inclusive damper model and concluded that the flow rate prediction cannot be made with an accuracy of better than 10%, while the experimental study demonstrated the strong dependence of discharge coefficient on the Reynolds number, geometric properties of the parts, and other design factors. As a result the modeling of damper valves is considered to be quite complex.

Furthermore, a hydraulic damper employs different configurations of valving resulting in asymmetric damping characteristics in compression and rebound. The majority of the damper designs, however, employ two parallel flow path, where one of them remains functional at all times and is referred to as the 'bleed flow path'. The flow through this path alone yields rapid change in the damping force and thus the high damping coefficient at low velocities, as shown in Figure 2.1. The second path becomes active when the pressure differential approaches a preset value. The effective flow area

thus increases at a higher velocity resulting in relatively lower damping coefficient (Figure 2.1).

Furthermore, consideration of compressibility of oil inside the damper results in greater complexity in damper characteristics. The thermal expansion and contraction of the cylinder walls and damper components may also cause variations in the chamber pressures and the fluid volume. This effect, although being similar to the fluid compressibility, is of second order (Warner, 1996). The combined effect of the fluid compressibility and compression/extension of the cylinder, however, can be effectively incorporated using a coefficient modified to include oil and cylinder wall effects (Lang, 1985). The fluid compressibility can be expressed as:

$$\frac{dP}{dV_c} = -\frac{1}{\beta . V_c} \tag{2.2}$$

Where $\beta$ is the compressibility of the liquid, $V_c$ is the chamber volume, P is the chamber pressure, and $dV_c$ is the change in volume due to compressibility. The dependency of $\beta$ on the pressure may be attributed to a number of factors: (i) the compressibility of oil decreases with increase in pressure (Hanly, 1967), (ii) any air volume entrapped in the oil results in an increase of the effective compressibility (Wahi, 1967), and (iii) variations in effective fluid compressibility caused by nonlinear deformation of rubber O-rings and other components with fluid pressure. Among these factors the entrapped air is known to affect the fluid compressibility most significantly (Warner, 1996).

Furthermore, the temperature sensitivity of the damping force can be characterized upon consideration of thermal expansion of the oil and the damper body. The influence of temperature changes on the component dimensions in considered to be relatively small compared to the thermal expansion of the fluid (Warner, 1996). Equation (2.3) illustrates that a decrease in fluid density caused by an increase in the oil temperature yields reduced damping force. The ratio of damping forces developed at two different temperatures can thus be directly related to the inverse ratio of fluid volumes corresponding to the two temperatures, given by:

$$\frac{F_{dT}}{F_{dT_{ref}}} = \frac{V_{OILTref}}{V_{OILT}} \tag{2.3}$$

Where $F_{dT}$ and $V_{OILT}$ are the damping force and the volume of oil, respectively at an operating temperature $T$; $F_{dT_{ref}}$ and $V_{OILTref}$ are the damping force and the volume of oil, respectively at a reference temperature $T_{ref}$. Owing to the strongly nonlinear dependency of damping force on valve flows, operating temperature, compressibility etc., the analytical modeling of dampers is considered to be quite complex. Consequently, the majority of the models are based upon regression analysis of the measured data. Such models are damper-specific and require identification of several coefficients.

## 2.3 Modeling of the Damping Characteristics

The dampers are designed to yield variable and asymmetric characteristics to achieve improved ride and road holding performance (Rakheja and Ahmed, 1992). The complex nature of the damping characteristics, however, poses considerable challenges

associated with analytical modeling and analyses as discussed in the previous section. Owing to such complexities, the majority of the studies on vehicle ride dynamics, pavement loads and road-holding analysis consider either linear or linear equivalent damping characteristics (Walker,1996; Joo, 1991; Rengarajan, 1991; Rakheja and Ahmed, 1994; Su, 1990). Such analyses neglect the effects of damping asymmetry and nonlinear variations with the relative velocity, but facilitate preliminary design analysis and exploration of different damping concepts. Alternatively, a few studies have characterized asymmetric damping properties by a piecewise linear describing function, as illustrated in Figure 2.3 (Rajalingham and Rakheja, 1993; Rakheja and Ahmed, 1994; 2003; Ahmed, 2001). In this formulation, the low and high speed damping coefficients in compression ($C_1$, $C_2$) and rebound ($C_3$, $C_4$) for a specific damper are identical from the mean of the laboratory-measured data, while neglecting hysteresis. The velocities ($\alpha_c$, $\alpha_e$), where the transitions from low speed damping coefficients ($C_1$ and $C_3$) to the high speed coefficients ($C_3$ and $C_4$) occur, are also identified from the measured data. The piece-wise linear describing function models of symmetric and asymmetric suspension dampers have been effectively employed in ride dynamic models of different Vehicles (Rakheja and Ahmed, 1993). The piecewise linear representation is considered adequate to study the effects of damping asymmetry and nonlinearity. A number of different piecewise linear models, however, may be considered to investigate the fundamental response behavior of symmetric as well as asymmetric damping. These models are described in the following subsections.

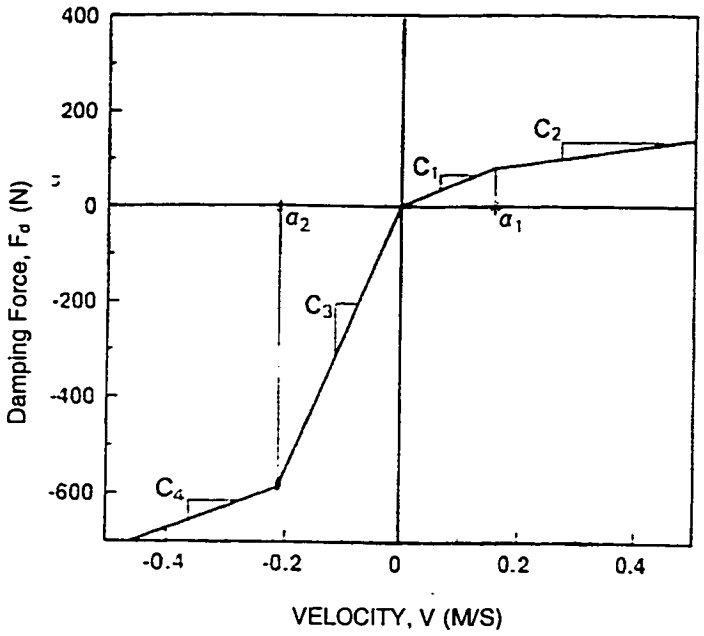


Figure 2.3: A piecewise linear damper characterization of asymmetric force-velocity characteristics (Rakheja and Ahmed, 1993).

### 2.3.1 Piecewise Linear Models

An asymmetric damping property could be simply characterized by a single-stage force-velocity curve, as shown in Figure 2.4. Such damping characteristics reveal rebound damping coefficient considerably higher than that in compression. A single-stage damping would imply the presence of a single flow path, while the flow resistances in compression and rebound would differ. A model of this type has been used in a recent study (Rajalingham and Rakheja, 2003), as shown in figure 2.5. The damping force due to such a damper can be expressed as:

$$F_d = \begin{cases} c_1 \dot{z}; & \text{for } \dot{z} \le 0 \\ c_3 \dot{z}; & \text{for } \dot{z} \ge 0 \end{cases} \tag{2.4}$$

where $C_1$ and $C_3$ are compression and rebound damping coefficients, respectively. $F_d$ is the damping force and $\dot{z}$ is the piston velocity.

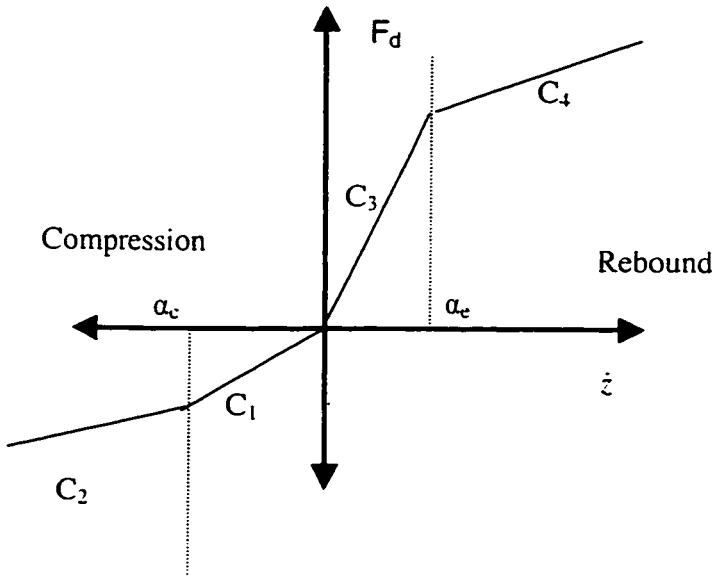


Figure 2.4: Piecewise-wise linear representation of a two-Stage Asymmetric curve

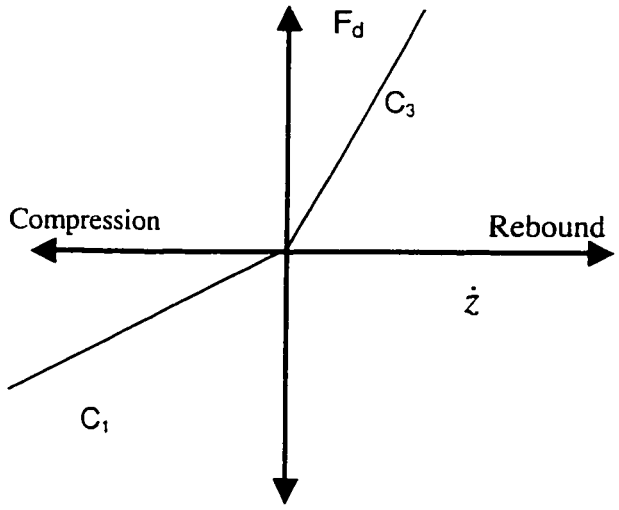


Figure 2.5: A single-stage asymmetric Damping Model

Denoting p as the asymmetry factor ($C_3/C_1$), the damping force may be expressed as:

$$F_d = \begin{cases} C_1\dot{z}; & \text{for } \dot{z} \le 0 \\ pC_1\dot{z}; & \text{for } \dot{z} \ge 0 \end{cases} \tag{2.5}$$

The dampers, however, invariably exhibit two or more stages of damping where the low speed damping coefficient is considerably larger than those attained at medium or high velocities, as evident from Figures 2.1 and 2.4. A few studies have considered multi-stage damping either in the form of regression models (Thompson, 1970; Sharp and Crolla, 1987; Chaudhury, 1998, Purdy, 2000) or piecewise linear models (Rajalingham and Rakheja, 2003; Hac and Youn, 1993; Rakheja and Ahmed, 1993, 1994). The piecewise linear models reported in these studies consider two-stage damping, although symmetric in compression and rebound. A symmetric force-velocity characterization of a damper is often realized through reduction or simplified representation of the asymmetric force-velocity properties to facilitate linear analysis in the convenient frequency domain (Rakheja and Ahmed, 1993). The force-velocity characteristics, symmetric in compression and rebound illustrated in Figure 2.6, reveal high damping coefficient ($C_1$) corresponding to a lower velocity and a lower damping coefficient ($C_2$) at higher velocities. The transition from low to high damping coefficient occurs at a preset velocity $\alpha$. The damping force may be expressed as:

$$F_d = \begin{cases} C_1\dot{z}; & \text{for } |\dot{z}| \le \alpha \\ C_1\alpha\,\mathrm{sgn}(\dot{z}) + C_2[(\dot{z} - \alpha\,\mathrm{sgn}(\dot{z})]; & \text{for } |\dot{z}| \ge \alpha \end{cases} \tag{2.6}$$

Where,

$$\mathrm{sgn}(.) = \begin{cases} 1; & \text{for } (.) \ge 0 \\ -1; & \text{for } (.) \le 1 \end{cases}$$

The sgn function is taken as 0 when $\dot{z}=0$.

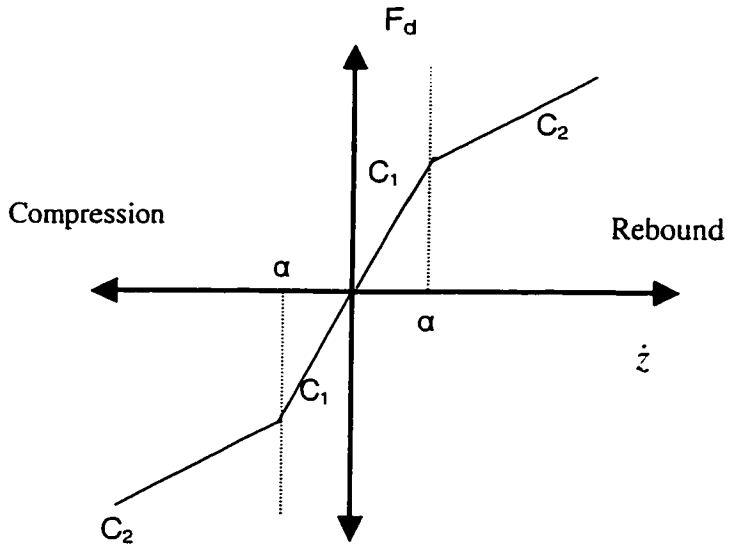


Figure 2.6: Idealized representation of force-velocity characteristics symmetrical compression and rebound.

Denoting the ratio of high speed damping coefficient to the low speed coefficient as a damping reduction factor attributed to the flows through the valve ($\gamma=C_2/C_1$), the damping factor could be expressed in terms of the low speed damping coefficient $C_1$:

$$F_d = \begin{cases} C_1\dot{z}; & \text{for } |\dot{z}| \le \alpha \\ (1-\gamma)C_1\alpha\,\mathrm{sgn}(\dot{z}) + \gamma C_1\dot{z}; & \text{for } |\dot{z}| \ge \alpha \end{cases} \tag{2.7}$$

The composite force-velocity curve of a typical hydraulic damper, however, exhibits multi-stage and asymmetric damping characteristics, as illustrated in Figure 2.1. Such a composite curve can be obtained from the hysteresis loop of the force-velocity

diagram by computing mean values of the peak forces for given velocities. The resulting composite curve consists of variable damping properties at different velocities. Although such composite force-velocity characteristics neglect the contributions due to fluid compressibility and thermal effects, they are considered to adequately describe the mean characteristics and the damping asymmetry. On the basis of laboratory characterization of 14 different bus suspension dampers, it was shown that the damping characteristics for the purpose of vehicle ride dynamic analysis can be effectively represented by the composite curve (Rakheja et al., 2001). The force-velocity curve illustrated in Figure 2.4 effectively applied to describe the low speed and high speed asymmetric damping characteristics.

The damping curve reveals high damping constants ($C_1$ and $C_3$) corresponding to bleed-control at low piston velocity in compression and rebound, and low damping constants ($C_2$ and $C_4$) due to blow-off flows at high piston velocity. The transitions from high to low damping in compression and extension occur at certain preset velocities, $\alpha_c$ and $\alpha_e$, respectively, in compression and rebound. The damping force can then be expressed as:

$$F_d = \begin{cases} C_1 \dot{z}; & \text{for} \alpha_c \le \dot{z} \le 0 \\ C_1\alpha_c + C_2(\dot{z}-\alpha_c); & \text{for } \dot{z} \le \alpha_c \\ C_3 \dot{z}; & \text{for } 0 \le \dot{z} \le \alpha_e \\ C_3\alpha_e + C_4(\dot{z}-\alpha_e); & \text{for } \dot{z} \ge \alpha_e \end{cases} \qquad (2.8)$$

Denoting $p=C_3/C_1$ as the asymmetry factor corresponding to low piston velocity, and compression and rebound damping reduction factors as, $\gamma_c=C_2/C_1$ and $\gamma_e=C_4/C_3$, the damping force can be expressed in term of low speed damping coefficient, $C_1$:

$$F_d = \begin{cases} c_1 \dot{z}; & \text{for} \alpha_c \le \dot{z} \le 0 \\ (1-\gamma_c)C_1\alpha_c + \gamma_c C_1 \dot{z}; & \text{for } \dot{z} \le \alpha_c \\ pC_1 \dot{z}; & \text{for } 0 \le \dot{z} \le \alpha_e \\ (1-\gamma_e)pC_1\alpha_e + p\gamma_e C_1 \dot{z}; & \text{for } \dot{z} \ge \alpha_e \end{cases} \qquad (2.9)$$

## 2.4 Analytical model of a nonlinear suspension spring

Apart from the suspension dampers, the suspension springs also exhibit nonlinear progressive hardening characteristics. The leaf, air and rubber springs employed in medium size and heavy vehicles, invariably exhibit nonlinear force-deflection characteristics, where the spring rate tends to increase with increase in the load. An increase or decrease in the load tends to cause a shift in the static equilibrium position in the absence of a ride height control. Moreover, the air springs yield asymmetric force-displacement behavior due to compressibility of the air (Quaglia and Sorli, 1998; Rakheja et al., 1999). This asymmetry coupled with the nonlinear characteristics, may influence the downward drifting phenomenon associated with asymmetric dampers. Majority of the reported studies on vehicle ride dynamics tend to consider either linear or linearized spring characteristics (Rengarajan, 1991; Haque et al., 1995; Rakheja and Ahmed, 1994; Su, 1990; Joo, 1991). The influence of stiffness nonlinearity on the 'packing down' or 'ride height drifting' behavior has not been investigated.

An air spring exhibits force-displacement characteristics as a hysteresis loop as shown in Figure 2.7. Owing to relatively small hysteresis magnitudes, a composite mean force-displacement curve can be used to characterize the force-displacement characteristics as shown in Figure 2.8 (Rakheja et al., 1999).

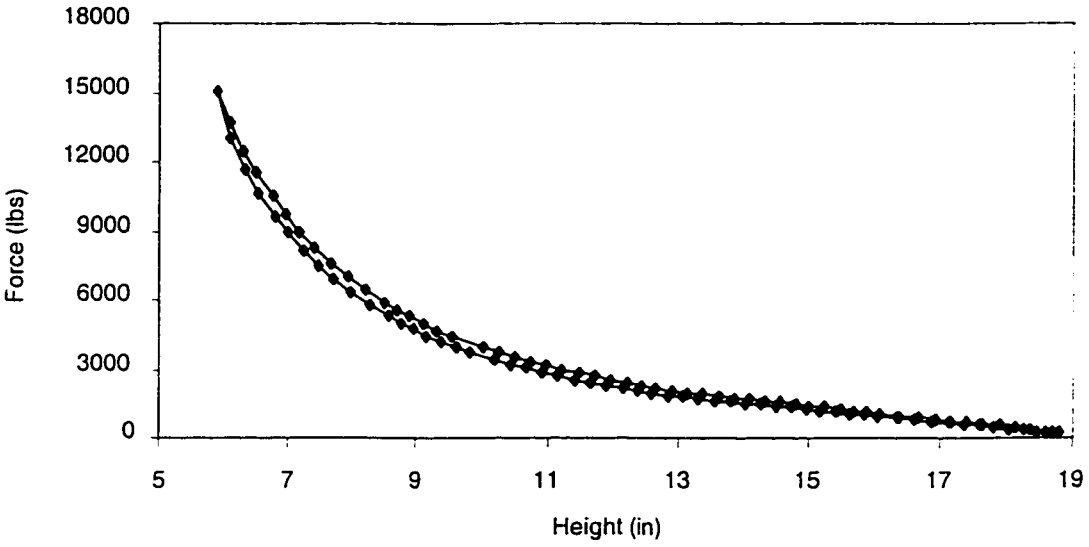


Figure 2.7: Force-displacements characteristics of an R11-130 air spring (Rakheja et al., 1999).

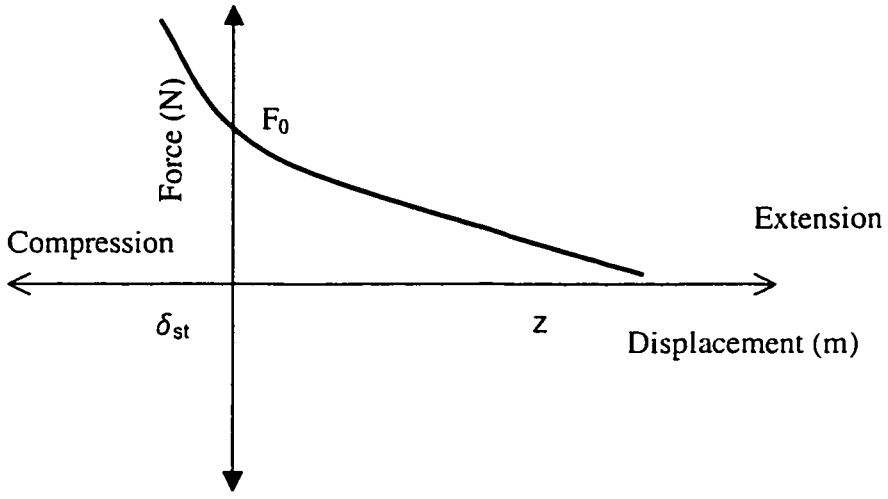


Figure 2.8: Force-deflection characteristics of an air suspension spring

The study suggested that, the force-deflection characteristics of air springs can be established as a function of the preload, while the static ride height is maintained at the recommended value. The instantaneous restoring force developed by an air spring is related to the instantaneous pressure and the effective area:

$$F_{Asd}(\delta) = (p_A - p_{atm}) A_E(\delta_s) \tag{2.10}$$

where $p_A$ is the absolute gas pressure, and $A_E$ is the effective area as a function of the spring deflection $\delta_s$ with respect to static design height. The instantaneous pressure and effective area are nonlinearly dependent on the air bag height, which may be clearly observed from the measured data. The instantaneous gas pressure may be related to the static charge pressure and the spring deflection using the gas law. Assuming a polytropic process, the instantaneous pressure may be derived from:

$$p_A(\delta_s) = \frac{p_0 v_0^n}{(v_0 - A_E \delta_s)^n} \tag{2.11}$$

where $p_0$ is the absolute pressure corresponding to static ride height, $v_0$ is the static volume and $n$ is the polytropic constant.

The resulting curve reveals progressively hardening characteristics, which can be alternatively described by a cubic force-deflection relationship during compression. The softening behavior in the rebound suggests nearly linear force-deflection relationship. The force-deflection relationship may thus be expressed as:

$$f_s = \begin{cases} F_0 - (K_1 z + K_2 z^3); & \text{for } z < \delta_{st} \\ F_0 - K_1 z; & \text{for } z > \delta_{st} \end{cases} \tag{2.12}$$

Where $f_s$ is the spring force, $K_1$ and $K_2$ are the linear and cubic stiffness coefficients, $\delta_{st}$ is the static deflection of the spring which depends upon the load, $F_0$ supported by the spring. Equation (2.12) can be used characterize the nonlinear and asymmetric force-deflection characteristics of suspension springs, similar to the damper models.

## 2.5 A Quarter-Vehicle Model

A vehicle model to be selected for the purpose of vibration analysis is largely dependent on the objective of the analysis. The objective here is to illustrate a simple but credible model that can be utilized for fundamental investigation into the ride height drifting or 'packing down' phenomenon of the suspension system. The model is thus required to characterize the vertical dynamics of the sprung and unsprung masses under road-induced excitations. The analytical model should be capable of predicting the bounce responses of the sprung and unsprung masses where the nonlinear characteristics of the suspension elements can be adequately represented. A quarter vehicle model is commonly used to obtain a qualitative insight into the functions of the suspension, particularly the effects of the sprung and unsprung masses, spring stiffness, and damping concepts on the dynamic responses of the masses, rattle space, and the tire and suspension forces. A quarter vehicle model constrained along the vertical axis can be formulated using 1 to 3 degrees-of-freedom (DOF) (Genta, 1997).

A single-DOF model is used to study various concepts in suspension assuming negligible contribution due to unsprung mass of the wheel and axle assembly and visco-elastic properties of the tire, as shown in Figure 2.9(a). A two-DOF quarter vehicle model is used most commonly, which incorporates the dynamics of the unsprung mass and elastic properties of the tire, as illustrated in Figure 2.9(b). A three-DOF quarter-vehicle

model may further include the secondary suspension, such as body mounts, seat suspension or cab suspension as illustrated in Figure 2.9 (c). A two-DOF quarter vehicle model would be adequate for the study of asymmetric/symmetric and linear/nonlinear properties of suspension components, as it could fully describe the essential bounce motions of the vehicle sprung mass, wheel and suspension components. This model contains no representation of the geometric effects of having four wheels, and any effect of roll and pitch motions.

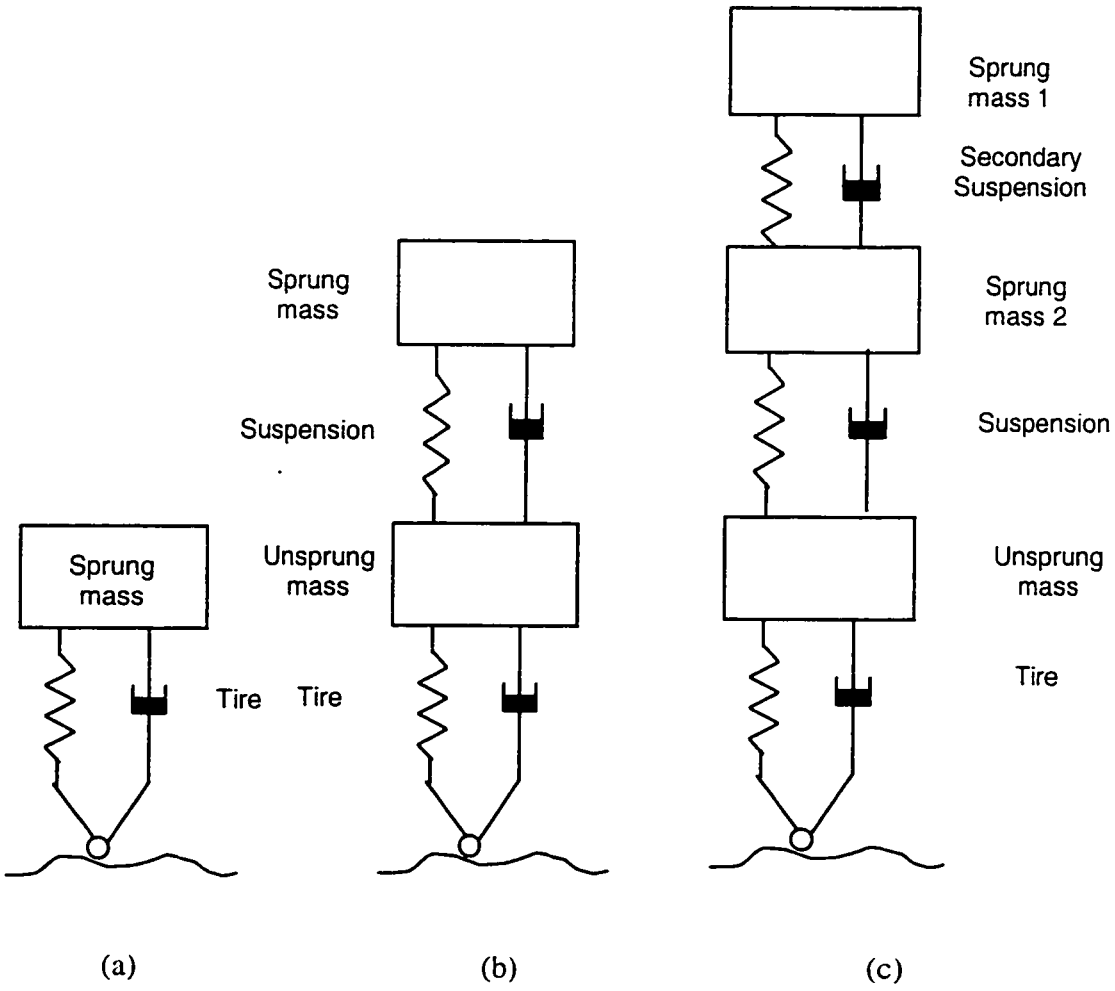


Figure 2.9: a) Single-DOF, b) Two-DOF and c) Three-DOF quarter-vehicle models.

A quarter vehicle model is also useful for representation of wheel load variations and suspension system forces (Sharp and Crolla, 1987). The most common and simple two-DOF quarter vehicle ride model that can be utilized for evaluation of sprung and unsprung mass bounce characteristics is presented in the Figure 2.10 (Ahmed, 2001). Here, the suspension components are modeled as non-linear elements for the ride analysis. The mass of the vehicle supported by the suspension is represented by the sprung mass $m_s$ while the masses due to wheel and tire assembly, and the brakes, are lumped together with portions of the steering and suspension masses, and represented as the equivalent unsprung mass, $m_u$. The sprung mass, $m_s$ of the vehicle model is derived upon subtracting the unsprung mass $m_u$ from the total of the vehicle mass supported by a single tire.

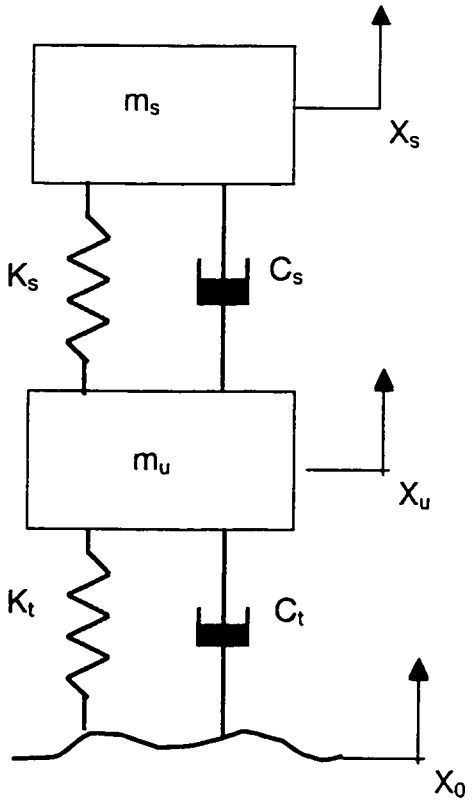


Figure 2.10: A two-DOF quarter vehicle Model.

The differential equations describing the motions for a nonlinear two-DOF quarter vehicle model subject to road excitation $x_0$ can be expressed as:

$$m_s \ddot{z}_s + F_D(\dot{z}) + f_s(z) + m_s g = 0 \tag{2.13}$$

$$m_u \ddot{z}_u - F_D(\dot{z}) - f_s(z) + F_t(z_1) + m_u g = 0 \tag{2.14}$$

Where $F_D$ and $f_s$ are suspension damping and spring forces respectively, as described by the component models in equations (2.4), (2.6), (2.8) and (2.12). It should be noted here that $F_D$ is the function of the relative velocity, $\dot{z} = \dot{X}_s - \dot{X}_u$. The spring force $f_s$ is the function of relative displacement, $z=X_s-X_u$. $F_t$ is the force developed by the tire. Assuming linear spring rate and viscous damping due to tire, the tire force can be expressed as:

$$\begin{aligned} F_t(z_1) &= k_t(z_1 - \delta_t) + C_t \dot{z}_1; && \text{for } (y_2 - \delta_t) \le 0 \\ &= o; && \text{otherwise} \end{aligned} \tag{2.15}$$

where $z_1=X_u-X_0$, represents the relative deflection of the tire and $\delta_t$ is the static tire deflection.

## 2.6 Summary

In this chapter, a suspension system with a nonlinear spring and asymmetric damper has been analytically modeled and incorporated within a two degrees-of-freedom quarter-vehicle model. Since the 'packing down' phenomenon is a net effect due to vertical motions of sprung and unsprung masses, a quarter vehicle model is considered to be sufficient for this investigation. An air spring that exhibits cubical force-displacement

characteristics in compression and linear properties in extension is considered for suspension spring. The nonlinear and asymmetric force-velocity characteristics of the hydraulic suspension dampers are modeled using piece-wise linear properties with asymmetry between compression and extension. The parameters of this damper model could be varied to represent either a single-stage or multistage asymmetric damping characteristics. The differential equations of motion for quarter-vehicle model derived in this chapter are solved in the following chapter to study the influence of asymmetric suspension properties on the response of the sprung and unsprung masses.

# CHAPTER 3

# VEHICLE RIDE ANALYSIS

## 3.1 General

The shock and vibration attenuation performance of a suspension system is evaluated from the response to known dynamic excitations. These evaluations may be performed either in laboratory or via computer simulation of the suspension dynamics as described by a mathematical model. Generally, it is more practical, versatile and economical to perform the analysis via computer simulation rather than laboratory or field-testing. A mathematical model validated against known characteristics provides a powerful tool for detailed analysis, evaluation of parametric sensitivity and functional limits. Since low frequency ride in terms of sprung and unsprung mass vertical motions and influence of nonlinear suspension are the focus of this investigation, the use of a simplified quarter vehicle model was justified in the chapter two. The nonlinear equations of motion for a quarter car model were presented in the previous chapters. This chapter is devoted to the ride analysis of the model with nonlinear suspension system. The simulations are carried out utilizing Matlab 'simulink' for various sinusoidal excitations. A set of baseline parameters for the vehicle and suspension are adopted from literature. The model with nonlinear damper and linear spring is first validated by comparing the simulated results over a wide frequency range with those published earlier. The validated model is then used systematically to simulate time history of sprung and unsprung masses to characterize the ride responses. The responses are examined to establish the influence of suspension nonlinearity and asymmetry on the drift of sprung mass dynamic

equilibrium referred to as drift. The influence of some asymmetry parameters on drift is also examined and presented in this chapter.

### 3.2 Basic System parameters

Basic system parameters for the quarter vehicle model are adapted from literature (Rakheja and Ahmed, 1993) and are typical of those used for a mid-size passenger car. These parameters are presented in Table 3.1. The table further presents a set of baseline parameters for the nonlinear damper and spring of the suspension as established in chapter 2. Parametric sensitivity of the response for the suspension parameters around their baseline values are investigated and presented in the next chapter.

Table 3.1

| Parameters | Value |
|---|---|
| Parameters for linear system | |
| Sprung mass, $m_s$ | 240 kg |
| Unsprung mass, $m_u$ | 40 kg |
| Linear suspension damping coefficient, $C_{eq}$ | 975 N-s/m |
| Linear suspension spring coefficient, $K_{eq}$ | 16000 N/m |
| Tire damping co-efficient, $C_t$ | 200 N-s/m |
| Tire stiffness co-efficient, $K_t$ | 120000 N/m |
| Non-linear Suspension Damping and spring Parameters: | |
| High damping coefficient at compression side, $C_1$ | 514.5 N-s/m |
| High damping coefficient at extension side, $C_3$ | 2747.5 N-s/m |
| Low damping coefficient at compression side, $C_2$ | 177 N-s/m |

Table 3.1 (continued)

| | |
|---|---|
| Low damping coefficient at extension side, $C_4$ | 462 N-s/m |
| Preset velocity at extension side $\alpha_e$ | 0.1524 m/s |
| Preset velocity at compression side $\alpha_c$ | -0.2163 m/s |
| Asymmetry ratio, p | 5.34 |
| Nonlinear stiffness co-efficient, $K_1$ | 12000 N/m |
| Nonlinear stiffness co-efficient, $K_2$ | 1.953e6 $N/m^3$ |
| Static equilibrium position of the sprung mass, $\delta_{st}$ | -0.01 m |

## 3.3 Model Validation

Dynamic responses of the vehicle and suspensions have been extensively investigated for either linear or equivalent linear suspension components (Thompson, 1970; Sharp and Crolla, 1987; Rengarajan, 1991; Wong, 1993; Rakheja and Ahmed, 1994), and can be readily compared with the developed model for its validation. Ahmed and Rakheja (1994) presented an equivalent linearization for nonlinear asymmetric damping in vehicle suspension. The study utilizing a quarter-car model compared the responses of the equivalent linear model in frequency domain obtained as exact solution through numerical integration. Figure 3.1 shows the published results in term of displacement transmissibility of the sprung and unsprung masses for frequencies in the range of 0.1 to 10 Hz. The parameters used in this study are (Rakheja and Ahmed, 1994):

Sprung mass, $m_s$= 240 kg.

Unsprung mass, $m_u$=40 kg,

Tire damping co-efficient, $C_t$= 200 N-s/m

Tire stiffness co-efficient, $K_t$ =120000 N/m

Linear suspension spring co-efficient, $K_{eq}$= 16000 N/m

High damping co-efficient at compression side, $C_1$ = 514.5 N-s/m

High damping co-efficient at extension side, $C_3$= 2747.5 N-s/m

Low damping co-efficient at compression side, $C_2$ =177 N-s/m

Low damping co-efficient at extension side, $C_4$=462 N-s/m

Preset velocity at extension side $\alpha_e$= 0.1524 m/s

Preset velocity at compression side $\alpha_c$= -0.2163 m/s

The model developed in this study and simulated using Matlab simulink is assigned the above parameters for simulation under sinusoidal excitation of amplitude 0.05 m. The steady state time response computed at selected frequencies is used to establish the frequency domain transmissibility in the range of 0.2 to 10 Hz. The results established as sprung mass ($X_s/X_0$) and unsprung mass ($X_u/X_0$) transmissibility are presented in Figure 3.2 in logarithmic scale. These results are identical to Figure 3.1 both in trend and quantity, and provide a positive validation of the present model and its simulation using simulink. It should be pointed that, these results (Figure 3.1 and 3.2) are influenced by the excitation amplitude due to strong nonlinearity of the suspension elements. It was thus important to carry out the validation for the same input as that used by Rakheja and Ahmed (1994).

### 3.4 Ride analysis of the Vehicle Model

The model for vehicle ride and simulation methodology, which is validated in the previous section, can be used for systematic analysis of ride properties. The primary objective is the analysis of ride is to examine the influence of suspension nonlinearity

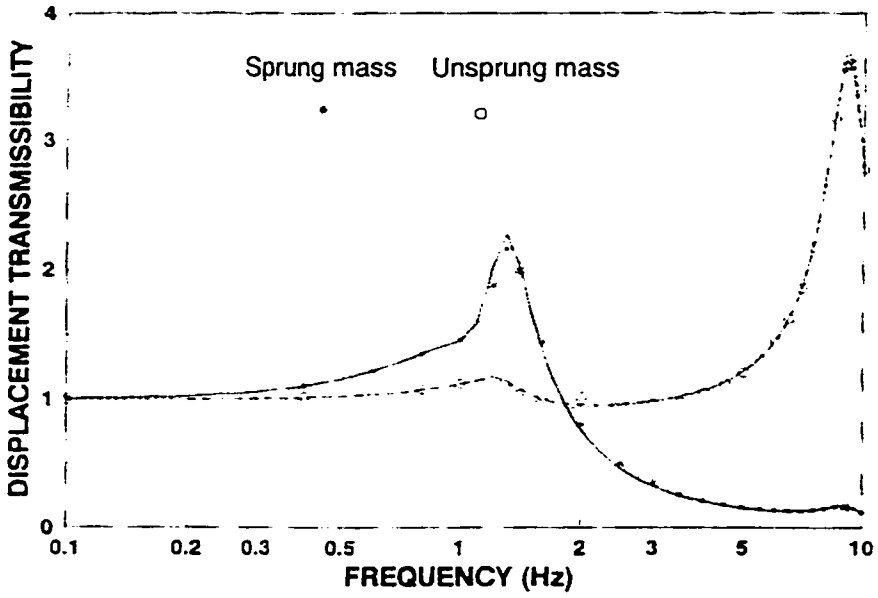


Figure: 3.1: Displacement transmissibility of a quarter car model with nonlinear suspension from local equivalent linearization method and its comparison with exact solutions (Rakheja and Ahmed, 1994)

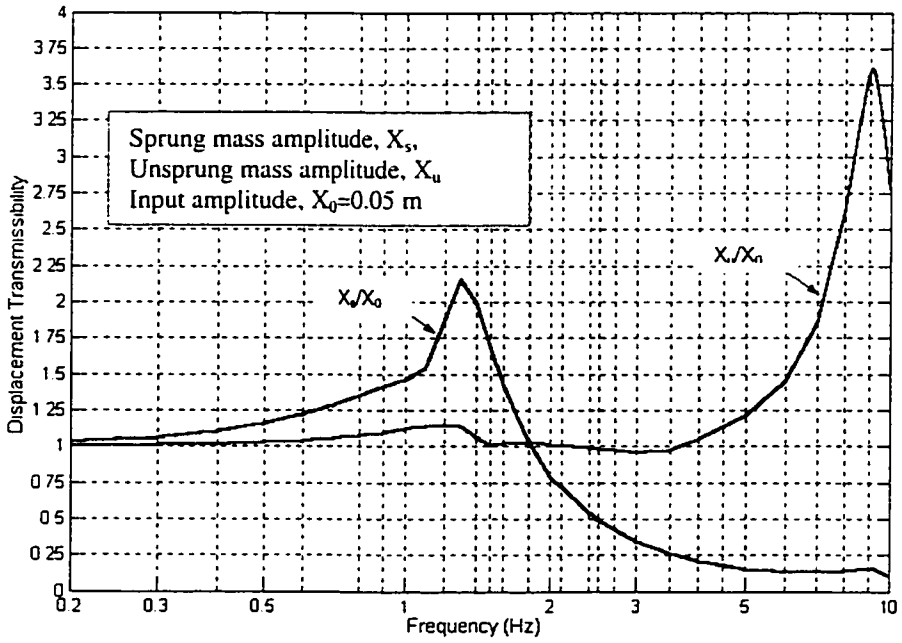


Figure 3.2: Displacement transmissibility of the developed model from simulink time response.

and asymmetry on the drift of sprung and unsprung mass at dynamic equilibrium. For a through understanding of the suspension influence, it is however necessary to introduce one of the characteristics at a time. For this reason, the model is simulated for a range of suspension characteristics from fully linear to nonlinear, asymmetric with nonlinear spring.

All results are obtained in time domain for a set of sinusoidal excitations in the frequency ranges of 0 to 20 Hz. Results of interest are: motions of sprung and unsprung masses, relative motions and velocities across the suspension. These results are recorded once the steady state is reached. The following sub-sections present the results in sequence starting from the linear suspension.

### 3.4.1 Linear suspension

A full linear system is established by selecting an equivalent linear parameter for suspension stiffness and damping. The linear system responses are obtained by setting all nonlinear damping parameters $C_1$ and $C_4$ to the value of 975 N-s/m, while linear suspension stiffness is set to the value of 16000 N/m.

Steady state time history of the responses to sinusoidal excitation of amplitude 0.05 m are examined at several frequencies. A sample set of results at the wheel-hop natural frequency of 9.5 Hz is presented in Figure 3.3. As the results indicate, for symmetric linear suspension, the responses are symmetric about the static equilibrium, which is indicated by position zero. Variation of relative amplitude symmetrically about zero is the indication used to establish drift of the ride. The drift is defined as shift of the zero line in the relative amplitude response. As expected, for the linear suspension there is no drift and the response shown in Figure 3.3 are typical of a linear system.

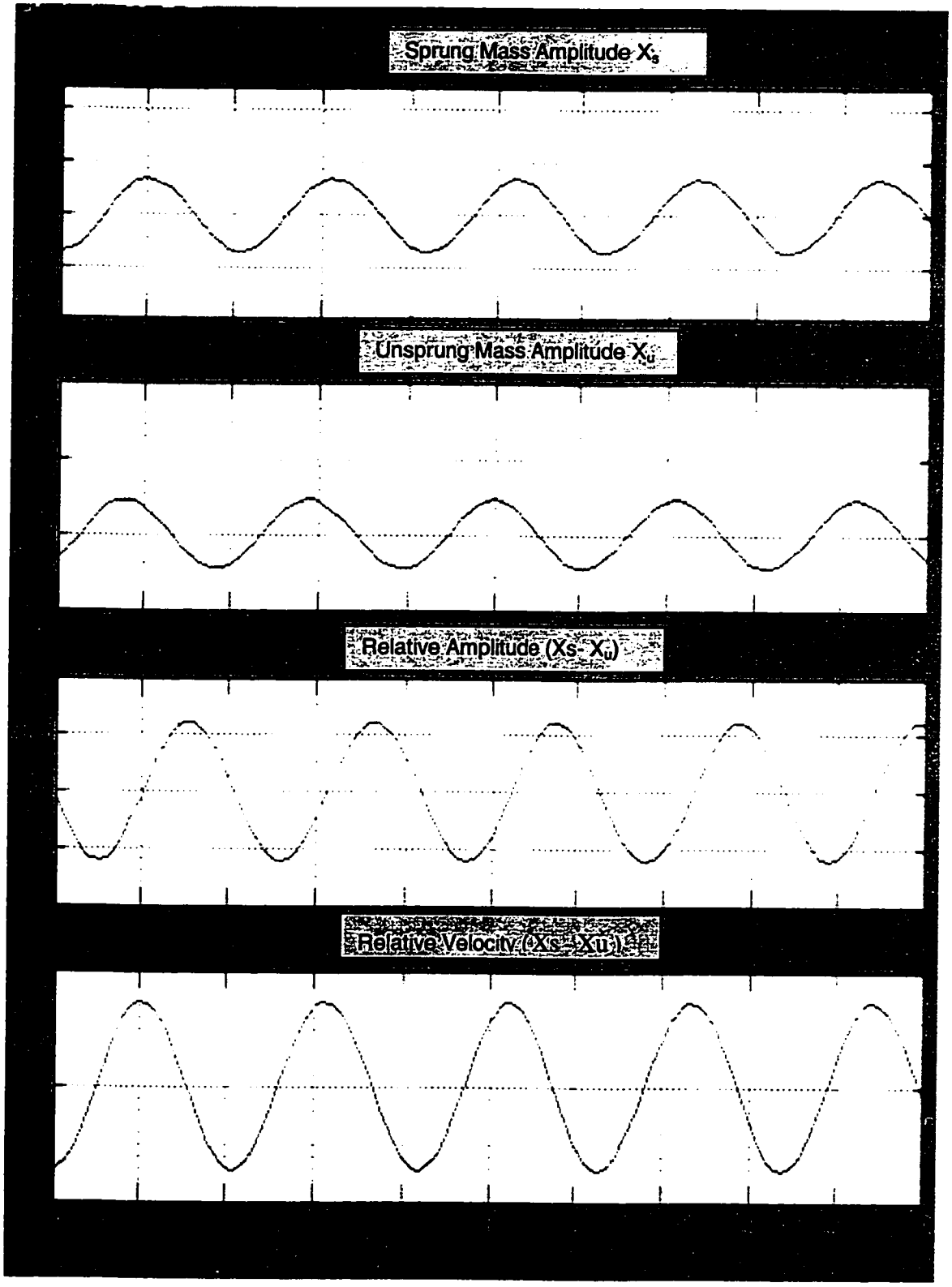


Figure 3.3: Linear suspension ride responses at 9.5 Hz

### 3.4.2 Suspension with Nonlinear Symmetric Damping

Neglecting the difference in compression and extension strokes of the suspension, the model can be simplified to a nonlinear but symmetric characteristic. Such a nonlinear damper characteristics is shown in Figure 2.6. A similar characteristic is considered in investigations of suspension modeling and performance (Rakheja and Ahmed, 1993). As discussed in chapter 2, a symmetric nonlinear damper is represented by a high and low damping with a preset velocity $\alpha$. Furthermore, the characteristic is symmetric in compression and extension. The high and low damping for this case is taken as the average of baseline high and low damping presented in Table 3.1. The resulting values utilized for this section are $C_1=C_3=1631$ N-s/m and $C_2=C_4=320$ N-s/m. The preset break velocities where damping change is taken as $\alpha_{c,c}= \pm 0.1524$ m/s.

Similar to linear system, steady state responses are examined for frequencies 0.5 to 20 Hz. A sample result for excitation frequency of 9.5 Hz is presented in Figure 3.4. For nonlinear symmetric damping it is observed that the effective damping in the suspension is sensitive to the amplitude of excitation. It is expected since the extent of high damping value utilized depends on the magnitude of relative velocity across the damper in relation to the preset break velocity ($\alpha$).

An examination of results presented in Figure 3.4 indicate symmetric variation in the relative amplitude about the static equilibrium. Thus similar to linear response, symmetric nonlinear suspension does not lead to any drift in the ride height.

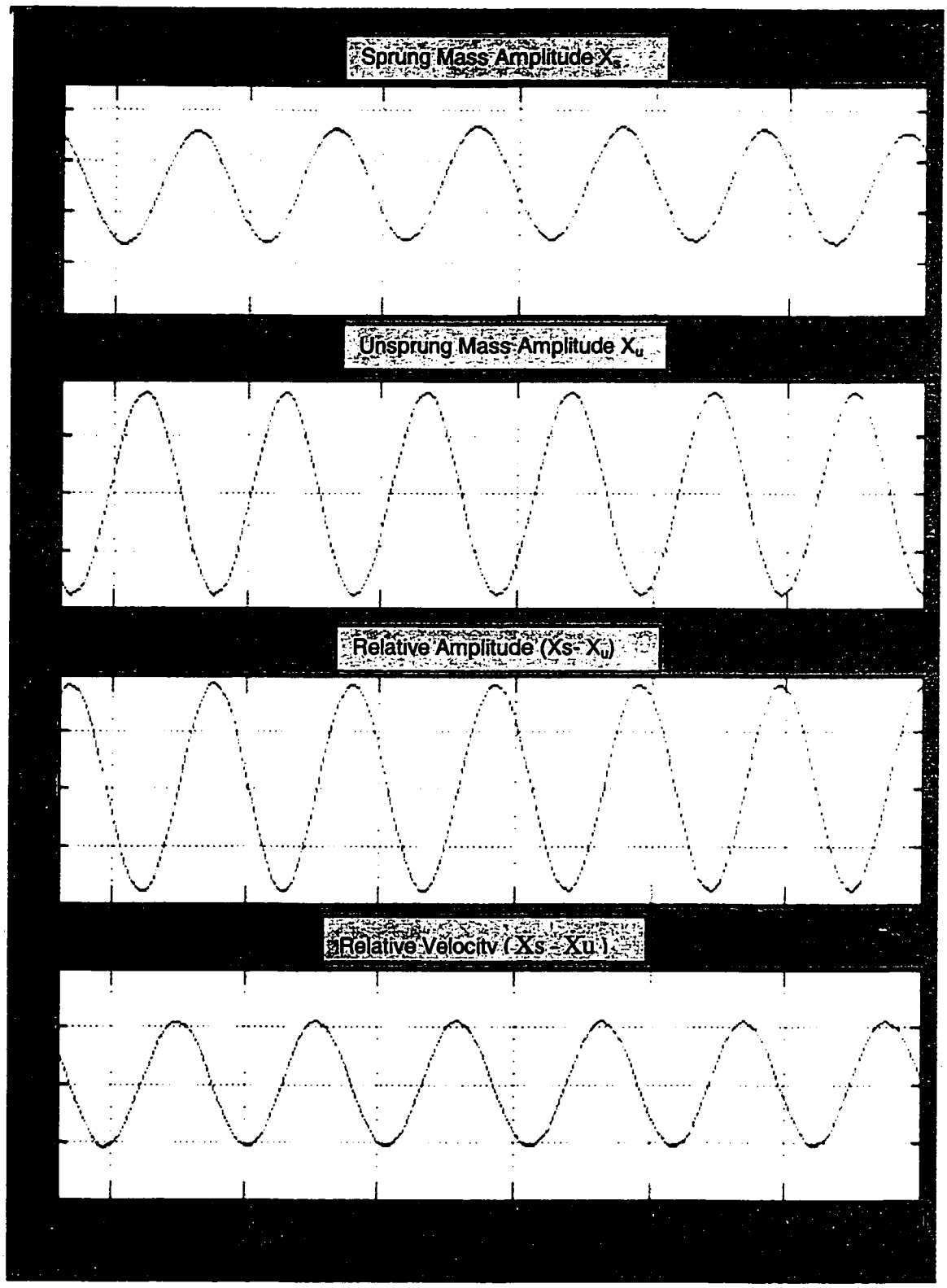


Figure 3.4: Ride response for a nonlinear symmetric damper at 9.5 Hz.

### 3.4.3 Ride Analysis of a Nonlinear Damper

As discussed in chapter 1 and modeled in chapter 2, suspension dampers are designed to provide variable damping with asymmetry between compression and extension. The damping Force-Velocity curve reveals high damping constants corresponding to bleed-control at low piston velocity, and low damping constants due to blow-off at high piston velocity. The transition from high to low damping in compression and extension occurs at certain preset velocity. Such a characteristic idealized by four piecewise linear segments is shown in Figure 2.4. These four coefficients used in this investigation are given in the Table 3.1, and are $C_1$= 514.5 N-s/m and $C_3$=2747.5 N-s/m, $C_2$=177 N-s/m, $C_4$=462 N-s/m. The preset velocities in extension and compression are: $\alpha_e$=0.1524 m/s, $\alpha_c$=-0.2163 m/s, respectively. Prior to considering a damper with two-stage in compression and two-stage in extension, this investigation first examines a single-stage asymmetric characteristics. A two-stage asymmetric damper can be simplified to a single-stage damper model (Figure 2.5) by assigning a constant low damping value for compression and a constant high damping value for extension. This section finally considers a two-stage asymmetric damper model, which uses $C_1$ to $C_4$ with $\alpha_c$ and $\alpha_e$ to describe force in compression and rebound.

#### 3.4.3.1 Ride Analysis of a Single-Stage Damper Model

The single-stage asymmetric damper is modeled by assigning $C_2$=$C_1$ and $C_4$=$C_3$ in the nonlinear Matlab simulink model such that the damper behaves as single-stage. The damping coefficients in compression and extension are taken as average baseline damping values in compression and extension of multi stage asymmetric damper. The compression and extension damping values are thus taken as: 345.6 N-s/m and 1604.75

N-s/m, respectively. These parameters provide an asymmetry ratio, p=4.64. The steady state time-history of the responses is obtained following the same steps as those in the previous cases. The results corresponding to wheel hope natural frequency (9.5 Hz) is shown in Figure: 3.5. These responses corresponding to asymmetry ratio of 4.64, defined as $C_3/C_1$. The relative amplitude across the damper in this case clearly indicates oscillation about a new equilibrium. For an excitation amplitude 0.05 m and damper asymmetry of 4.64, the zero line has shifted by –0.14 m, and is referred to as drift. Researchers observing such behavior (Warner, 1996; Emery, 2002) refer to such phenomenon as packing down of suspension. This behavior results from the fact that asymmetric damper generates unequal force in compression and extension. Since less force is developed against compression, the sprung mass tends to oscillate about a new equilibrium that is considerably lower than the static equilibrium. This will thus result in a reduction in the working space for the suspension by the amount of the drift. The results further reveal that the packing down of the sprung mass is primarily responsible for the drift of relative motion.

To examine the influence of asymmetry on the drift behavior, further results are obtained at wheel hop natural frequency for variation of 'p'. The results summarized as peak drift as a function of asymmetry ratio (p) for excitation amplitude 0.05 m are shown in Figure 3.6. This clearly attributes the phenomenon of drift to extent of asymmetry in the damping force. An extensive parametric study is carried out in the next chapter to examine influence of suspension parameters over a frequency range.

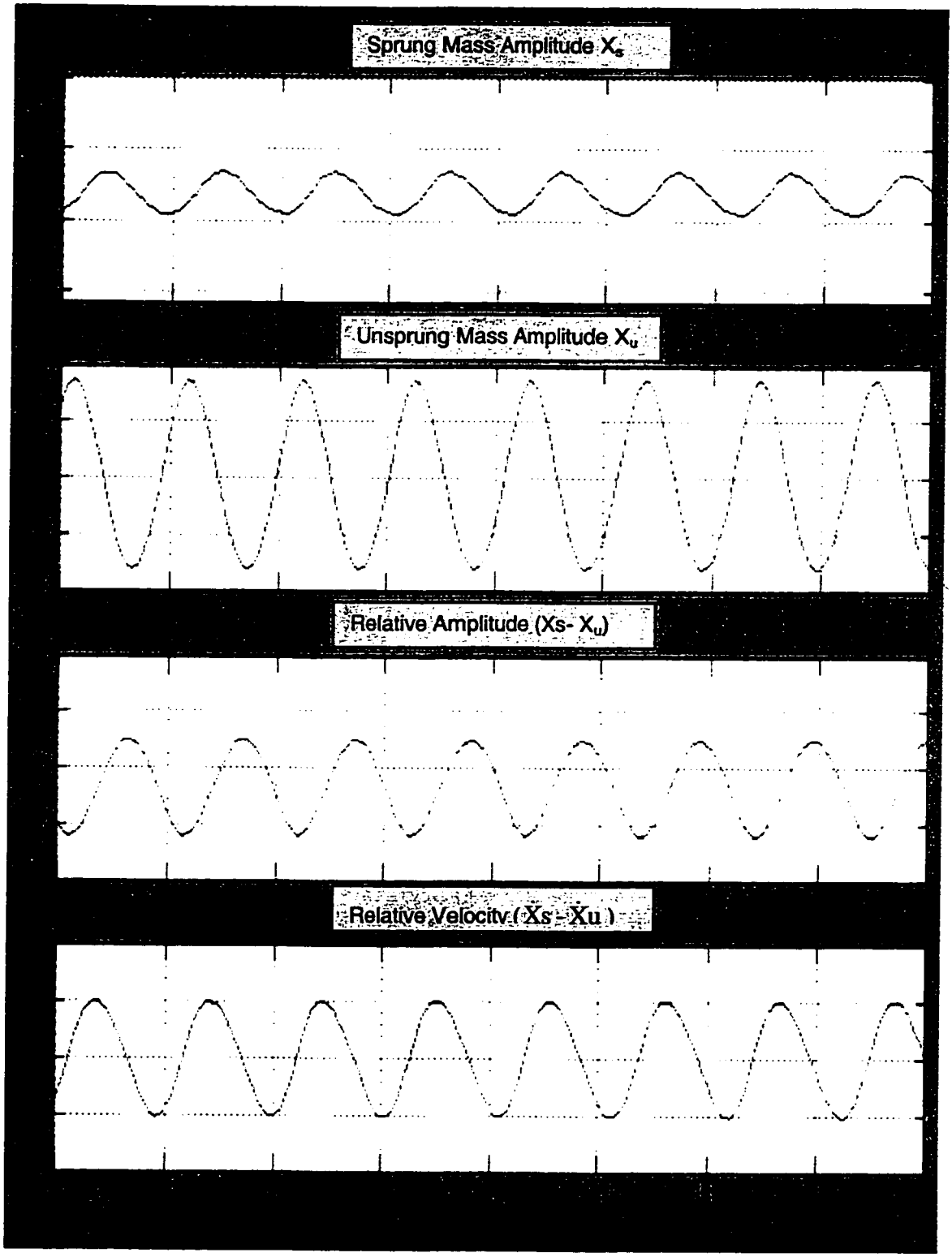


Figure 3.5: Ride response for a single-stage damper with asymmetry ratio 4.64 at 9.5 Hz.

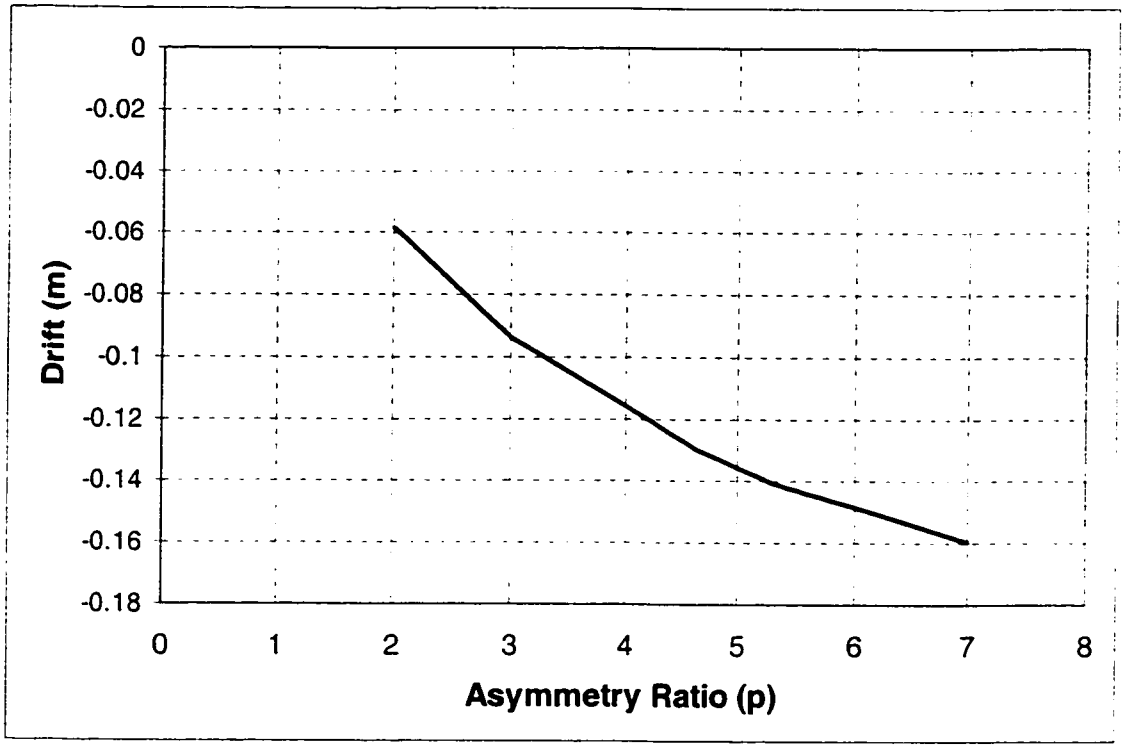


Figure 3.6: Effect of asymmetric ratios on the suspension drift for a single-stage damper at 9.5 Hz.

### 3.4.3.2 Ride Analysis of a Two-Stage Nonlinear Asymmetric Damper

Two-stage nonlinear asymmetric damper is represented by two damping constants for each of compression and extension strokes. The preset velocities are also defined to identify the relative velocity where the damping coefficients change. The simulation is carried out for the baseline parameters presented in Table 3.1 except for the suspension spring. Here the suspension spring is taken as linear with stiffness Ks= 16000 N/m. The baseline asymmetry ratio 'p' defined, as $C_3/C_1$ is 5.34. Figure 3.7 presents the simulated ride responses in time domain corresponding to the wheel hop natural frequency of 9.5 Hz. As is observed for single-stage asymmetric case, the two-stage asymmetry also leads to a shift in the ride height.

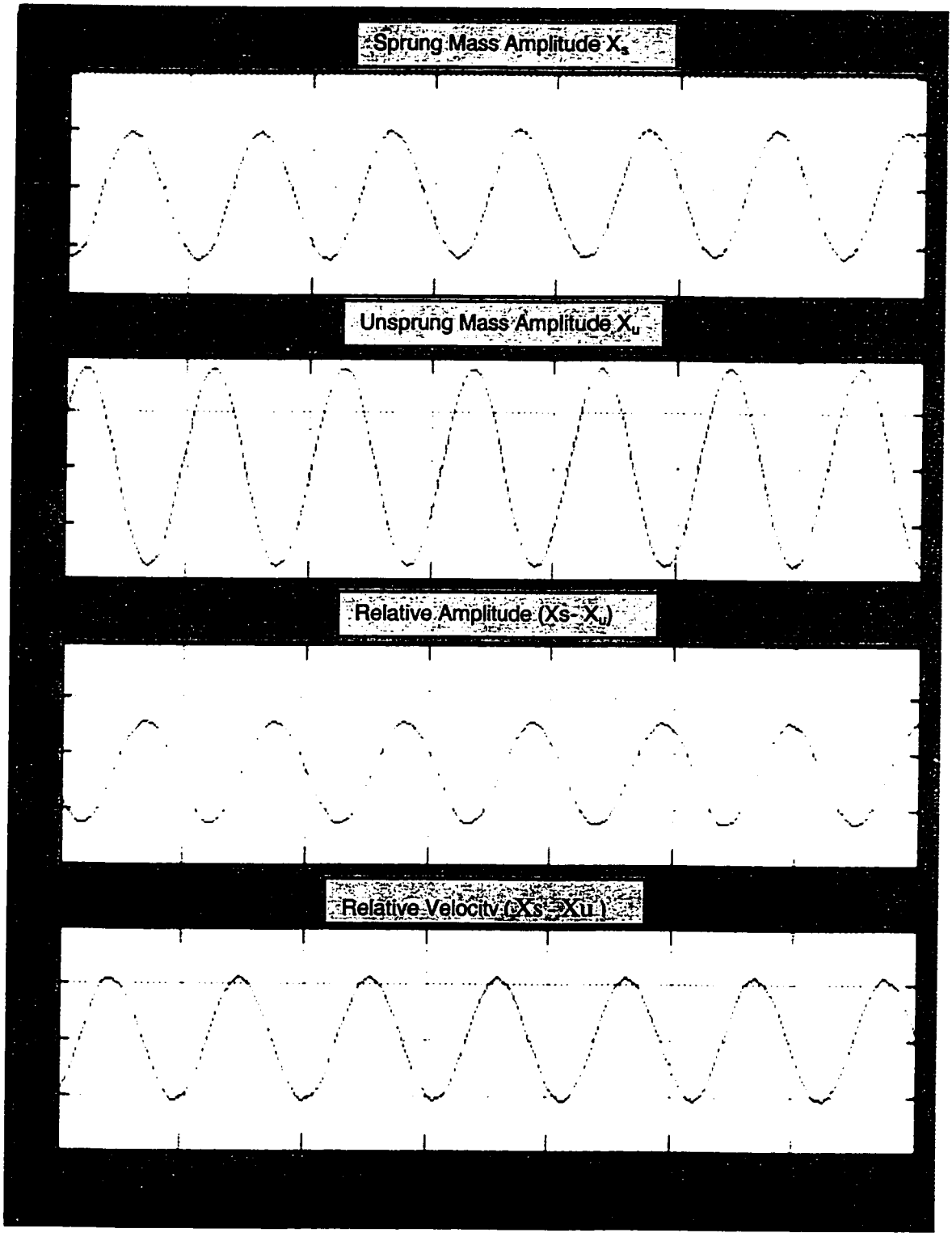


Figure 3.7: Ride response for a two-stage nonlinear damper with base line system parameters.

For p=5.34, the results in Figure 3.7 show –0.07 m shift from the mean line for relative amplitude across the suspension. The drift is thus established as –0.07 m. The magnitude of drift in this case of two-stage asymmetric damper is found to be less than that of a single-stage. Comparison of results with single-stage damper further indicates reduced magnitude of the sprung mass motion at 9.5 Hz. The change of response is a combined effect of change in equivalent damping and asymmetry realized with the baseline damper. For a two-stage asymmetric damper, four damping constants are involved and its asymmetry characteristics can only be defined by minimum of these parameters. These parameters defined as: asymmetry ratio ($C_3/C_1$), compression reduction factor ($C_2/C_1$) and extension reduction factor ($C_4/C_3$). Simulations are carried out for variation of one parameter at a time. In all cases the results are recorded corresponding to wheel hop natural frequency (9.5 Hz).

**a) Affects of Asymmetry Ratio**

The Asymmetry ratio for the two-stage nonlinear damper (p) is varied between 2 to 7 and the steady state magnitude of the drift is recorded for each simulation. The results summarized in Figure 3.8 presents the drift versus p relationship for excitation frequency 9.5 Hz. These results indicate a linear relationship between asymmetry ratios and ride drift. Compared to single-stage, the influence of p is significantly less for two-stage damper as it alters only high damping ratios at low velocities.

**b) Affects of Extension Reduction Factor of the Damper**

The damper extension reduction factor is defined as the ratio of two damping coefficients in the extension stroke and is defined as $C_4/C_3$. For the base line model, the extension reduction factor is 0.168 and the corresponding drift as shown in Figure 3.7 is –

0.07 m. Further results are obtained for extension reduction factor 0.05, 0.10 and 0.2. This is achieved by changing $C_4$ while $C_3$

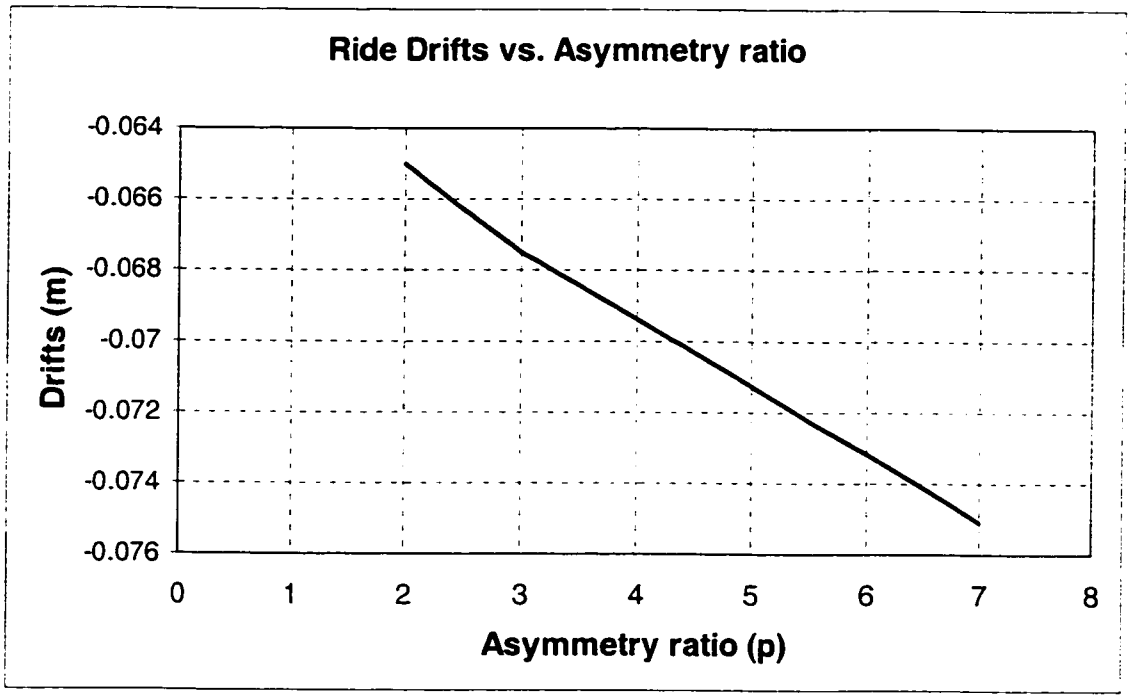


Figure 3.8: Drift as function of asymmetry for two-stage damper at 9.5 Hz.

and all other parameter maintained at the baseline value. The results as magnitude of drift for the selected extension reduction factor are shown in Figure 3.9. As the results show, increase in extension reduction factor reduces the drift to some extent. Since extension reduction factor is defined as $C_4/C_3$, an increase in the ratio using reduced $C_3$ leads to lower overall asymmetry of the damper. The reduced asymmetry in turn reduces the magnitude of drift.

**c) Affects of Compression Reduction factor**

Similar to extension reduction factor, compression reduction factor is defined as the ratio of the two damping coefficients on the compression side, and is defined as $C_2/C_1$. For the baseline parameters presented in Table 3.1, the compression reduction

factor is 0.34 and the corresponding drift as shown in Figure 3.7 is –0.07 m. To examine the effect of this parameter, further results are computed at 9.5 Hz for compression reduction factor 0.1, 0.5 and 0.8. This is achieved by changing $C_1$ while $C_2$ and all other parameters maintained at the baseline value.

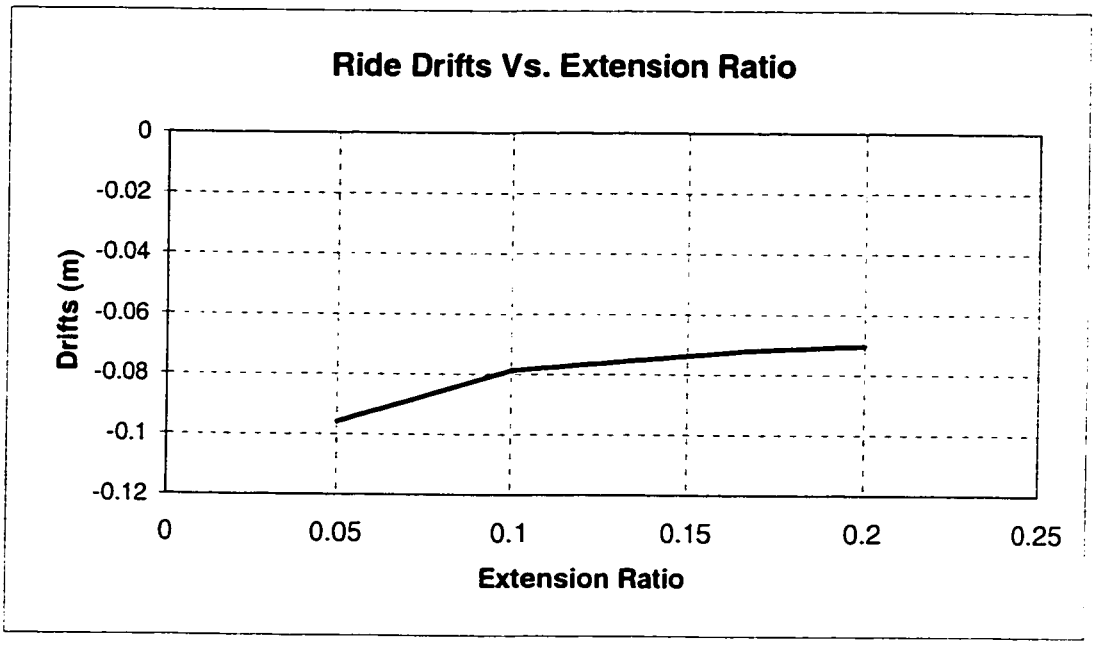


Figure 3.9: Drift as a function of extension reduction factor at 9.5 Hz.

The results as magnitude of drift for the selected compression reduction factor s are presented in Figure 3.10. These results show a slight increase in the drift as compression reduction factor is increased, and is trend is opposite to that of extension reduction factor. In the case of compression reduction factor, larger ratio requiring lower value of $C_1$ leads to increased asymmetry of the damper. In analyzing Figure 3.9 and 3.10 showing the effect of coefficient ratios, it should be pointed out that the variation in the ratios are achieved by modifying the coefficient corresponding to the higher velocity only. Effect of this is therefore dependent on the magnitude of relative velocity attained across the damper in the response.

A more meaningful conclusion can only be drawn from a comprehensive parametric study with variation in excitation amplitudes. Such study is carried out and presented in the next chapter.

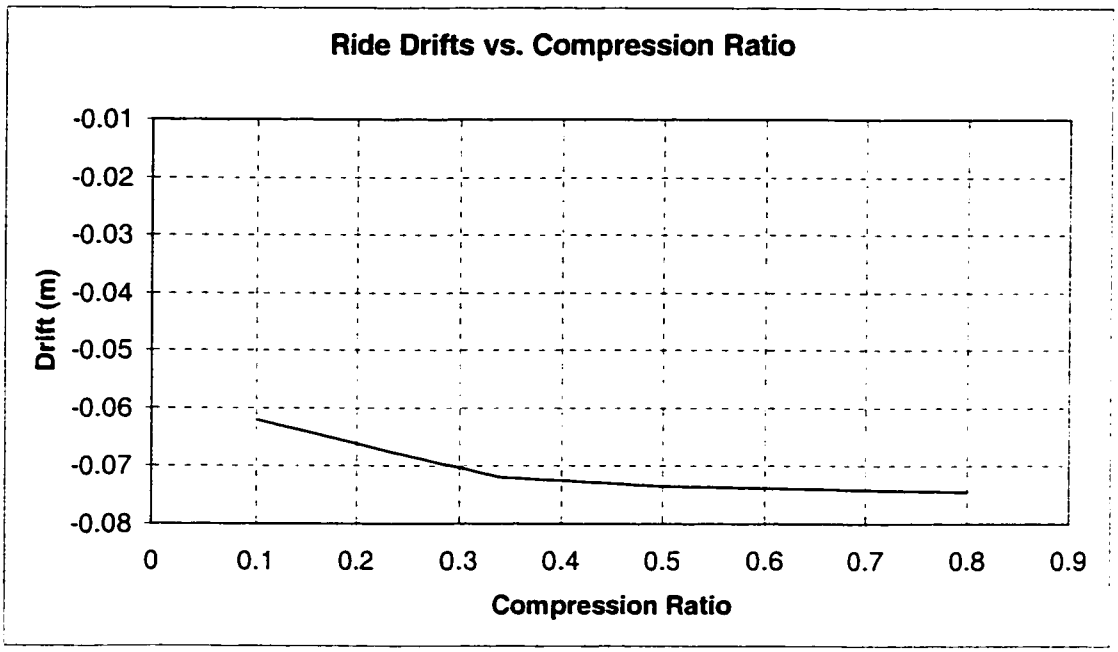


Figure 3.10: Drift as a function of compression reduction factor at 9.5 Hz.

## 3.5 Ride Analysis of a Nonlinear Asymmetric Damper and Spring

Simulation and analysis of results presented in section 3.4 dealt with nonlinear asymmetric damper with a linear suspension spring. Finally, in this section, the complete system as proposed to contain nonlinear damper and nonlinear spring is considered. The suspension spring as proposed in section 2.4 and represented by equation 2.12 is nonlinear with asymmetric characteristics. The asymmetry of the spring is however, opposite to that of the damper. The springs are significantly stiffer in compression than the rebound mode. The baseline spring parameters for the nonlinear representation are given in Table 3.1.

Similar to previous sections, the ride response results obtained from simulation at 9.5 Hz excitation are presented in Figure 3.11. An examination of responses of the sprung mass and suspension indicates small positive drift while the results due to same damper parameter with linear spring presented in Figure 3.7 showed significant negative drift. Such trend in response is attributed to the fact that the asymmetry of suspension spring is opposite to that of damper, and tends to cancel the effect of asymmetry. The results obtained so far for wheel hop natural frequency indicate that potentially once can find a nonlinear spring such that the drift due to asymmetric damper is zero. A constructive conclusion can however, be only drawn after an extensive parametric study over a wide frequency range with variation in spring parameters.

### 3.6 Summary

The vehicle Ride analysis model developed in chapter 2 with nonlinear asymmetric suspension and nonlinear spring is simulated in this chapter through Matlab simulink tool. The model and simulation is first validated by comparing nonlinear time history responses over a wide frequency range with those of published data. The validated model is utilized in a systematic manner to investigate the effect of suspension nonlinearity and asymmetry. Simulation results are obtained in sequence from linear system to full nonlinear. All the results presented and analyzed in this chapter corresponding to wheel hop natural frequency where the magnitude of relative motion across the suspension at its maximum and drift is most likely. The results clearly reveal the role of suspension damper asymmetry on the drift phenomenon. Damper with lower coefficient in compression than extension lead to 'packing down' behavior where the sprung mass and suspension motions are not about its static equilibrium, but about a new zero line lower

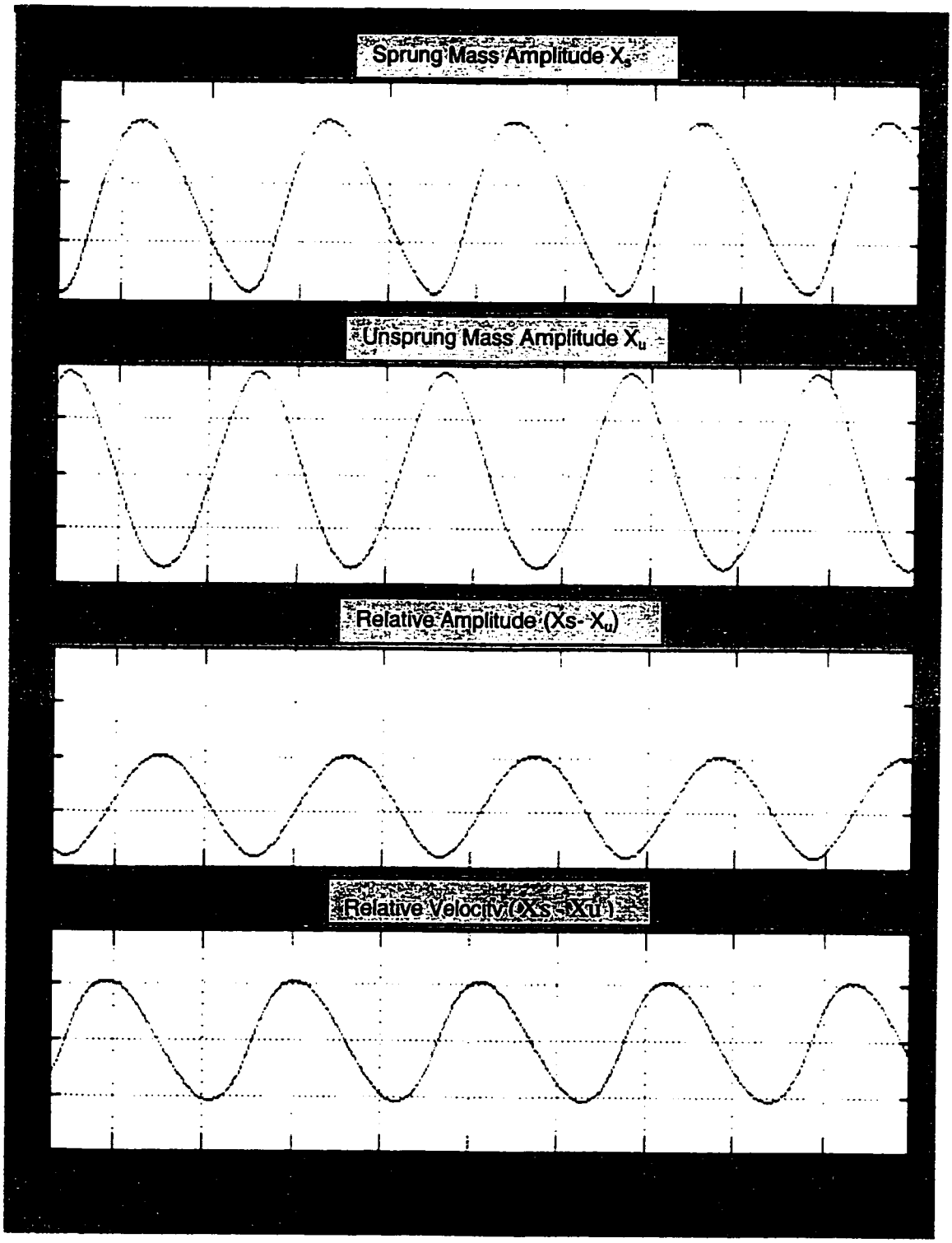


Figure 3.11: Ride analysis of an asymmetric damper and spring for excitation at 9.5 Hz

than the static equilibrium. The extent of this drift can be directly related to the asymmetry of the damper.

The drift due to asymmetry of damper can be identified from simulations with linear suspension stiffness. When nonlinear stiffness is introduced the drift is found to reduce significantly. This is attributed to the fact that suspension stiffness nonlinearity produces larger force in compression and is opposite to the asymmetry in the damper. Spring nonlinearity, thus tend to cancel the drift introduced by damper at the wheel hope frequency. Consequently there may exist stiffness characteristics that will neutralize the drift created by damper.

While it is obvious that asymmetry of damping leads to drift at wheel hop natural frequency, it is essential to characterize this over a wide frequency range. A comprehensive parametric study is undertaken in the next chapter to examine the influence of parameters over a wide frequency range as well as to explore the prospect of establishing a nonlinear spring characteristics to minimize the drift over the entire frequency range.

# CHAPTER 4

# INFLUENCE OF DAMPER PARAMETERS ON RIDE HEIGHT DRIFTING

## 4.1 General

The road vehicle ride model with nonlinear suspension characteristics developed in chapter 2 is simulated to examine the influence of suspension properties on the ride height drift phenomenon. The simulation results presented in chapter 3 in terms of time history clearly demonstrates that the nonlinearity and asymmetry in the damping property lead to drift in the ride height. The magnitude and the direction (up or down) of the drift depend on the magnitude of damping and asymmetry between extension and compression. In general, increased asymmetry with lower damping in compression leads to downward drift of the sprung mass and relative motion. The drift is also found to be maximum at the wheel hop natural frequency. The results presented in chapter 3 are obtained for a fixed sinusoidal input at the wheel hop natural frequency.

This chapter is devoted to the study of suspension parameters and their influence on the drift magnitude over a wide frequency range for different excitation amplitudes. A frequency range of 0 to 20 Hz is considered here as appropriate for ride performance study. The parameters that characterize nonlinear asymmetric damper include: the asymmetry ratio (p) defined as $C_3/C_1$; damping ratio ($\xi$) defined with respect to $C_1$; preset velocities ($\alpha_c$, $\alpha_e$); extension reduction factor ($\gamma_e$) defined as $C_4/C_3$; and compression reduction factor ($\gamma_c$) defined as $C_2/C_1$.

The nonlinear spring modeled in chapter 2 is also examined here for its effect in combination with linear and nonlinear asymmetric dampers. Finally, an attempt is made to establish parameters for a nonlinear spring that may minimize the influence of damper asymmetry on the ride height drift over the frequency range.

## 4.2 Influence of Suspension Parameters on Ride Height Drift

The proposed vehicle suspension system model comprises a cubical spring and a nonlinear asymmetric damping mechanism to achieve a full nonlinear asymmetric suspension system. The effects of suspension asymmetry on the drift of dynamic equilibrium as ride height drift, established from steady state time response at selected frequency are demonstrated in chapter 3. The results are obtained systematically from linear damping and stiffness characteristics to fully nonlinear suspensions. The results clearly demonstrate that the drift is only present in the case of asymmetric suspension characteristics. The section on parametric study thus only considers asymmetric damper characteristics with linear and nonlinear springs.

The influences of damper parameter are examined for two cases, namely: single-stage asymmetric damping and two-stage asymmetric damping. In these cases the spring is assumed linear. Finally a nonlinear spring is introduced with a two-stage damper and studied for the combined effect on the ride height drift behaviors.

### 4.2.1 Single-Stage Damper with a Linear Spring

As shown in Figure 2.5, a single-stage damper is essentially piecewise linear with lower coefficient in compression and can be considered for a reasonable representation of a real damper. The nominal parameters are taken as average value of coefficients in

compression and extension side which yields $C_1$= 345.63 N-s/m and $C_2$ =1604.75 N-s/m respectively. The simulations are carried out using Matlab simulink model in time domain as presented in chapter 3. Results are obtained by measurements of steady state time domain response for sinusoidal excitation of 0.05 m in the frequency range of 0 to 20 Hz. The magnitude of drift as defined in chapter 3 is established at discreet frequencies and presented in Figure 4.1. The results as shown indicate that for such damping characteristics the sprung mass experiences 'packing down' phenomenon over the entire frequency range. The drift increases rapidly producing a small peak at sprung mass natural frequency and reaches its peak value of –0.13 m corresponding to the wheel hop frequency where the relative amplitude between the sprung and unsprung masses is maximum.

The results of drift normalized by the relative amplitude plotted over the frequency range are shown in Figure 4.2. This shows interesting result, indicating that the normalized drift is a linear function of the frequency of excitation.

The baseline model with single-stage asymmetric damping and linear spring is next examined for influence of parameters. The parameters considered are asymmetry (p), amplitude of excitation ($X_0$) and damping ratio ($\xi$).

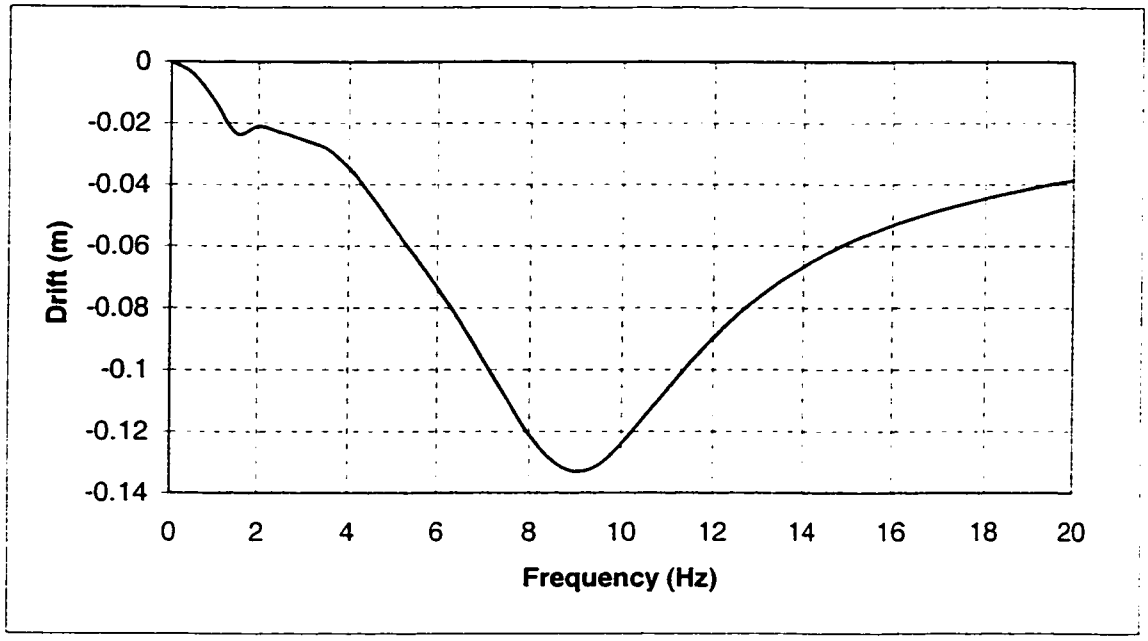


Figure 4.1: Frequency response of drift for baseline single-stage asymmetric damper

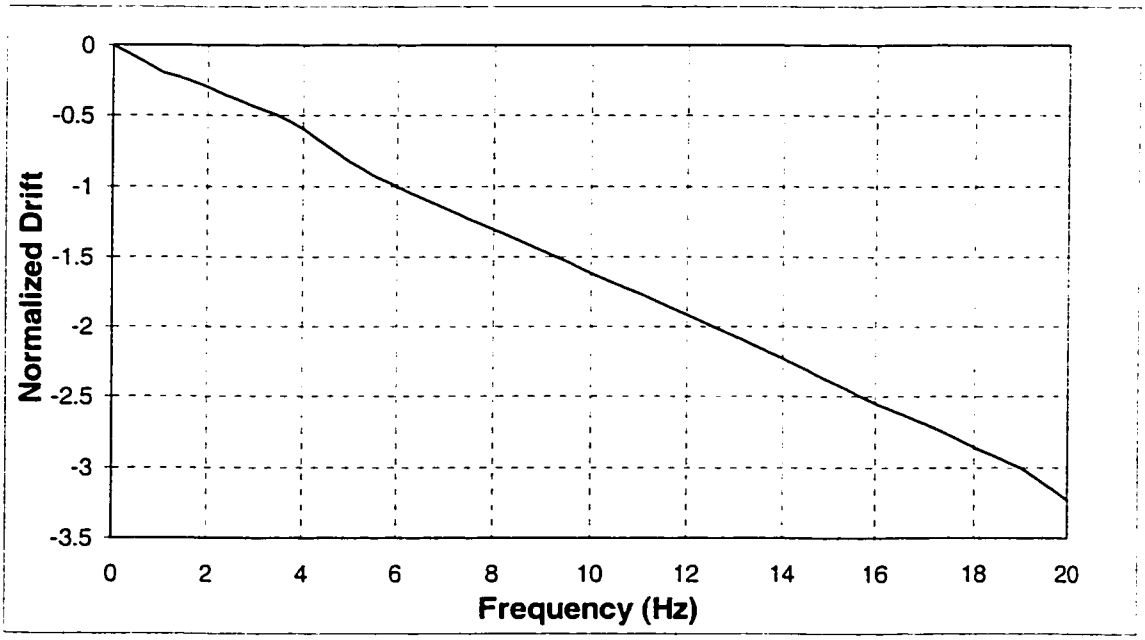


Figure 4.2: Normalized drift for single-stage asymmetric damper.

#### 4.2.1.1 Influence of Asymmetry (p)

The results presents in Figures 4.1 and 4.2 correspond to p=4.6, indicating that the damping coefficients in extension is 4.6 times that of compression stroke. Further results are obtained for p=2 and 3 over the frequency range and presented in Figure 4.3. As the results show, identical trend in drift is produced for all values of p whereas drift reduces with reduced asymmetry. The results normalized with respect to relative amplitude shown in Figure 4.4 also indicate linear relationship with frequency for all values of p. The rate of change of normalized drift with frequency shown in Figure 4.4 for p=2, 3 and 4.6 are found to be 0.08, 0.16 and 0.3 $Hz^{-1}$, respectively, indicating a near linear relationship of the drift rate with the asymmetry.

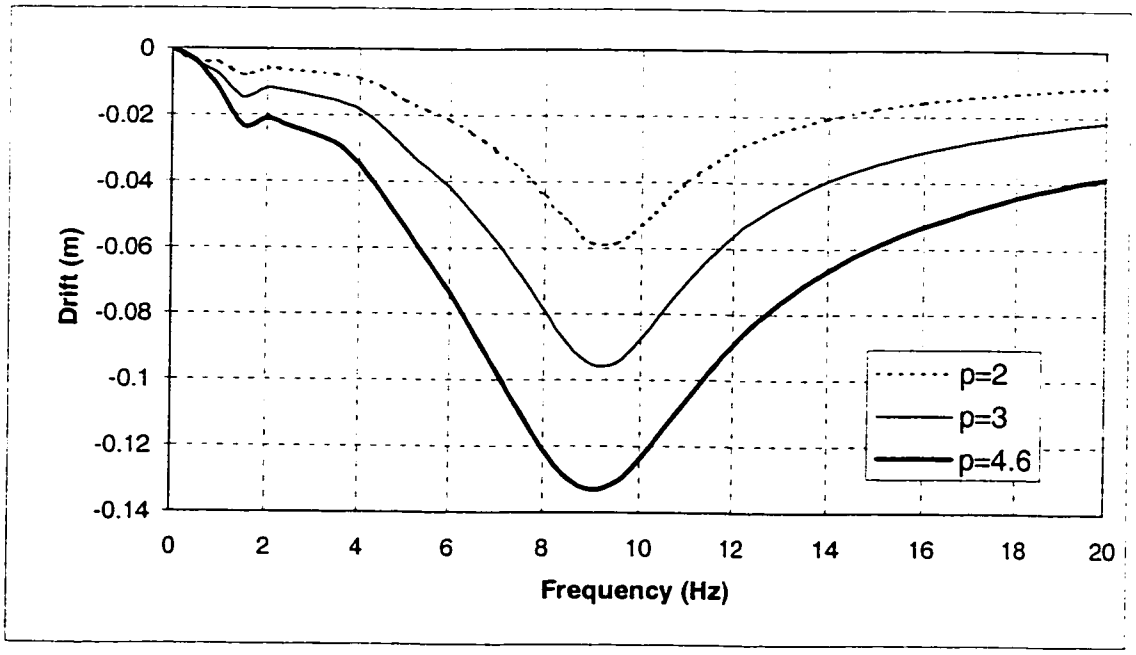


Figure 4.3: Frequency response of drift for different asymmetry in a single-stage damper

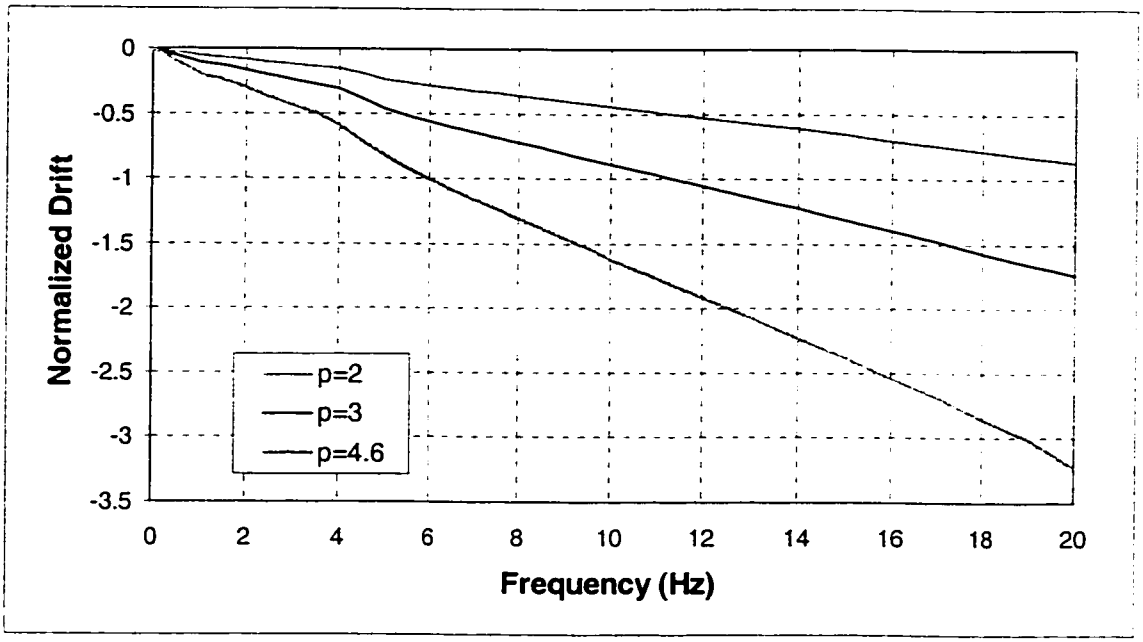


Figure 4.4: Normalized drift for a single-stage damper which various asymmetry

#### 4.2.1.2 Influence of excitation magnitudes ($X_0$)

Since relative amplitude across the suspension is a function of the excitation amplitude, it is expected that the magnitude of drift will also be affected by the input magnitude. To investigate the influence of excitation amplitude ($X_0$), the baseline model response is computed over the frequency range for $X_0$=0.03, 0.05 and 0.07 m. The results in terms of drift are presented in Figure 4.5. These results clearly demonstrate that the increase in excitation amplitude leads to larger drift over the entire frequency range with maximum influence around the wheel hop natural frequency.

The drift magnitude presented in Figure 4.5 normalized with respect to the relative amplitude across the damper at each frequency is presented in Figure 4.6. These results indicate that the excitation amplitude does not affect the normalized drift. This is

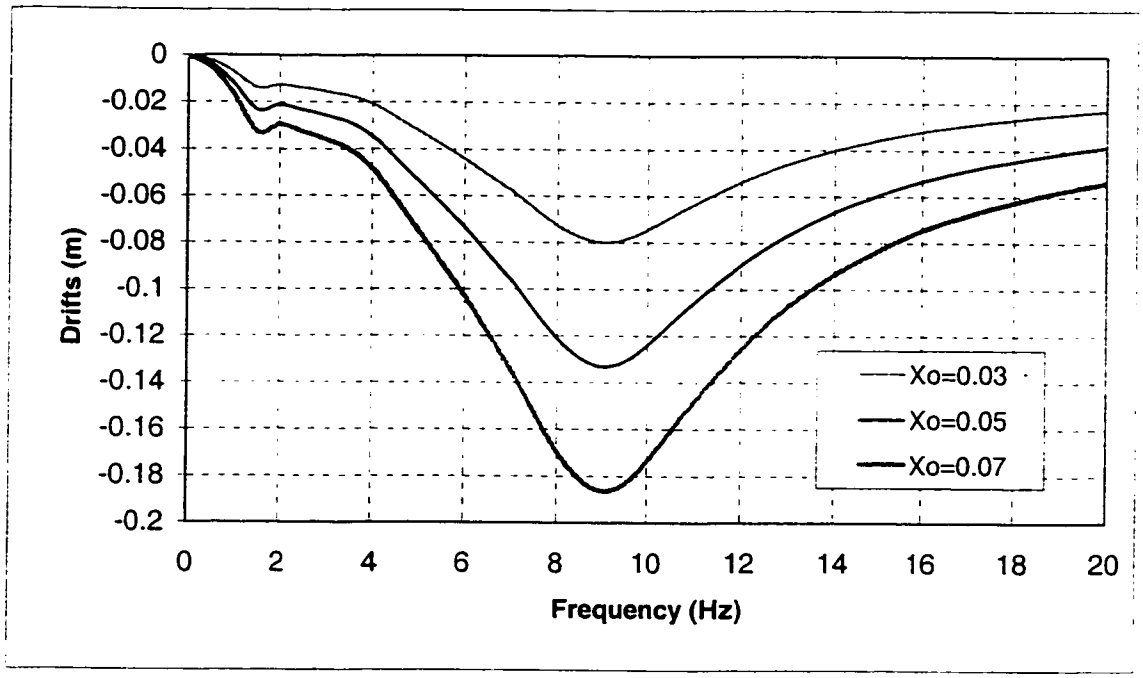


Figure 4.5: Frequency response of drift for a single-stage damper corresponding to different excitation amplitudes.

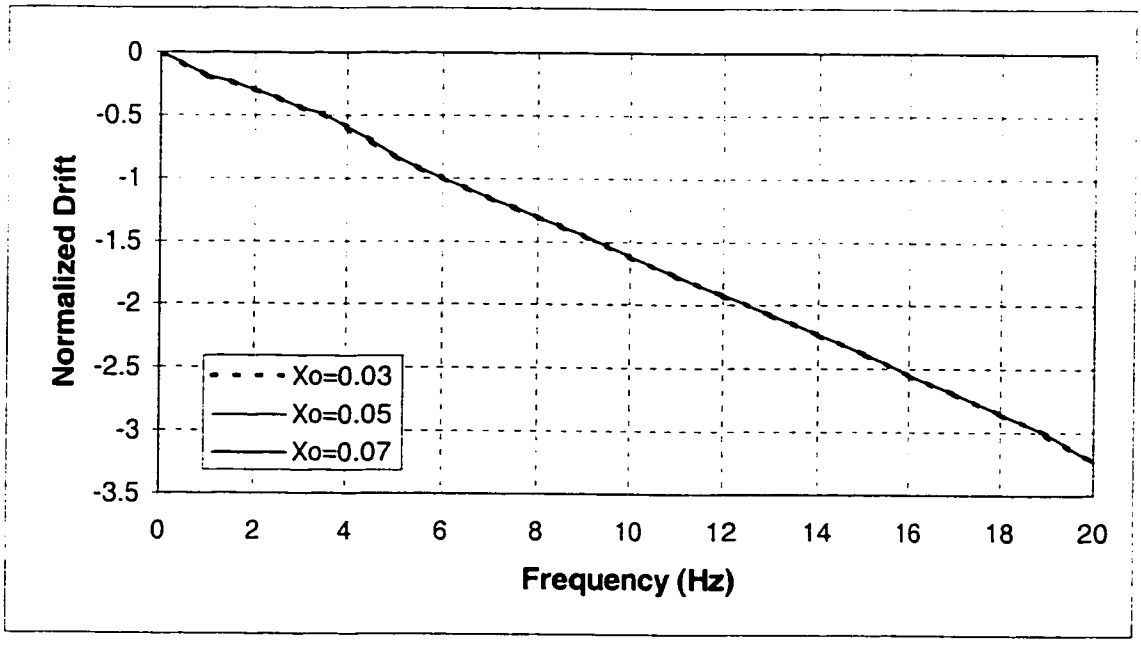


Figure 4.6: Normalized drift for a single-stage damper for various excitation amplitudes.

owing to the fact that an increase in $X_0$ leads to an increase in drift, which is proportional to the increase in the relative amplitude.

#### 4.2.1.3 Influence of Damping ratio ($\xi$)

A measure of damping offered by a single-stage asymmetric damper is defined as all damping ratio due to $C_1$ and expresses as $\xi = \frac{c_1}{2\sqrt{K_{eq} m_s}}$ where $K_{eq}$ is the equivalent linear coefficient of the suspension spring. For any change in damping ratio, both $C_1$ and $C_2$ are modified, since the asymmetry ratio 'p' is maintained constant and equal to the baseline value.

Simulation results in terms of drift over the frequency range for $\xi$ =0.08 to 0.2 are presented in Figure 4.7. These results show that for a fixed asymmetry, the drift decreases as the damping is increased, and the influence is maximum around the wheel hop frequency. The corresponding results in terms of normalized drift, ratio of drift to the magnitude of relative displacement response across the suspension is shown in Figure 4.8. Again a linear relationship can be established between normalized drift and frequency for all values of damping ratio considered.

It should be noted, that the results presented so far in this section are for single-stage asymmetric damper. A more realistic suspension damper typically exhibits multi stage nonlinearity in both extension and compression. The next section focuses on the parametric influence for suspension with two-stage nonlinear asymmetric damper.

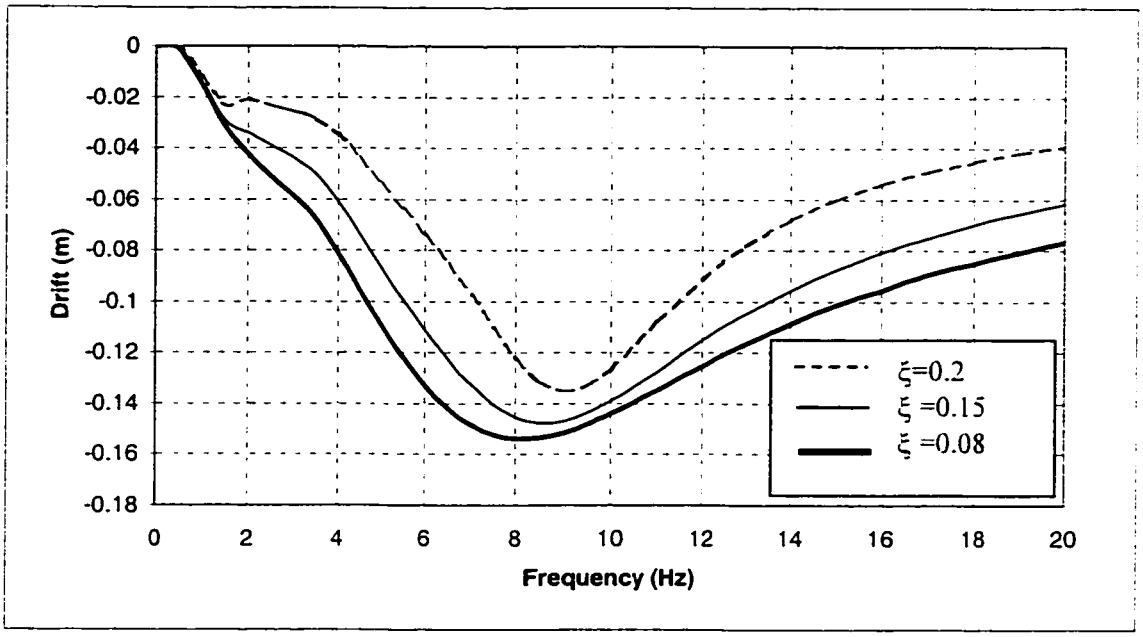


Figure 4.7: Drifts response for a single-stage nonlinear damper for variation of damping ration in frequency domain.

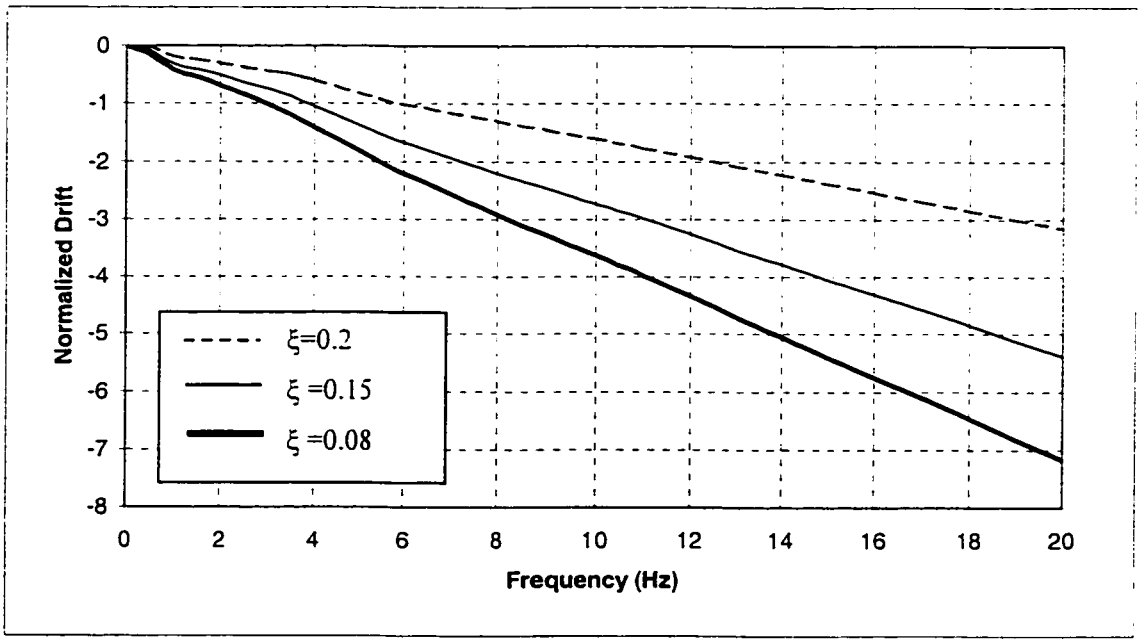


Figure 4.8: Normalized drift corresponding to different damping ratio for a single-stage nonlinear damper in frequency domain.

### 4.2.2 Two-Stage nonlinear asymmetric damper with a linear spring

The baseline ride model with linear suspension spring and two-stage asymmetric damper presented in chapter 2, and used for time simulation in chapter 3 is considered here for parametric study. This section focuses on the influence of asymmetry on the magnitude of drift from static equilibrium. The measure of asymmetry (p) as defined earlier represents the ratio of damping constant in extension to the compression strokes for low velocities. Hence, 'p' is defined as $C_3/C_1$ while $C_2$ and $C_4$ are maintained at their nominal value. The influence of $C_2$ and $C_4$ are examined later for variation of compression and extension reduction factor defined as $C_2/C_1$ and $C_4/C_3$, respectively. Other than the above damper parameters, this section also examines the influence of preset velocities and amplitude of excitation.

#### 4.2.2.1 Influence of Asymmetry (p)

The baseline asymmetry for a two-stage asymmetric damper as defined as $C_3/C_1$ is 5.34. Here the model is simulated for p=2, 5.34 and 8 over the entire frequency range of interest. The magnitude of drift for the selected values of p is shown in Figure 4.9. As the results show, larger asymmetry tends to larger drift over the entire frequency range. The trend is similar to that of a single-stage asymmetric damper, however, the influence in this case is significantly less due to the fact that asymmetry is defined with respect to $C_1$ and $C_3$ which is valid only upto the preset velocities.

The drift magnitude normalized by the relative amplitude across the suspension over the frequency range is presented in Figure 4.10. These results reveal that normalized drift changes with frequency in a nonlinear manner upto the wheel hop natural frequency, and increases linearly as frequency is increased further. It is recalled that for the case of

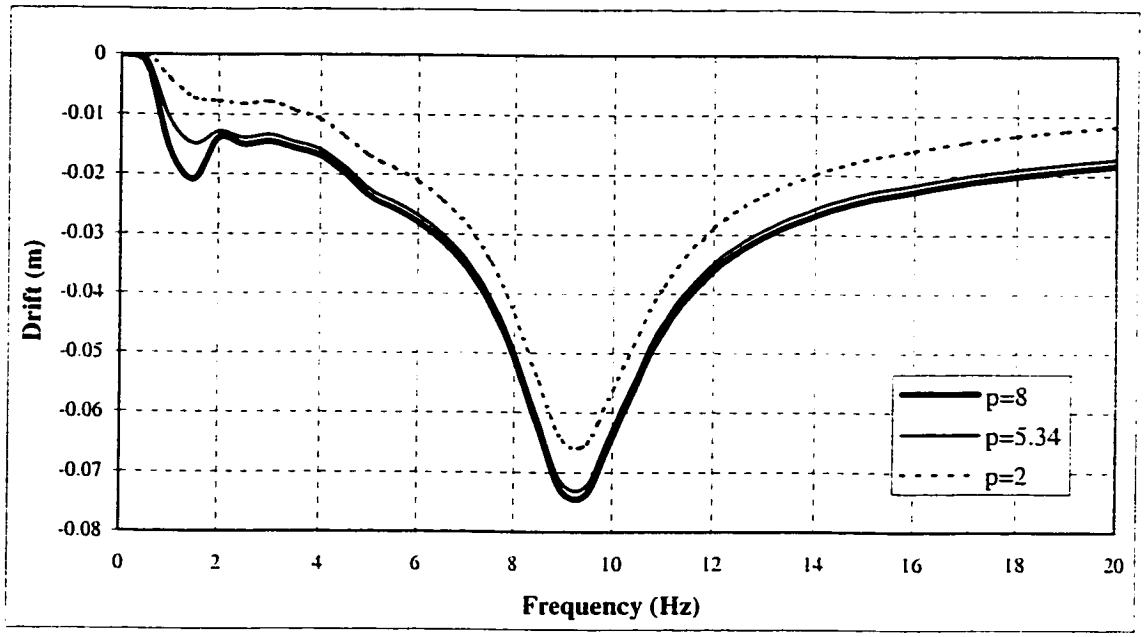


Figure 4.9: Frequency response of drift for a two-stage damping model corresponding to different asymmetries

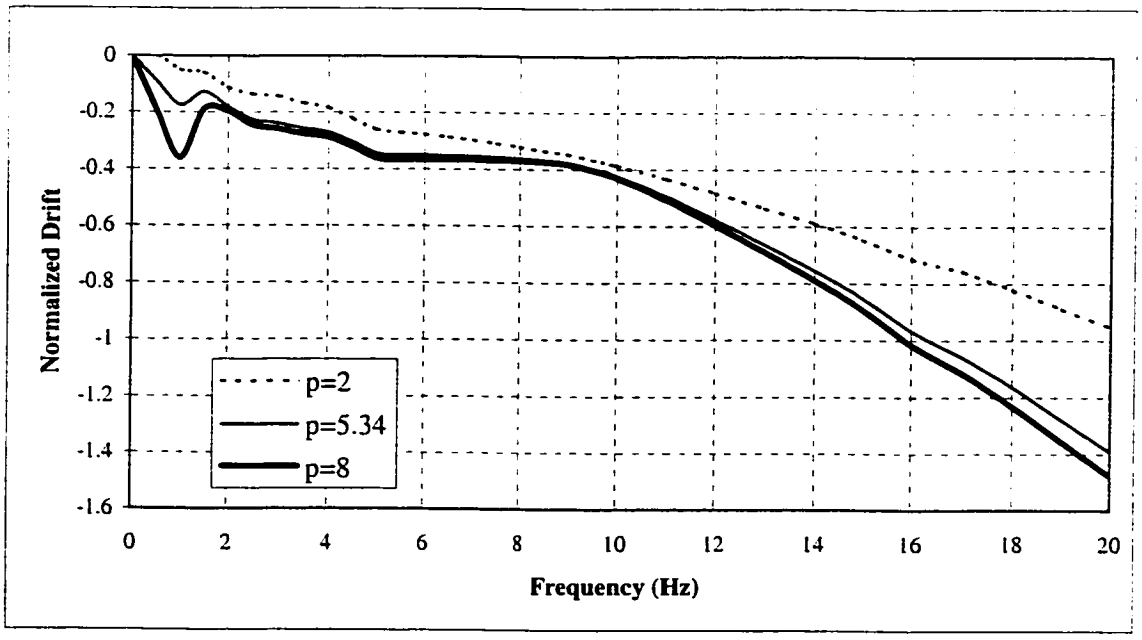


Figure 4.10: Normalized drift for a two-stage damper for various asymmetries

single-stage damper, this relationship was found to be linear. Such change in response can be attributed to the fact that other than asymmetry, the motion in this case goes through multi stage of damping over a cycle, especially for frequencies corresponding to one of the natural frequencies of the system.

#### 4.2.2.2 Influence of Breaking Velocities ($\alpha_e$, $\alpha_c$)

Breaking velocities are the damper preset velocities in compression $\alpha_c$ and in extension $\alpha_e$, where the damping constants change. The base line values used for these parameters are $\alpha_e$=0.1524 and $\alpha_c$=-0.2163 m/sec. The influence of the parameter is examined by changing one at a time. Figure 4.11 presents the drift magnitude for three sets of preset velocity in order to examine the trend of their influence over the frequency range. These results represent the baseline response as well as for change in $\alpha_e$ or $\alpha_c$ to a value of 1m/sec. As the results show, the increase in the extension preset velocity ($\alpha_e$) leads to a significant increase in the drift magnitude over the frequency range. On the other hand, an increase in compression reduction factor , preset velocity ($\alpha_c$) leads to slight reduction in the drift magnitude. This can be attributed to the fact that overall asymmetry of the damper increases when $\alpha_e$ is increased, whereas it decreases when $\alpha_c$ is increased. Such trend is also reflected from the normalized drift over the frequency range presented in the Figure 4.12. Once again the trend in the variation is similar to that of changing asymmetry presented in Figure 4.10.

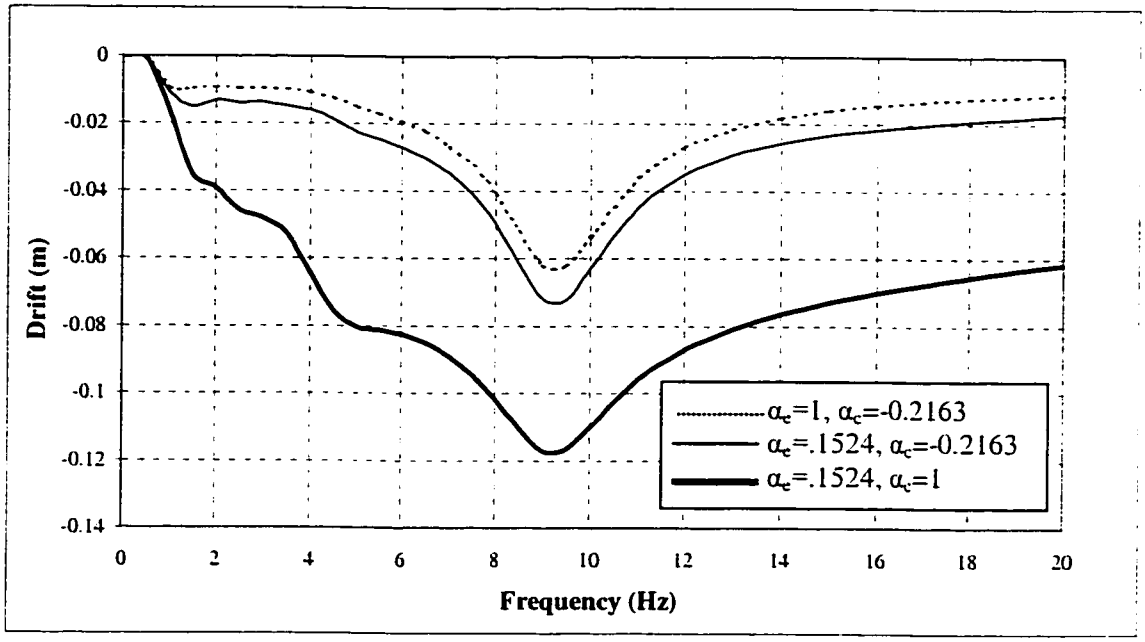


Figure 4.11: Frequency response of drift for a Two-stage damping model corresponding to different preset velocities

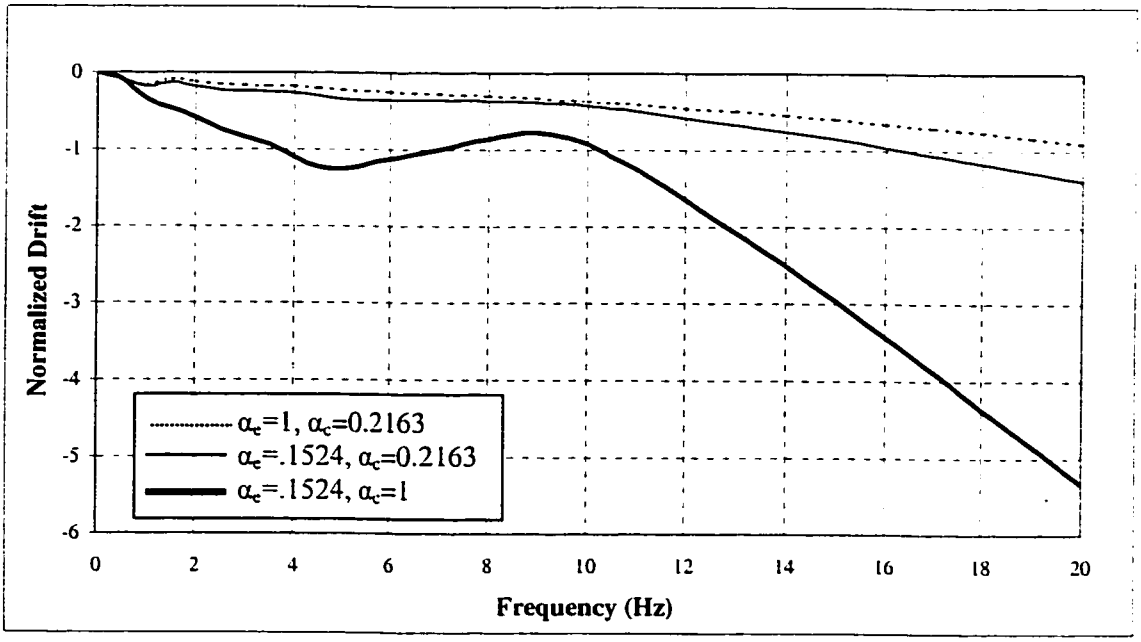


Figure 4.12: Normalized drift for a two-stage damper for various preset velocities.

#### 4.2.2.3 Influence of Excitation amplitudes ($X_0$)

The influence of excitation amplitude on the ride drift is examined for the baseline model under sinusoidal excitations. Simulation results are obtained for excitation amplitudes of 0.03, 0.05 and 0.1 m. The magnitude of steady state drift over the frequency range is presented in Figure 4.13. The results indicate that the drift increases with the increase in excitation amplitude throughout the frequency range. Furthermore, the increase in drift is proportional to the increase in the excitation amplitudes. The results further indicate that theoretically large excitation amplitude at the wheel hop frequency can lead to a very significant ride drift, severely limiting the suspension workspace.

These results in terms of normalized drift over the frequency range are presented in Figure 4.14. These results indicate relatively small effect of excitation amplitude until the wheel hop natural frequency. The influence is relatively large at higher frequencies. In comparison to single-stage damper, which showed negligible influence of the excitation amplitude, on the normalized drift (Figure 4.6), multistage does show some influence. This can be attributed to the strong nonlinearity that exists in the case of a multistage asymmetric model. Another interesting result observed here is the reversal of the trend from absolute drift as the amplitude of excitation is increased. In this case an increase in excitation amplitude leads to the fact that as input amplitude is increased, drift increases, while the increase in relative amplitude is even greater.

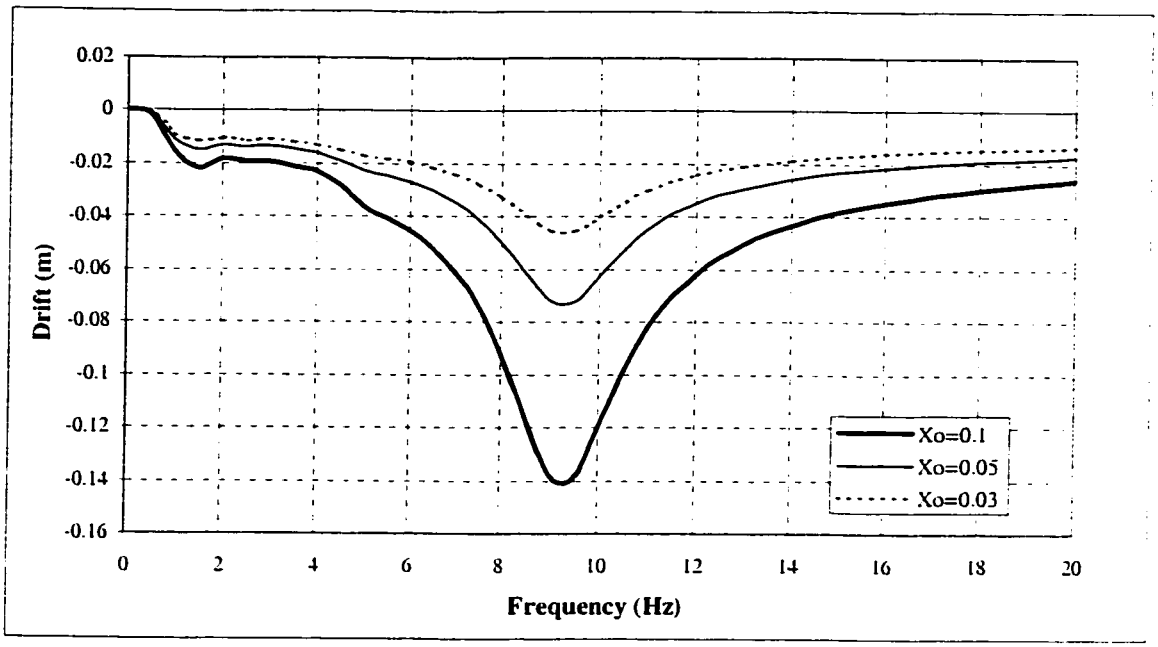


Figure 4.13: Frequency response of drift for a two-stage damping model corresponding to different excitation amplitudes

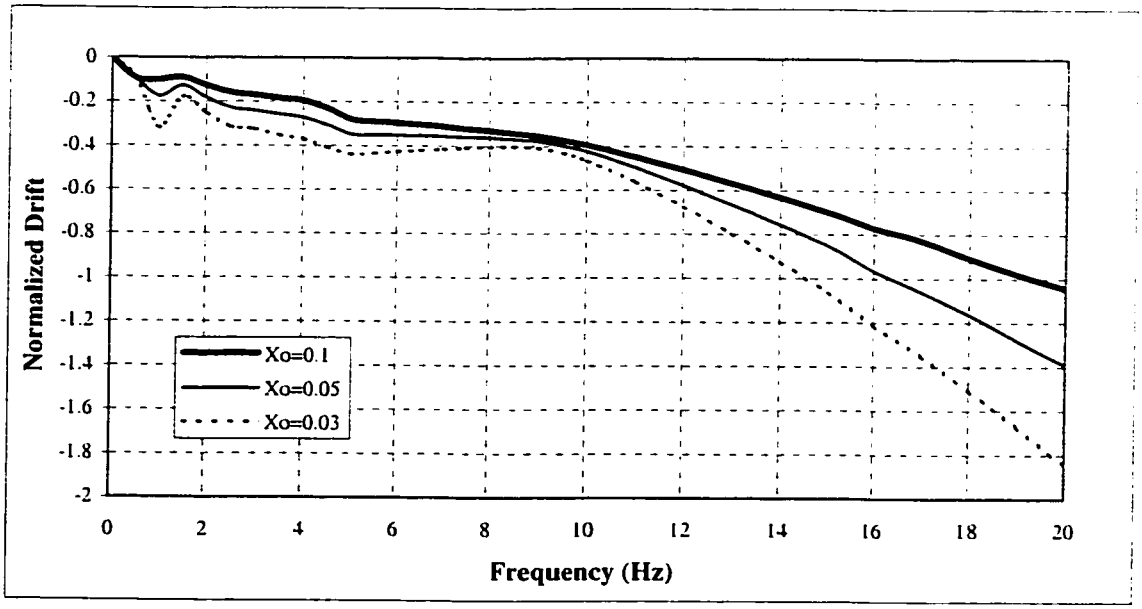


Figure 4.14: Normalized drift for a two-stage damper for various excitation amplitudes

#### 4.2.2.4 Affect of Extension Reduction Factor, ($\gamma_e$)

The damper extension reduction factor ($\gamma_e$) is defined as $C_4/C_3$ to characterize the extent of nonlinearity in the extension stroke. The variation is obtained by changing $C_4$ only in order to ensure that the asymmetry parameter 'p' is not altered. Baseline value of the parameter is 0.1682. Simulations are carried out for $\gamma_e$ =0.1, 0.168 and 0.5, where $\gamma_e$= 0.1 represents stronger nonlinearity with reduced damping in extension. The simulation results in terms of sprung mass drift over the frequency range for three values of $\gamma_e$ is presented in the Figure 4.15.

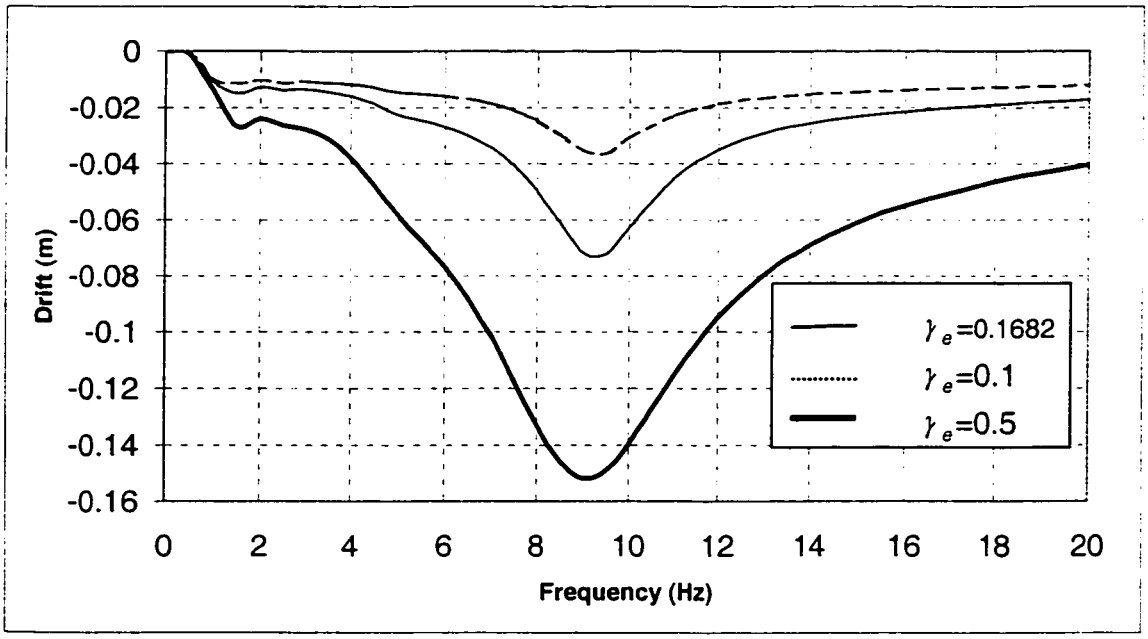


Figure 4.15: Frequency response of drift for a two-stage damping model corresponding to different extension reduction factors

As these results show, the extension reduction factor has very significant influence on the drift response over the entire frequency range. From the damper characteristics it is easy to see that although the asymmetry as defined by 'p' is held constant, an increase in $\gamma_e$ significantly increases these overall asymmetry of the damper. As a result an increase in $\gamma_e$ although increase damping, it also leads to significant increase in the drift magnitude over the frequency range. Same trend is also observed from normalized drift response presented in Figure 4.16.

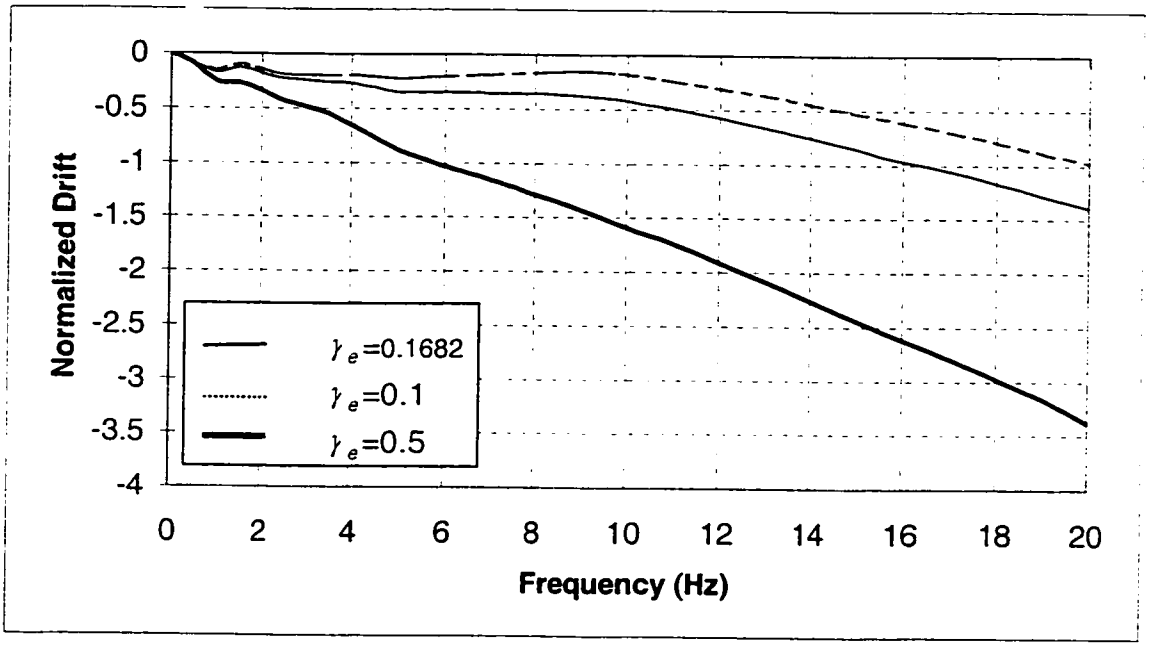


Figure 4.16: Normalized drift for a two-stage damper for various extension reduction factors

#### 4.2.2.5 Influence of Compression reduction factor s ($\gamma_c$)

The damper compression reduction factor ($\gamma_c$) is defined as $C_2/C_1$ to characterize the extent of nonlinearity in the compression stroke. The variation is obtained by changing $C_2$ only in order to ensure that asymmetry parameter 'p' is not altered. Baseline

value for the compression reduction factor parameter is 0.3416. Simulation are carried out for $\gamma_c$=0.1, 0.3416 and 0.5, where $\gamma_c$= 0.1 represents stronger nonlinearity with lower damping in compression. Figure 4.17 presents the drift magnitude for the three values of $\gamma_c$ over the frequency range. These results show opposite trend when compared with those obtained as influence of $\gamma_e$. In this case, an increase in $\gamma_c$ leads to significant decrease in drift around the wheel hop natural frequency. The results showing the influence of $\gamma_c$, therefore suggest that while increasing $\gamma_c$, increases damping, it also reduces overall asymmetry of the damper. This can easily be confirmed from the damper characteristics to demonstrate that although the asymmetry as defined by 'p' is held constant, an increase in $\gamma_c$ reduces the overall asymmetry of the damper. This trend is also reflected in the normalized drift trend presented in Figure 4.18.

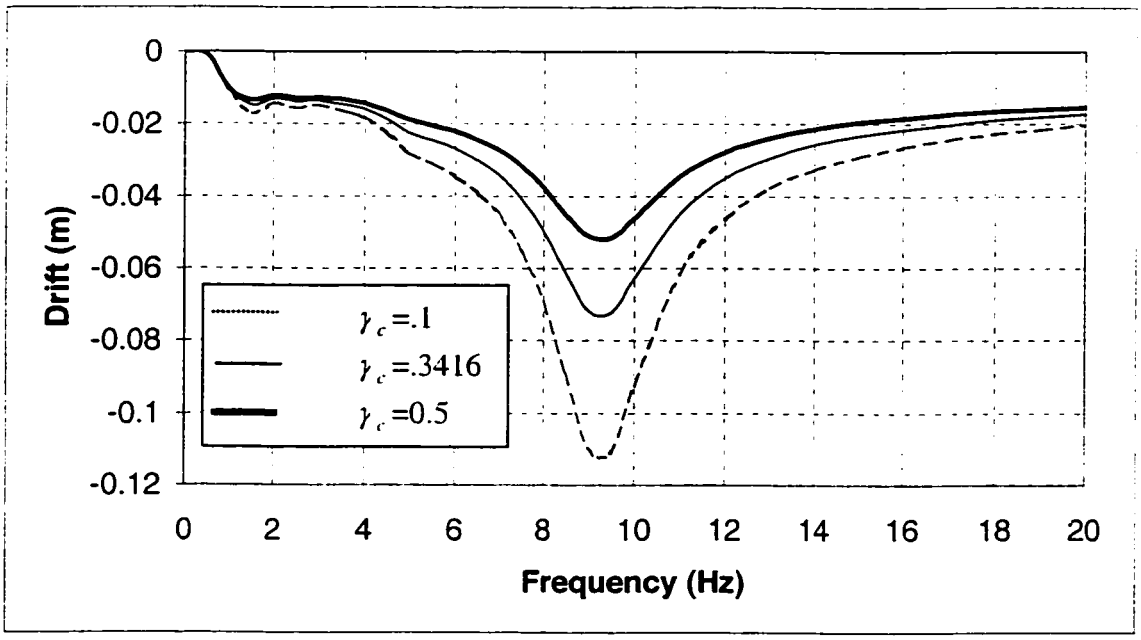


Figure 4.17: Frequency response of drift for a two-stage damping model corresponding to different compression reduction factors

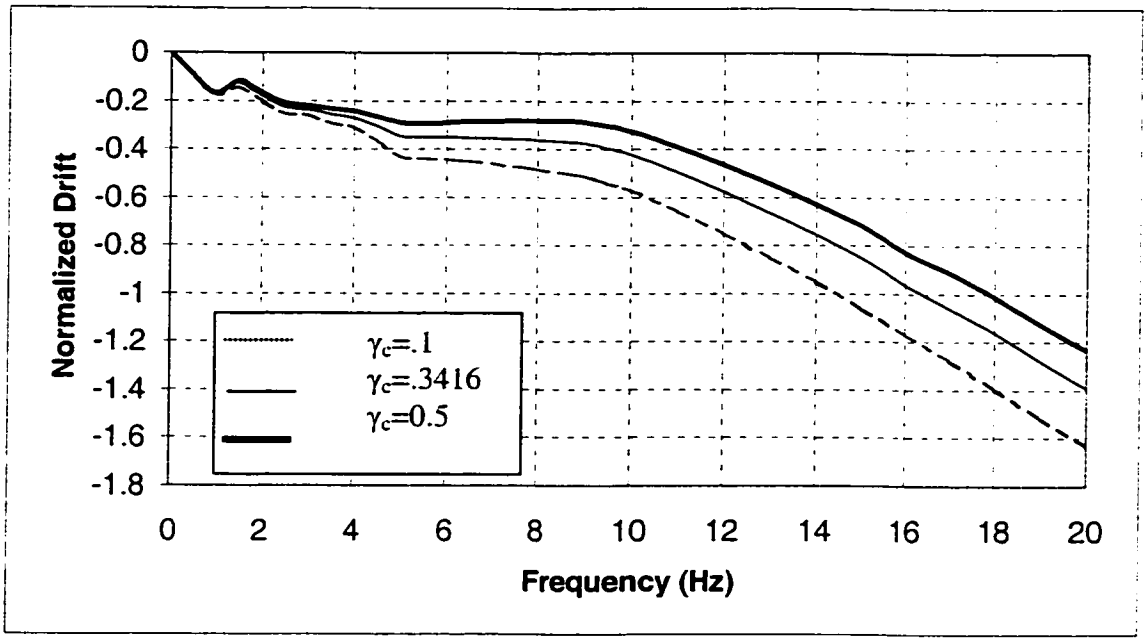


Figure 4.18: Normalized drift for a two-stage damper for various compression reduction factors

## 4.3 Ride Drift Characteristics for Suspension with Nonlinear Spring

The results of parametric study presented so far in this chapter consider a linear suspension spring. The spring was represented by an equivalent linear system to represent a cubical spring. In this section, a complete nonlinear suspension is considered incorporating the nonlinear asymmetric damper and a cubical nonlinear spring. The parameters used are presented for the baseline model in table 3.1, where $K_1$=12000 N/m and $K_2$=1.953e6 N/m$^3$ is used to represent the cubical spring. Simulations are carried out in steps to understand the influence of each component. The first simulation is thus carried out for linear damper with nonlinear spring, which is followed by a complete nonlinear suspension. Finally a parametric study is carried out to examine the influence of nonlinear spring parameter, $K_1$ on the overall drift response.

### 4.3.1 Nonlinear Spring with Linear Damper

The baseline quarter vehicle model with proposed cubical spring and a linear damper (C=975 N-s/m) is simulated in time domain for frequencies 0 to 20 Hz. The magnitude of drift is recorded for each frequency once the steady state is reached. The drift responses over the frequency range for excitation amplitude of 0.05 m and three different values of $K_1$ are presented in Figure 4.19. As the results show, the nonlinear spring also introduces drift over the frequency range with larger magnitude at the two natural frequencies. In this case, however, the drift is positive indicating a 'packing up' response of the sprung mass. It is expected since the cubical spring is a hardening spring that produces significantly larger force against compression than that in extension. As a result the center of oscillation for the sprung mass for large motions moves upward from the static equilibrium. As the spring parameter $K_1$ is increased reducing the asymmetry of the spring, the drift magnitude around the wheel hop frequency reduces. Such trend can be attributed to the fact that as $K_1$ is increased, the critical damping defined as $C_c = 2\sqrt{km}$ is increased, and the resulting damping ratio for the system $\xi = \frac{C}{C_c}$ decreases. This in turn produces larger sprung mass response at the resonance frequency, which also increases with the increase in stiffness. On the other hand, increasing stiffness values, it reduces positive drifts at wheel hop frequency. It should be noted here that, the peak of the drift responses shift while changing stiffness coefficients, that is due to, changing the stiffness coefficients also changes its natural frequencies.

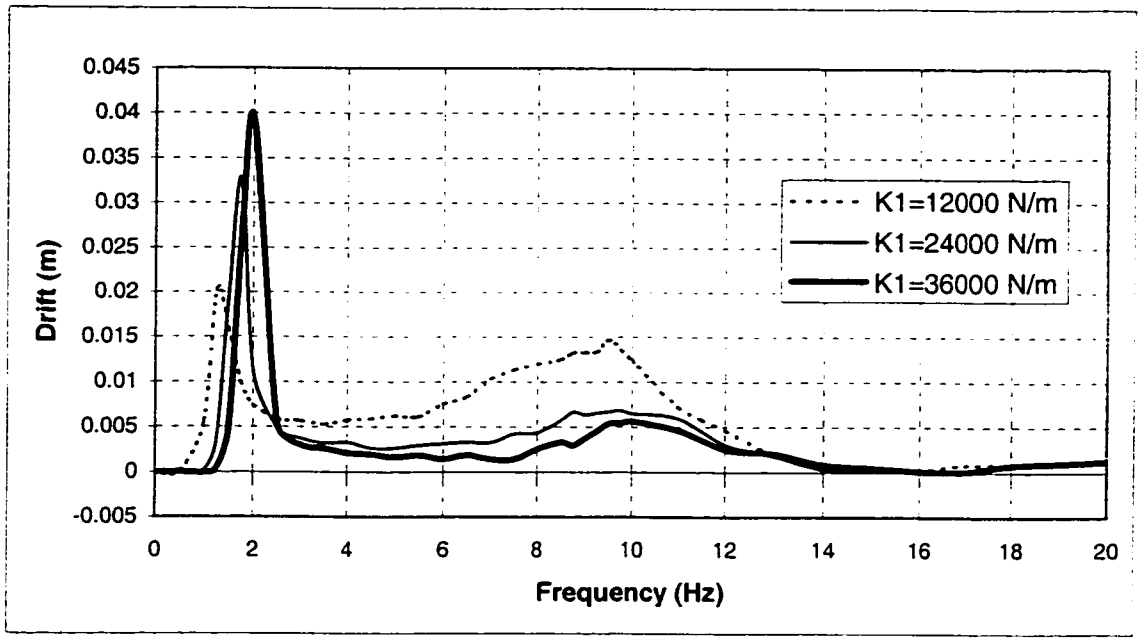


Figure 4.19: Frequency response of drift for a linear damper with nonlinear spring corresponding to different stiffness coefficient values

### 4.3.2 Nonlinear Spring with Nonlinear Damper

Based on the results obtained in Figure 4.19, it is expected that the frequency response of the drift produced by asymmetric damper will be significantly modified by the introduction of the nonlinear spring, especially around the natural frequencies. A combined effect of baseline asymmetric damper with the selected set of nonlinear spring over the frequency range is shown in Figure 4.20. As the results show, the combined effect yields more or less constant negative drift throughout the frequency range except for positive drift for a very narrow band around sprung mass natural frequency and around the wheel hop natural frequency. The results further reveal that it is possible to select a nonlinear spring characteristics that will minimize the drift magnitude due to asymmetric damper throughout most of the frequency range. However, this can be achieved at the expense of a larger drift at the sprung mass natural frequency. This trend

is also reflected in the normalized drift trend presented in Figure 4.21 which shows, the normalized drift is nearly linear after the wheel hop frequecies.

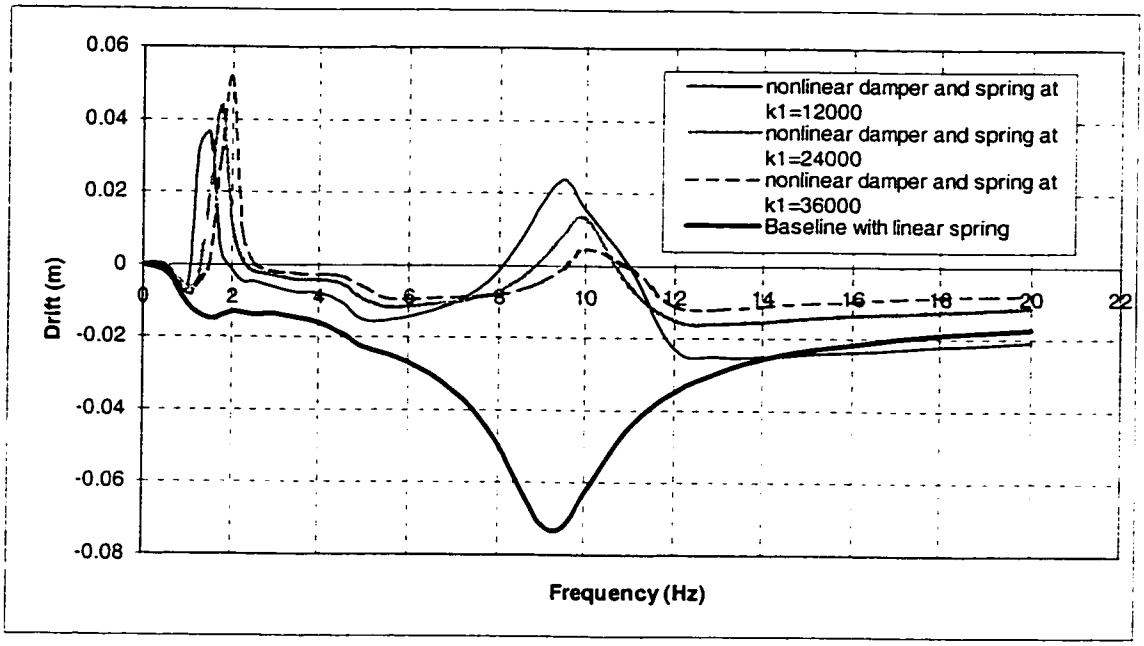


Figure 4.20: Frequency response of drift for a complete nonlinear model corresponding to different stiffness coefficient values

## 4.3 Summary

A comprehensive parametric study is performed to establish the influence of variation in design and operating parameters on the performance characteristics of linear, nonlinear, symmetric and asymmetric damper models associate with either linear or nonlinear spring. Simulations are presented in terms of frequency response of drift and normalized drift defined as drift/relative amplitude. The results are obtained for variation of one parameter at a time while others are held constant and equal to their nominal value. The parameters that are varied and their general influence on the drift behavior are summarized here. The specific conclusions are presented in the next chapter.

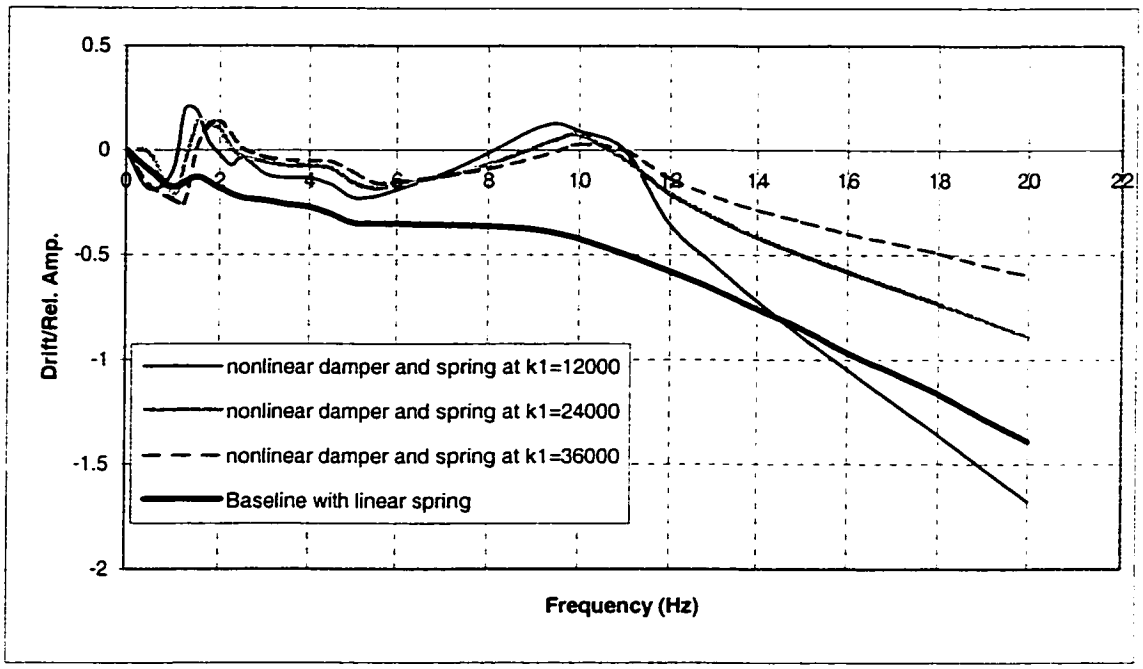


Figure 4.21: Normalized drift for a complete nonlinear model for various stiffness coefficients.

Increase in asymmetry (p) leads to increased drift with more influence on single-stage damper. Increase in excitation amplitude ($X_0$) increases the drift. Normalized drift is unaffected for single-stage damper while two-stage system show influence for larger frequencies. A change in preset velocities primarily changes the asymmetry characteristics. An increase in $\alpha_e$ reduces asymmetry and drift while increase in $\alpha_c$ increases asymmetry and resulting drift. An increase in damping ratio in general reduces the amplitude motions and resulting drift. For a fixed asymmetry ratio (p) an increase in compression reduction factor ($\gamma_c$) reduces overall asymmetry and resulting drift. A reverse of the above trend is observed for a change in extension reduction factor ($\gamma_e$) as an increase in $\gamma_e$ increases the overall asymmetry of the damper. Nonlinear hardening spring introduces positive drift around the system natural frequencies. The combined

effect of nonlinear spring and asymmetric damper reduces negative drift throughout the frequency range with significant positive drift introduced at sprung mass natural frequency. A suspension system designed with asymmetric characteristics for damper and spring to achieve improved ride and handling may thus introduce drift in dynamic equilibrium through out the frequency range. A suspension designer therefore, should also consider the resulting drift to ensure that it does not adversely affect the performance of the suspension system.

# CHAPTER 5

## CONCLUSION AND RECOMMENDATIONS FOR THE FUTURE WORK

### 5.1 General

Highly significant developments in suspension system have been realized during the past few decades through modeling, simulations, repetitive filed trials and tuning. Suspensions are designed with blow off and bleed-control valves to produce nonlinear asymmetric characteristics to provide improved ride performance over a wide frequency range and to ensure adequate wheel-road contact for handling. Although such designs have been extensively investigated, one of its characteristics, namely 'packing down' phenomenon was not reported until recently. Furthermore, such behavior has not been explored through analytical modeling and parametric study.

This investigation presents a detailed analysis of a simple quarter-vehicle model with comprehensive representation of suspension system to demonstrate the 'packing down' phenomenon or ride height drift characteristics of a modern suspension system. The suspension system considered incorporates a nonlinear asymmetric damper and nonlinear cubical spring to represent air spring system. The model developed for ride analysis is validated against published frequency response results. A detailed parametric study is also carried out to investigate the influence of various suspension damper and spring parameters in the ride height drift characteristics over a frequency range of 0-20 Hz.

Simulations are carried out in time domain using "Matlab simulink' for selected amplitudes of excitations and frequencies within the range. Steady state response is then

used to establish the centre of oscillations for sprung and unsprung masses. Results are extracted to represent drift magnitude and normalized drift (ratio of drift over relative motion across the suspension).

The major conclusions drawn from the response results, and a list recommendation for future works are presented in the following subsections.

## 5.2 Major Conclusions

The study utilizing a validated vehicle ride model is carried out in several stages to systematically characterize the ride drift phenomenon of modern vehicle suspension. The major conclusions that can be drawn from the results presented and observed are:

a) Suspension nonlinearity has no influence on the drift as long as characteristics is symmetric.

b) Ride drift is a phenomenon directly related to the asymmetry of suspension damping. Drift increases as damper asymmetry is increased.

c) Both single-stage and multi stage asymmetric damper lead to ride drift where single-stage produce larger drift.

d) Lower damping in compression than extension lead to drift down or 'packing down' and vice versa.

e) There is drift at all frequencies with a slight increase at sprung mass resonance and is maximum for frequencies corresponding to wheel hop or unsprung mass resonance.

f) Normalized drift defined as drift/relative amplitude increases linearly with increasing frequency for single-stage damper whereas for two-stage damper linear

relationship only exists for frequencies greater than the wheel hop natural frequency.

### 5.2.1 Parametric Study

All suspension damping parameters that characterize a nonlinear asymmetric damper will change the effective damping and asymmetry of the damper. Some general and specific conclusions drawn from the parametric study are as follows:

a) A parameter that reduces effective damping without affecting asymmetry will increase the drift magnitude.

b) A parameter that increases asymmetry without affecting the damping will increase the drift magnitude.

c) A change in parameter for damper affects both effective damping and asymmetry. It is therefore, difficult to identify the cause when only one parameter is changed at a time that affects both damping and asymmetry.

d) For single-stage asymmetry, increase in asymmetry or excitation amplitude increases drift in a similar manner.

e) The rate of change for normalized drift for a single-stage damper is unaffected by the amplitude of excitations indicating proportional increase in drift and relative motion with excitation amplitude.

f) For two-stage damper, asymmetry as defined with respect to high damping has relatively less effect on the drift magnitude.

g) Based on the parameters considered, the influence of excitation amplitude has opposite effect on drift and normalized drift.

h) Drift is highly influenced by the increase in break velocity ($\alpha_e$) in extension than that of increase in break velocity ($\alpha_c$) in compression.

i) An increase in two-stage extension reduction factor ($\gamma_e$), decreasing the effective damping, also decreases the drift magnitude significantly as it tends to reduce the asymmetry. A change in $\gamma_e$ thus has more influence on asymmetry.

j) An increase in two-stage compression reduction factor ($\gamma_c$), decreasing effective damping.

k) Nonlinear cubical spring with softer stiffness in extension leads to upward drift at the natural frequencies.

l) A suspension with asymmetric damping and hardening spring exhibit positive drift at natural frequencies while the drift is negative at other frequencies.

m) The drift around one natural frequency can be minimized by selecting spring parameters, at the expense of larger drift at the other natural frequency.

Finally it is concluded that both asymmetric spring and damper leads to drift in dynamic equilibrium, the drift can be significant for realistic asymmetric damper with linear spring. Suspension design should therefore consider such behavior as it may effect the available suspension working space and ride height at some frequencies. Vehicle systems with different load in front and rear or suspension with different characteristics in front and rear may result in a different ride height in the front and rear, and thus affecting the pitch orientation. Further studies should therefore be carried out to investigate the phenomenon of vehicle suspension drift. A list for possible further studies summarized in the following.

## 5.3 Recommendations for Future Investigations.

The present work yields a dynamic model that provides a basic insight to the drift phenomenon of the conventional suspension system with asymmetric properties. The knowledge gained from this investigation is a starting point and establishes the direction for future works.

a) More elaborate pitch plane vehicle model should be studied with the proposed damper models to study dynamic equilibrium in bounce as well as pitch modes.

b) Experimental validation of the results obtained may be under taken by laboratory and field testing of an instrumented vehicle.

c) A more refined damper model with temperature effect, friction and valve dynamics may be undertaken to explore the drift phenomenon.

d) The present investigation examined the response to deterministic excitation. Future work may examine the response of the suspension to stochastic road excitations.

e) In the present work, a conventional damper and a gas spring are considered for a mid size car parameters. Various types of suspension systems such as hydropneumatic, semi active configurations, interconnected suspension etc. should be considered in conjunction with different on-road, off-road and tracked vehicle configurations.

## REFERENCES


1. Ahmed, A. K. W., "Ground Transportation Systems", Encyclopedia of Vibration, Academic Press, 2001, pp. 603-620.
2. Bacon Miles E., "Automotive Steering, Suspension, and Wheel Alignment", McGraw-Hill Book Company, 1988.
3. Bastow Donald, "Car Suspension and Handling, London", Second Edition, PenTech Press, UK, 1988.
4. Bert, C.W. "Material Damping: An Introductory Review Of Mathematical Models, Measures and Experimental Techniques", Journal of Sound and Vibration. Vol. 29(2), 1973, pp. 129-153
5. Causemann, Peter, "Automotive Shock Absorbers", Verlag Moderne Industrie, Augsburg, Germany, 2000.
6. Chaudhary, S., "Ride and Roll Performance Analysis of a Vehicle with Spring Loaded Interconnected Hydropneumatic Suspension", M.A.Sc. Thesis, Concordia University, Canada, 1998.
7. Choi S. B., Lee S. K. and Park Y. P. "A Hysteresis Model for the Field-Dependent Damping Force of a Magneto-rheological Damper", Journal of Sound and Vibration 245(2), 2001, pp. 375-383.

8. Crolla, D. A. and Horton, D. N. L., "Application of Linear Sensitivity Methods to Vehicle Dynamics problems", The University of Leeds, UK, 1991.

9. Ellinger Herbert E. and Hathaway Richard B., "Automotive Suspension and Steering Theory and Service", Prentice Hall, New Jersey 07632, 1989.

10. Emery M, "The Not so Fine Art of Suspension", Quickbrit Publishing Inc, 2002

11. Genta, G., "Motor Vehicle Dyanmics: Modeling and Simulation", Politecnico di Torino, Italy, 1997.

12. Gillespie, Thomson D., "Fundamentals of Vehicle Dynamics", Society of Automobile Engineers, USA, 1992.

13. Hac, A., Youn, I. "Optimal semi-active suspension with preview based on a quarter car model", Proceedings of the American Control Conference, v.1, p 433-438, 1991.

14. Hanly, F J., "Fluids for High-Pressure Industrial Hydraulic Systems." SAE Technical Paper No. 670697, 1967.

15. Haque, M. M., Ahmed, A. K. W. and Sankar, S., "Simulation of Displacement Sensitive Non-Linear Dampers via Integral Formulation of Damping Force Characterization", Journal of Sound And Vibration vol. 187 (1)., Canada, 1995, pp. 95-109

16. Harrison, R F and Harmond, J. K. "Approximate Time Domain, Non-stationary Analysis of Stochastically Excited, Nonlinear Systems with Particular Reference to the Motion of Vehicles on Rough Road", Journal Sound and Vibration, 105, (3), 1986, pp. 361-371.

17. Horton, D. N. L. and Crolla, D. A., "Theoretical Analysis of a Semi-Active Suspension Fitted to an Off-Road Vehicle", Vehicle System Dynamics, 15, 1986, pp. 351-372.

18. Hrovat, D. "Survey of Advanced Suspension Developments and Related Optimal Control Applications," Automatica, Vol. 33, No. 10, 1997.

19. Ikenaga S., Lewis F. L., "Active Suspension Control Using a Novel Strut and Active Filtered Feedback: Design and Implementation" Automation and Robotics Research Institute, The University of Texas at Arlington, Texas, USA, 1999.

20. Joo, F., "Dynamic Analysis of a Hydropneumatic Suspension System", M.A.Sc Thesis, Concordia University, Montreal, 1991.

21. Karnopp, D. C., Crosby, " The Active damper- A new Concept for Shock and Vibration Control," Shock and vibration Bulletine, 43(4), June, 1973, pp. 119-133.

22. Lang, H. H., "A Study of the Characteristics on Oil Seals for Gas Pressurized Shock Absorbers of Automotive Suspension," SAE Technical paper No. 850333, 1985

23. Michael, W. Sayers and Dongsuk, Han, "A Generic Multi body Vehicle Model for Simulating Handling and Braking", IAVSD Symposium, Ann Arbor, USA, 1995.

24. Nigam, N. C., "Introduction to Random Vibrations", The MIT Press, Cambridge, Massachusetts, 1983.

25. Oueslati F, Sankar S., "A class of semi-active Suspension Schemes for Vehicle Vibration Control", Journal of Sound and Vibration, 172(3), 1994, pp. 393-411.

26. Oueslati, F., "A Comparative Study of Advanced Suspensions Based On an In-Plane Vehicle Model", MASc Thesis, Concordia University, 1990.

27. Parkin, M. J., "Suspension System: Developments from 1900 to the Present Day", Mechanical Engineering Department, University of Bath, UK, 1999.

28. Purdy, D.J., "Theoretical and experimental investigation into an adjustable automotive damper", Proceedings of the Institution of Mechanical Engineers, Part D: Journal of Automobile Engineering, 214-3-2000, pp. 265-283. 2000

29. Quaglia, G., Sorli M., "Experimental and Theoretical Analysis of An Air Spring With Auxiliary Reservoir", Dept. of Mechanics, Politecnico di Torino, Corso Duca degli Abruzzi, Torino, Italy, 1998.

30. Rajamoni, R. and Hedrick, J. K., "Semi-active Suspensions A Comparison Between Theory and Experiments", University of California at Berkeley, USA, 1991.

31. Rakheja S. and Rajalingham C., "Influence of Suspension Damper Nonlinearity on Vehicle Vibration Response to Ground Excitation", Journal of Sound and Vibration, in press.

32. Rakheja S., Mcmanus, S. J. and K. A. St. Clair, "Evaluation of Vibration and Shock Attenuation Performance of a Suspension Seat with a Semi-Active Magnetorheological Fluid Damper", Journal of Sound and Vibration 253(1), 313-327, 2002.

33. Rakheja, S., Ahmed, A. K. W., "Frequency Response Analysis of Symmetric and Asymmetric Nonlinear Vehicle Suspensions", CSME, Special issue, Vol 17, No. 4B, Canada, 1993.

34. Rakheja, S. and Ahmed, A. K. W., "An Algorithm for Simulation of Nonlinear Mechanical Systems Using Energy and Force Similarity of its Elements", Finite Elements in Analysis and Design 18, pp.141-154, Concave Research Center, Concordia University, 1994.

35. Rakheja, S., Ahmed, A. K. W., "An Equivalent Linearization Technique for the Frequency Response Analysis of Asymmetric Dampers", Journal of Sound and Vibration, 153(3), 1992, pp 537-542.

36. Rakheja, S., "Computer Aided Dynamic Analysis and Optimal Design of Suspension Systems for Off-Road Tractors", Ph.D. Thesis, Concordia University, 1983.

37. Rakheja, S., Ahmed, A.K.W., Yang, X. and Guerrette, C., "Optimal Suspension Damping for Improved Driver and Road Friendliness of Urban Buses," SAE Technical Paper, 199-01-3728, 1999.

38. Rengarajan S., "An Analytical and Experimental Investigation On the Vibration Isolation Performance of Semi-Active Suspensions", M. A. Sc. Thesis, Concordia University, Canada, 1991.

39. Scibor-Rylski, A. J., "Road Vehicle Aerodynamics", Pentech Press Limited, London, 1975.

40. Segel, L. and Lang, H. H., "The Mechanics of Automotive Hydraulic Dampers at High Stroking Frequencies", Proc. 7$^{th}$ IAVSD Symposium on the dynamics of vehicles on roads and on railways tracks (ED. A. H. Wickens), Cambridge UK, 1981, pp. 194-214.

41. Sharp R. S. and Crolla D. A., "Road Vehicle Suspension System Design- A Review," Vehicle System Dynamics, Vol. 16, 1987, pp. 167-192.

42. Snowdon, J.C. "Vibration And Shock in Damped Mechanical Systems", John Wiley and Sons, Inc. USA, 1968.

43. Su, H., "An Investigation of Vibration Isolation Systems Using Active, Semi-Active and Tunable Passive Mechanisms with Applications to Vehicle", Ph.D. Thesis, Concordia University, Montreal, 1990.

44. Tanaka. N. and Kikushima, Y. "Optimal Design of Active Vibration Isolation Systems", Trans. ASME, J. Dynamic Systems, Measurement and Control, Vol 110, Jan 1988, pp.42-48.

45. Thompson, A. G., "Optimization Damping in a Randomly Excited Non-linear Suspension", Proc. Inst. of Mech. Engrs, 184(2A), 1969-70, 169-178.

46. Thompson, W. T., "Theory of Vibration with Applications", Prentice-Hall, Englewood Cliffs, N. J., 1965.

47. Wahi, M. K., "Oil Compressibility and Polytropic Air Compression Analysis for Oleopneumatic Shock Strut", Journal of Aircraft, Vol. 13, No. 7, 1976, pp. 527-530,

48. Walker, D.G., Stein, J.L. and A.G. Ulsoy, "An Input-output Criterion for Linear Model Deduction". Proceedings of the 1996 ASME International Mechanical Engineering Congress and Exposition - Dynamic Systems and Control Division, Symposium on Automated Modeling, November, Atlanta, GA. Published by ASME, New York, NY. 1996.

49. Warner Brian, "An Analytical and Experimental Investigation of High Performance Suspension Dampers, Concordia University, Canada, 1996.

50. Warner, B., "Adjustable Damper Means for Shock Absorber", United States Patent No. 4872537, October 10 1989.

51. Williams, M., "Shocked", Four Wheeler Magazine, Eastern Ontario Trailblazers, Canada, 2000.

52. Wong J. Y., "Theory of Ground Vehicles", 2nd Edition, John Wiley and Sons Inc., USA, 1993.

53. Wu X., Griffin, M. J., "A Semi-Active Control Policy to Reduce the Occurrence and Severity of End-Stop Impacts in a Suspension Seat with an Electrorheological Fluid Damper", Journal of Sound and Vibration 203, 1997, pp. 781-793.

54. Youn I. and Hac A., "Semi-Active Suspensions with Adaptive Capability", State University of New York at Stoony Brook, New York 11794, USA, Journal of Sound and Vibration, 180 (3), 1995, pp. 475-492.